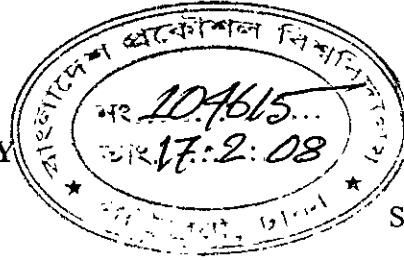# AN EXPERIMENTAL INVESTIGATION OF WIND LOAD ON TALL BUILDINGS WITH SQUARE CROSS-SECTION HAVING ROUNDED FACET.

A THESIS PREPARED BY

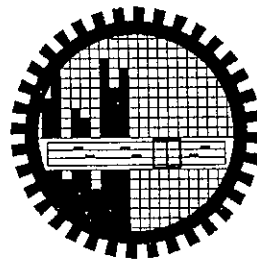Nripendranath Biswas   Student No.: 040510041P

The thesis is submitted to the Department of Mechanical Engineering, Bangladesh University of Engineering & Technology (BUET), Dhaka, Bangladesh in partial fulfillment of the requirements for the degree of Master of Science in Mechanical Engineering.

SUPERVISED BY

DR. AMALESH CHANDRA MANDAL
Professor
Department of Mechanical Engineering
BUET, Dhaka.

DEPARTMENT OF MECHANICAL ENGINEERING
BANGLADESH UNIVERSITY OF ENGINEERING AND TECHNOLOGY,
(BUET)
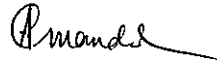Dhaka-1000, Bangladesh
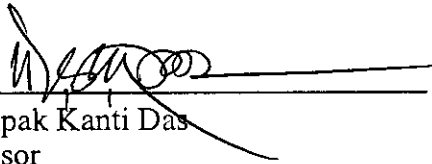January, 2008

RECOMMENDATION OF THE BOARD OF EXAMINERS

The Board of Examiners hereby recommends to the Department of Mechanical Engineering, Bangladesh University of Engineering and Technology (BUET), Dhaka, the acceptance of the Thesis on "An Experimental Investigation of Wind Load on Tall Buildings with Square Cross-Section having Rounded Facet", submitted by Nripendranath Biswas, Roll No.: 040510041P, Session: April-2005, in partial fulfillment of the requirement for the degree of Master of Science in Mechanical Engineering.

Dr. Amalesh Chandra Mandal   Chairman
Professor
Department of Mechanical Engineering
BUET, Dhaka.

Dr. Dipak Kanti Das   Member
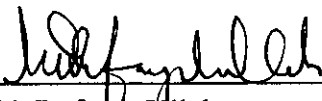Professor
Department of Mechanical Engineering
BUET, Dhaka.

Dr. Md. Maksud Helali   Member
Professor and Head   (Ex-Officio)
Department of Mechanical Engineering
BUET, Dhaka

Dr. Md. Refayet Ullah   Member
Professor   (External)
Department of Naval Architecture
and Marine Engineering
BUET, Dhaka.

ii

CANDIDATE'S DECLARATION

This is to certify that the work presented in this thesis is an outcome of the investigation carried out by the author under the supervision of Dr. Amalesh Chandra Mandal, Professor, Department of Mechanical Engineering, Bangladesh University of Engineering & Technology (BUET), Dhaka and that it has not been submitted elsewhere for the award of any degree or diploma.

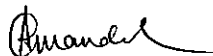**Prepared by**

_____

Nripendranath Biswas (040510041P), Author

Supervised by

_____

Dr. Amalesh Chandra Mandal
Professor
Department of Mechanical Engineering
BUET, Dhaka.

Dedicated

To

My Parents

ACKNOWLEDGEMENTS

The Author

v

ABSTRACT

An experimental investigation of the static pressure distribution on the square cylinders with rounded facet is conducted. The study includes both the single cylinder and the group consisting of two cylinders. The test is conducted in open circuit wind tunnel at a Reynolds number 5.4×10^4 based on the face length across the flow with uniform flow of velocity 13.6 m/s.

The study is conducted, initially on a single cylinder with various facet widths at zero angle of attack. The five different dimensionless facet widths are considered in the study with a view to observing the effect of the facet widths on the static pressure distribution.

Then a group of cylinders is taken into consideration for the study. Each group consists of two cylinders; one in front of the other is kept along the flow direction. The static pressure distribution is monitored on each cylinder in the group varying the inter spacing between the front and the rear cylinder.

The drag coefficient is determined from the static pressure distributions by the numerical integration method. It is observed from the results that the drag coefficient depends on the facet widths significantly. With the facet widths on the cylinder, the drag reduces remarkably compared to that on the sharp edged cylinders. However, with further increase of facet widths, drag does not change significantly.

CONTENTS

LIST OF FIGURES

NOMENCLATURE

A	Frontal area of the cylinder
C_d	Co-efficient of drag
C_l	Co-efficient of lift
C_p	Mean pressure co-efficient
D	Width of cylinder normal to the flow direction
Δd	Strip width of the mid portion in the vertical direction
$\frac{dp}{dn}$	Pressure gradient
F	Denotes upstream cylinder
F_d	Drag force per unit length of the cylinder
F_l	Lift force per unit length of the cylinder
h	Width of facet
h'	Any height from test section from bottom surface
Δh	Strip width of the mid portion in the horizontal direction / deflection in manometer limb
H	Depth of cylinder in the flow direction
H_0	Tunnel test section
L	Longitudinal spacing
P	Local static pressure
P_0	Free stream static pressure
ΔP	Difference of ambient and local static pressure
ΔP_h	Pressure differences in the horizontal strip
ΔP_v	Pressure differences in the vertical strip
r	Facet radius
R	Denotes downstream cylinder
R_e	Reynolds number
u	Mean axial velocity
U_∞	Free stream velocity
V	Mean wind speed at a height Z
V_c	Mean wind speed at the gradient height Z_c
x	Latitude
α	Angle of attack
γ_w	Specific weight of manometer water
ρ	Density of air
ω	Angular velocity of the earth

CHAPTER - 1

INTRODUCTION
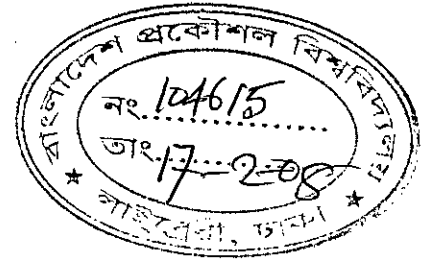
1.1 Background

During the last few decades wind loadings on buildings and structures have been considered as one of the most important engineering problems. A group of skyscrapers, chimneys, towers, the flow induced tubes in heat exchangers, bridges, oil rigs etc. need detailed investigation in regard to flow patterns and aerodynamic loads. There has been lots of in research works concerning laboratory simulations, full-scale measurements, theoretical predictions and numerical calculations for flows over the bodies of various shapes. However, the problem of wind loading is not a new one. Galileo and Newton considered the subject for study in the 17th century. A number of failures of bridges, transmission towers, buildings etc. stimulated the researchers to do investigation in this field. Some of the pioneer researchers in the field are Smeaton (1759), Vogt (1880), Irminger (1891), Eiffel (1900) and Stanton (1907).

Irminger in 1891 published results of measurements on models, which was probably the first-ever wind tunnel test and Eiffel in the period up to 1900, following completion of the famous tower, conducted studies on the flow velocities and tower movements from a laboratory at the top of the tower.

The study of wind effect was first limited to loading on buildings and structures only, possibly because of its most dramatic effects are seen in their collapses. In mid-sixties researchers started the study of less dramatic, but equally important environmental aspects of the flow of wind around buildings. These include the effects on pedestrians, weathering, rain penetration, ventilation, heat loss, wind noise, air pollution etc. The pioneer researcher in this field is T. V. Lawson [36] of the University of Bristol. A number of works of the environmental aspects of wind are being studied at the Building Research Establishment at Garson and the University of Bristol, UK.

It is true that researchers from all over the world have contributed greatly to the knowledge of flow over bluff bodies [42] but the major part of the reported works are of fundamental nature involving the flow over single body of different profiles. Most of the researchers have conducted research works either on a single cylinder or on a group of cylinders having square or rectangular sections mainly. But the flow over either square or rectangular cylinders with rounded facet problems has not been studied till now especially in-groups to date, although this is a problem of practical significance. It will contribute towards the knowledge of wind loads on either a single or a group of buildings of square or rectangular section with rounded facet.

1.2 Nature of the Wind

The wind behavior is discussed in this section in brief. The characteristics of the wind, which are more or less related to the present study, have been taken into consideration for discussion in a nutshell.

1.2.1 Wind Velocity

Winds are named by the direction they come from. Thus a wind from south, blowing toward the north is called a south wind. Windward refers to the direction a wind comes from, leeward to the direction it blows toward. When a wind blows more frequently from one direction than from any other it is called a prevailing wind. Wind speed increases rapidly with height above the ground level, as frictional drag declines. Wind is commonly not a steady current but is made up of a succession of gusts, slightly variable in direction, separated by lulls. Close to the earth the gustiness is developed due to irregularities in the wind are caused by the conventional currents. All forms of turbulence play a part in the process of transporting heat, moisture and dust into the air aloft.

There are various parameters, which control the flow behavior [12]. They are; (i) Vortices in front of the building, (ii) Opening through buildings, (iii) Spacing of rows, (iv) Wakes of buildings, (v) Long straight streets, (vi) Narrowing streets, (vii) Corners, (viii) Courtyards.

The mean wind speed varies with height. The variation of wind speed has been expressed

by Davenport [19] as

$$V = V_c (Z/Z_c)^a \quad \text{...} \quad (1)$$

where, V is the mean wind speed at a height Z, V_c is the mean wind speed at the gradient height Z_c. The value of V_c depends upon the geographical locality, but Z_c is a function of terrain. Values of Z_c and the exponent "a" suggested by Davenport [19] are as follows:

-For open terrain with very few obstacles   : a=0.16, Z_c = 300 meters.

-For terrain uniformly covered with obstacles 10-15 m height: a =0.28, Z_c =430 meters.

-For terrain with large and irregular objects   : a =0.40, Z_c =560 meters.

However, in the present study the uniform velocity of wind is considered for the experimental investigation. Since the study is limited to the tall buildings only, this assumption will be very reasonable.

1.2.2 Generation of Wind

The source of wind energy is the sun that emits solar radiation, which causes differential heating of the earth surface and the atmosphere. In the atmosphere there is a general convective transport of heat from lower to higher latitudes in order to make the earth's radiation imbalance [34]. It is for this reason that the atmosphere is a restless medium in which circulation of all sizes is normal.

Wind is simply air moving in a direction that is essentially parallel with the earth's surface. The atmosphere is fixed to the solid-liquid earth in gravitational equilibrium and so moves with the earth in its west to east rotational movement. Wind, therefore is air movement in addition to that associated with rotation. In large-scale circulation covering several thousand miles, horizontal motion greatly exceeds vertical motion. Thus, a wind that takes several days to cross an ocean may move up or down only a few miles. The vertical component of movement is much greater in small-scale circulation such as thunderstorms and tornadoes. In a thunderstorm, air may ascend to the top of the atmosphere in about an hour.

Wind is complex in origin. Usually its direct cause lies in differences between

3

atmospheric densities resulting in horizontal differences in air pressure. That is, it represents natures attempt to rectify pressure inequalities. When these horizontal pressure differences develop, a gradient of pressures exists. But in spite of the direct part played by pressure differences, the ultimate source of average for generating and maintaining winds against the drag is mainly from the differences in heating and cooling between high and low latitudes.

1.2.3 Forces Governing Winds

Four forces operate to determine the speed and direction of winds: (i) pressure gradient force, (ii) Coriolis force, (iii) Frictional force, (iv) Centrifugal force.

i) Pressure Gradient Force

This sets the air in motion and causes it to move with increasing speed along the gradient. The magnitude of the force is inversely proportional to the isobar spacing. Since the gradient slopes downward from high to low pressure, direction of airflow is from high to low pressure along the pressure gradient. But due to the rotation of the earth, the trajectory of an air particle moving from high to low pressure is very indirect, except close to the equator.

ii) Coriolis Force

This is the deflecting force of the earth's rotation that affects only the direction of wind. Except at the equator, winds and all other moving objects, no matter what their direction, are deflected to the right of the gradient in the Northern Hemisphere and to the left in the Southern Hemisphere. The force acts at right angles to the direction of motion. Coriolis force is stronger in higher latitudes. When pressure gradient is balanced by the coriolis force, wind blows parallel with the isobars and it is called geotropic wind. The geotropic wind V_c can be estimated from the expression as suggested by Davenport [19].

$$V_c = (dp/dn) (2\rho\omega.sinx) \dots\dots\dots\dots\dots\dots\dots\dots\dots\dots\dots\dots\dots\dots (2)$$

Where, dp/dn is the pressure gradient, ω is the angular velocity of the earth, x is the latitude and ρ is the air density.

Outside the atmospheres friction layer may be extended up to 1000 meter above the earth's surface. Winds actually do blow in a direction almost parallel with the isobars with low pressure on the left and high pressure on the right in the Northern Hemisphere.

iii) Frictional Force

This affects both wind speed and direction. Friction between the moving air and the earth's land-sea surface tends to slow the air's movement. Because of the frictional effects of the land-sea surface upon air flowing over it, surface air does not flow essentially parallel with the isobars as it does aloft, but instead crosses them at an oblique angle. The greater the friction, the wider is the angle the wind direction makes with the isobars. Winds over irregular land surfaces usually form angles varying from 20^0 to 45^0 with the isobars. But over oceans, the angle may be as little as 10^0.

iv) Centrifugal Force

This force comes into the picture only when air moves in a curved path. Centrifugal force is a major factor only when the wind is strong and the radius of curvature small as they are in tropical hurricanes, tornadoes and the centers of a few usually well-developed cyclonic storms. The flow of air which is necessary to balance pressure force, coriolis force and centrifugal force in absence of frictional force is called gradient wind. This happens at heights greater than 500 meters or so.

1.2.4 Wind Loading on Structures

The development of modem materials and construction techniques has resulted in the emergence of a new generation of structures. Such structures exhibit an increased susceptibility to the action of wind. Accordingly, it has become necessary to develop tools enabling the designer to estimate wind effects with a higher degree of refinement than has previously required. It is the task of the engineer to ensure that the performance of structures subjected to the action of wind will be adequate during their anticipated life from the standpoint of both structural safety and serviceability. To achieve this end, the designer needs information regarding (i) the wind environment, (ii) the relation between that environment and the forces it induces on the structures, (iii) the behavior of the structure under the action of the forces.

The action of wind on building considering the load effect may be classified into two major groups; the static effect and the dynamic effect. There are many other effects like generation of noise, the risk of the hazard, the penetration of rain, uncomfortable wind for the pedestrians etc. But they are not usually considered for structural design. Since all wind loading are time-dependent because of varying speeds and direction of winds, winds loading are never steady. Static load is referred to as the steady (time-variant) forces and pressure tending to give the structure a steady displacement. On the other hand, dynamic effect has the tendency to set the structure in oscillation. A steady wind load on a building is very difficult to achieve. In fact always wind loads are of a fluctuating nature because of varying speeds and directions of winds. The type of wind and stiffness and roughness of the structure determine the nature of loading on a building. When a building is very stiff the dynamic response of the structure may be neglected and only the static leads may be considered. This is because the natural frequency of an extremely stiff building is too high to be excited by wind. In the present study the effect of static loading is taken into account due to steady wind. Since natural winds are continually fluctuating it is generally assumed that these fluctuations are so irregular and random that the response of a structure will not differ from that due to a steady wind of the same average speed. Very recently the dynamic response of building has been considered for study because of the modern tendency to build more slender and lighter structures.

1.3   Importance of the Study

Housing and mankind is the basic primary need next to food and clothing; clear air and portable water being very essential for existence. In Bangladesh strong wind is an annual natural hazard due to its geographical location. On the other hand, most of the existing house and those which are going to be built in the next few decades are likely to be non-engineered, mostly with thatched roofs and are vulnerable to wind [57]. Strong wind is causing immense loses of rural dwellers by making their houses collapse fully or partially by lifting of roof etc [4]. Almost 70% of the population in the rural sector and 50% of the population in the urban sector are living below the poverty line with earnings too little to pay for all needs [14]. It is this group of people most impoverished that is to be provided

6

with good housing. According to the recent ADB report [16] (Lewis and Chisholm), 1999, 82% of the dwellings are in rural areas. About 75% of the dwelling in rural areas is of kutcha construction (Mud, Bamboo, Woven Bamboo etc.) and that 23% of urban and more than 40% of rural dwellings are of a temporary nature. They can rarely survive against even a moderate intensified storm. Evidence from the field in strong wind-prone areas indicates that there is a socially perceived need of more engineering knowledge and improved construction of domestic dwelling [5].

The first International Conference [21] on wind effect was held in 1963 at Teddington, UK where an International Study group was established from research workers, consultants and designers. Subsequent conferences had been held at four yearly intervals in Ottawa 1967 [24], Tokyo 1971 [59], London 1975 [10], and Colorado, USA 1979 so on. The conference proceedings contained results of extensive research works on 'Wind Effect on Buildings and Structures'- which hitherto had been the internationally agreed title of the subject. The European title had been Industrial Aerodynamics and in North America, the term Wind Engineering had been used in the same context. At the fourth International Conference [1975], it was agreed to adopt the title 'Wind Engineering for All Future Activities'.

The most serious direct effect the wind can have upon a man is to blow him over. That can cause injury and sometimes death. Two old ladies in the UK died in 1972 after being blown over by wind close to tall buildings. This kind of inconveniences was only realized after the construction of buildings that were allowed to be built by default. Very recently destructive wind tunnel testing has been conducted in Australia [1, 2] to comply with regulatory requirements of Australian Buildings.

Now-a-days the effect of wind regarding both wind loading and environmental problem is considered as one of the important design criterion in order to design a tall building in a free standing condition and as a part of a group of buildings. In Bangladesh urban environmental problems due to buildings is not yet recorded. However, the cities are rapidly growing with emphasis given to the construction of multistoried buildings to cope with the urban population pressure. The need to build in more windy sites or the need to

locate a number of tall buildings close together will undoubtedly create problems not yet encountered by architects and town planners of Bangladesh.

The knowledge of wind loading on a single tall building or on a group of tall buildings is essential for sound planning and design. For designing groups of tall building, knowledge of the effect of wind loading on a group of tall buildings is essential because the interference of the neighboring buildings on a simple tall building makes the nature of wind loading different from that on a free standing building.

One approach to the problem of predicting the flow around buildings in close proximity is to develop an understanding of the nature of flows on relatively simple arrangement of bodies by Wind Tunnel experiments [53]. With these ends in view, the present investigation of pressure distributions about square or rectangular cylinders with rounded facet with varying side ratios has been carried out. Square or rectangular cylinders with rounded facet ideally may represent the shape of same tall buildings. So, a study on groups of square or rectangular cylinders with rounded corners arranged simply in the staggered form, which would be helpful in the analysis of wind effects on same groups of buildings. This type of study may provide the engineers and architect sufficient information in choosing the shape of the tall buildings either in a freestanding condition or in a group.

Apart from wind loading problems, construction of high rise building can produce local environmental problems like unpleasant wind conditions near ground level (e.g. blowing dust off the ground), too high wind load on people, too high speeds in streets and passengers or stagnation of air in certain areas causing air pollution. Though the problem regarding the wind loading on buildings and structures is common to all parts of the world and it is expected that the solution will not be significantly different from country to country, yet research work should be carried out in this field considering the climatic conditions and problems of this country, so that a clear picture about the nature of wind loading can be obtained applicable to our country. After all, engineers, architects and planners want to provide safe and comfortable conditions in open air pedestrian areas, and therefore need knowledge of wind flow around rectangular rounded buildings and

how to control it by good design.

1.4 Why model Study

Differences between wind tunnel and full-scale result can occur due to Reynolds number inequality, incorrect simulation of the atmospheric boundary layer and small-scale difference between wind tunnel and prototype model. In most wind tunnel tests the full scale Reynolds number rarely be achieved [44]. Boundary layer separation depends on Reynolds number. For sharp edged structures, separation point does not depend on Reynolds number. On the other hand the flow field around curved surfaces is very much Reynolds number dependent, so tests on these configurations must be treated with care. The crosswind scales in wind tunnels are often less than reality. This can cause underestimation of cross wind effects. The scale difference between wind tunnel model and prototype is found in the high frequency fluctuation. High peaks found on the cladding in full-scale are not found in the wind tunnel. Those effects may be caused by structural details that are not simulated in the wind tunnel model.

After all, full-scale experiments are both costly and difficult to perform [62]. For the present study with staggered buildings full-scale experiments will not only be complex and costly but it would be difficult to record reliable pressure distributions simultaneously on the groups of buildings as there will be variation of speed and direction of wind with time. The flow around buildings in actual environment is very complex and formulation of a mathematical model to predict the flow is difficult. Thus model study is a must and the results obtained under simulated condition in the laboratory are considered to be quite satisfactory for practical purposes.

1.5 Aim of the Study

The aims of the study are as follows:
i.   To measure the static pressure distribution around a single square cylinder with rounded facet at different angles of attack.
ii.   To measure the pressure distribution around square cylinder with rounded facets at different facet widths.

9

iii. To measure the pressure distribution around staggered square cylinders with rounded facets at zero angle of attack.

iv. To observe the effects of different longitudinal spacing between the cylinders.

v. To determine the wind load from the static pressure distributions.

vi. To make comparisons of wind loads with various square cylinders having rounded facets.

It is expected that the wind load on the square or rectangular cylinders with rounded facets will decrease appreciably compared to those with sharp edge. The results will enable the engineers and architects to design building more efficiently. Since the results will be expressed in the non-dimensional form; they will be applicable to the prototype building as well.

1.6   Scope of Thesis

In this section a brief description of the various themes which have been presented in the different chapters has been taken into account.

In chapter 1, The wind characteristics and its effects has been described in short. The importance of the study has been discussed in the chapter. The aim of the study has also been incorporated in a nutshell.

The review of the various previous research works has been provided **in Chapter 2.** The works, which are either directly related or a little inline with the present study has been summarized in this chapter.

The experimental set-up and the measuring equipment have been provided in **Chapter 3.** The different forms of the cylinders are presented in this chapter, which are considered for the experiment.

In Chapter 4, The mathematical model in order to calculate the pressure coefficient, drag coefficient has been described in a nutshell. The procedure of finding the coefficients numerically from the experimental static pressure distribution values has been discussed.

10

The Chapter 5 includes the most vital part of the thesis. In this chapter the results has been discussed in the most systematic way. The pressure distributions around the cylinders and the drag developed on the cylinders have been discussed elaborately.

Finally in Chapter 6, the conclusions from the results of the experimental investigation are given. Some recommendations are also provided for the future researchers.

CHAPTER - 2

REVIEW OF LITERATURE

During the last half century much attention has been paid to the study of the wind loading. The occurrences of certain disastrous collapse of suspension bridges and damage to buildings and structures should not be encountered as minor criteria for design purposes. Till now extensive research work has been carried out on isolated bluff bodies. But interference with each other is a very recent endeavor. Very little information is available concerning the flow over staggered cylinders with rounded facets, although this is a problem of practical significance. The present work would be contributed towards the knowledge of wind actions on groups of tall buildings and structures. A brief description of some of the papers related to the present state of the problem is cited here.

Nakamura and Matskawa [45] experimentally investigated the vortex excitation of rectangular cylinders with a long side normal to the flow in a mode of lateral translation using free and oscillation methods.

Hua C K [23] performed measurements of fluctuating lift and the oscillating amplitudes on a square cylinder in a wind tunnel test.

Okajima [48] conducted experiments in a wind tunnel and in a water tank on the vortex shading frequencies of various rectangular cylinders.

Baines W D [6] described in his paper the effects of velocity distribution on wind loads and flow patterns around buildings. He has measured pressure distributions on models of walls and rectangular block structures in a wind tunnel. Tall buildings with square sections have also been included in his study. The tests were conducted both in an artificially produced velocity gradient used to simulate natural conditions, and in a constant velocity field for comparison with standard procedures.

Matsumoto M [41] has conducted an investigation on the aerodynamic forces acting on an oscillating square prism in a steady flow both experimentally and theoretically. First, a

few experiments are performed in order to examine the aerodynamic forces, in the direction of the wind stream and in a plane normal to it, acting on an oscillating square prism. Karmon's theory about a thin plate is extended to the case of a square prism and the aerodynamic forces in a plane of the direction of the wind stream are obtained, which have to correlate with the experimental results fairly well.

Parkinson G V and Modi V J [49] describe in their paper about the characteristics of the separated flow over two-dimensional bluff bodies that relate to two forms of the aeroelastic instability of the bodies, vortex-excited and galloping transverse oscillation. Bodies investigated included cylinders of square, rectangular, circular, and elliptical.

Hussain H S and Islam O [24] measured co-efficient of pressure and co-efficient of lift on circular, parabolic and elliptic shell roof in a uniform velocity. The investigation was performed in a small wind tunnel with Reynolds number varying between 1.7 to 3, 50,000 based on model width. The scale of the model was quite high (1:40). The variation of the Reynolds number was obtained by varying the velocity only. As the experiment was carried out in a uniform velocity, the estimated results were higher than it would be in reality.

Keffer [31] investigated the wake produced by the two-dimensional cylinder of diameters 12.7 mm, 7.93 mm and 4.76 mm with straining the flow. The tunnel speed was held constant at 5.48 m/s so that the corresponding Reynolds number based on cylinder diameters were 4630, 2890 and 1740 for cylinder diameters of 12.7 mm, 7.93 mm and 4.76 mm respectively. The mean quantities were measured with a pitot-static tube. Experimentally he found that the wake width increased with distance along the downstream. The mean velocity distribution of the wake profile was in no way self-preserving.

Gartshore [22] investigated the two-dimensional wake of a square (6.35 mm) rod at adverse pressure gradients and at the pressure gradient for exact self-preservation. The velocity ratio was maintained approximately constant and the flow through wake having Reynolds numbers 6300 and 7300 were based on the conditions at the trailing edge.

Pearistein A J and Mantle W J [50] investigated that at low Reynolds numbers (R_e), the

13

flow past axisymmetric and attached. For bluff bodies (e.g. spheres, mindrops and torpedoes) the flow separates as R_e increases ultimately transition to unsteady axsymmetric flow becomes unstable with respect to an oscillatory helical instability at R_e 175.1. The critical R_c and predicted Strouhal number (dimensionless frequency) agree well with previous experiments. We are extending this work to the case where the body falls or rises freely under the action of gravity. In that case, the rigid body motion can couple to the flow disturbances, leading to a lower critical R_c.

Pearlstein A J, Petteni F and Wang L [51] conducted computational investigations of the stability of the steady (asymmetric) 2-D flow past a rotating cylinder, as well as the time periodic 2-D flow to which it loses its stability as the Reynolds number (R_c) is increased. To date, they have shown that the critical R_c at which the steady flow becomes unstable to 2-D disturbances depends nonmonotically on the dimensionless rotation rate, and that the frequency of the critical mode that evolves from the Hopf bifurcation has several discontinuities along the stability boundary, corresponding to transitions from one mode to another.

Peris R [52] in his paper describes many items, one of that is the investigation of galloping oscillation on square cylinders.

Bearman P W and Trueman D M [8] investigated the base pressure co-efficient, drag co-efficient and Strouhal number of rectangular cylinders with one face normal to the flow direction. They found that when D/H $\approx$ 0.62, when D is section depth and H is section width normal to the wind direction, the drag co-efficient was maximum (about 2.94). By introducing a splitter plate into the wake region they found that the increased drag effect was completely eliminated. This finding demonstrated that the high drag was associated with the regular shedding of vortices. They also showed that the further the vortices could be persuaded to form away from the body, the higher the base pressure. They suggested that for higher values of D/H (>0.6) the vortices were forced to form further downstream because of the influence of the trailing edge corners.

Yasuhara, Nakamura and Yujiohya [47] attempted to study vortex shedding from square prisms placed to smooth and turbulent approaching flows. They make flow visualization and measured the velocity and pressure for the flow past prisms of variable length with

14

square section. They found that square prisms shed vortices in one of the two-fixed wake planes, which were parallel with the plate sides. The plane of shedding was switched irregularly from one to the other. They further showed that the vortex shedding from a square prism with D/H = 0.5 and a cube was similar, while for a square prism with D/H - 2.0, no such vortex shedding was observed.

Davis R W and Moore E F [20] carried out a numerical study of vortex, shedding from rectangular cylinders. They attempted to present numerical solutions for two-dimensional time dependent flow about rectangles in infinite domains. They investigated the initiation and subsequent development of the vortex shedding phenomena for Reynolds number varying from 100 to 2800. They found that the properties of these vortices were strongly dependent on the Reynolds number. Lift, drag and Strouhal number were also found to be influenced by Reynolds number. The computer simulation described in the paper was carried out on a UNIVAC 1108.

Lee B E [36] made an elaborate study of the effect of turbulence on the surface pressure field of a square prism. He presented measurements of the mean and fluctuating pressures on a square cylinder placed in a two-dimensional uniform and turbulent flow. It was observed that the addition of turbulence to the flow raised the base pressure and reduced the drag of the cylinder. He suggested that this phenomenon was attributable to the manner in which the increased turbulence intensity thickened the shear layers, which caused them to be deflected by the downstream corners of the body and resulted in the downstream movement of the vortex formation region. The strength of the vortex shedding was shown to be reduced as the intensity of the incident turbulence was increased. Measurement of drag at various angle of attacks (0^0 to 45^0) showed that with increase in turbulence level the minimum drag occurred at smaller values of angle of attack.

Roberson J A, Crowe C L and Tseng R [55] measured pressure distribution on rectangular rods placed in a cross flow with the rods oriented at small angle of attack with respect to the direction. The Reynolds number based on the minimum dimension of the rod was 40000 and the turbulence intensity of the cross flow ranged between 1% and 10%. They concluded that the free stream turbulence had a significant effect on the

pressure distribution about bodies of rectangular cross-section. With small angle of attack these bodies had a significantly lower pressure on their windward side wall than did the same bodies with zero angle of attack. To study the pressure distribution on bodies that more nearly represent building configurations, tests were made on bodies of square cross section placed on the floor of the wind tunnel. It was found that decreasing relative height of the body had an attenuating effect on the negative pressure on the windward side wall and it also increased the critical angle of attack.

Roberson J A, Chi Y L, Rutherford G S and Stine M D [54] carried out experiments on circular cylinders, spool shaped bodies, cup-shaped bodies, square rods and rectangular rods to observe the effect of turbulence on the drag of these bodies. For square rods with their axes parallel to the flow direction it was found the C_d decreased approximately 25% when the turbulence intensity increased from 1% to 10%. Two rectangular rods used; one had a square cross section and the other had a length (in the free stream direction) to breadth ratio of two. The drag was measured with the axes of the rectangular rods oriented normal to the free stream direction. It was noted that on the sides of the square rod the pressure change with a change in turbulence intensity was about the same as for the face: while for the rectangular rod, the change in pressure on the sides was large, and it was small on the rear face. They concluded that bodies, which have shapes such that reattachment of the flow is not a factor, experience an increase in C_d with the increased turbulence intensity. On the other hand bodies for which reattachment or near reattachment of flow occur with increased turbulence may experience either a decrease or increase in C_d with increased turbulence intensity depending upon the shape of the body.

Barriga A R, Crowe C T and Roberson J A [7] studied the effects of angle of attack, turbulence intensity and scale on the pressure distribution of a single square cylinder placed in a turbulent cross flow. They found that when the square cylinder was positioned in a cross flow with one face normal to the flow direction, only drag force was produced, but in the same flow a negative lift force was developed at small positive angle of attack, the magnitude of which dependent on the turbulence characteristics of the cross flow. It was suggested that the negative lateral force on the square cylinder oriented at a small positive angle of attack was due to the relatively large negative pressure co-efficient in the separated zone on the windward side wall. It was also concluded that the effect of

16

turbulence intensity was to decrease the pressure near the front corner of the windward side wall and promote flow reattachment near the rear, giving rise to a very significant increase in aerodynamic moment.

Nakamura Y and Ohya Y [46] studied the effects of turbulence on the mean flow past square rods. Measurements were made on square rods with different lengths with their square face normal to the flow to investigate the effects of turbulence intensity and scale on the mean flow characteristics. The turbulence intensity varied from 3.5% to 13% and the length to size ratio of d/h for the rods ranged from 0.1 to 2.0 where, d was the length of the rod. It was found out that there were two main effects of turbulence on the mean flow past a three-dimensional sharp edged bluff body. Small-scale turbulence increased the growth rate of the shear layer, while large-scale turbulence enhanced the roll up of the shear layer. The consequences of these demands depend on the shape of the bluff body. For a square plate, both small and large-scale turbulence reduced the size of the base cavity. As the length of the square rod was increased beyond the critical (0.6 times the heights), the shear-layer-edge direct interaction controlled the near wake eventually leading to flow reattachment. The effect of small scale turbulence was to promote the shear layer direct interaction.

Vickery B J [61] presented in his paper the results of the measurements of fluctuating lift and drag on a long square cylinder. He attempted to establish a correlation of lift along the cylinder and the distribution of fluctuating pressure on a cross section. It was found that the magnitude of the fluctuating lift was considerably greater than that for a circular cross section and the span wise correlation much stronger. It was also reported that the presence of large-scale turbulence in the stream had a remarkable influence on both the steady and the fluctuating forces. At small angle of attack (less than 100) turbulence caused a reduction in base suction and a decrease in fluctuating lift of about 50%.

Bostock B R and Mair W A [11] studied the pressure distributions and forces on rectangular and D-shaped cylinders placed in two-dimensional flow with a Reynolds number of 190000. It was found that for rectangular cylinders a maximum drag co-efficient was obtained when the height D (normal to the stream) of the section was about 1.5 times the width H. Reattachments on the sides of the cylinders occurred only for D/H

less than 0.35.

Sakamoto H and Arie M [58] collected experimental data on the vortex shedding frequency behind a vertical rectangular prism and a vertical circular cylinder attached to a plane wall and immersed in a turbulent boundary layer. They tried to investigate the effects of the aspect ratio (height / width) of these bodies and the boundary layer characteristics on the vortex shedding frequency. Measurements revealed that two types of vortex were formed behind the body, depending on the aspect ratio; they were the arch-type vortex and the Karman-type vortex. The arch-type vortex appeared at an aspect ratio less than 2.0 and 2.5 for rectangular and circular cylinders respectively. The Karman-type vortex appeared for the aspect ratio greater than the above values. The whole experiment was conducted at a turbulence level of 0.2% and free stream velocity of 20 m/s. The aspect ratio was varied from 0.5 to 8.0.

Castro I P and Robins A G [13] describe in their paper the flow around surface mounted cubes in uniform, irrotational and sheared, turbulent flows. The shear flow was simulated atmospheric boundary layers with a height ten times the body dimension. They presented measurements of body surface pressures and mean and fluctuating velocities within the wake region. These measurements reflected the effects of upstream turbulence and shear on the wake flow. It was found that in the reversed flow region directly behind the body the addition of upstream turbulence and shear considerably reduced the size of the cavity zone. Unlike the case of uniform flow the separating shear layers reattached to the body surface. Measurements for a variety of cube size boundary layer height ratios further revealed that reattachment occurred even for cube heights larger than the boundary layer height. They found that in the case of uniform flow approaching the cube at 45 degrees, the near wake and pressure fields were dominated by strong vortex shed from the top edges of the body.

Mandal A C [38] performed the study on the staggered square cylinders. The test was conducted in an open circuit wind tunnel at a Reynolds number of 27800 based on the side dimension of the square model. The maximum blockage area was 6.96 percent. Three cylinders were arranged in the staggered form (one in upstream and two in downstream flow) varying the longitudinal and transverse spacing and measurements of

pressure coefficients were taken for the upstream and downstream cylinders. Experiments were also carried out for drag coefficients, lift coefficients, total force coefficients and moment coefficients. After all, it is concluded from the results that wind loading on a building is generally less severe when the building forms part of a group than when it is free-standing.

Lanoville A, Gartshore I S and Parkinson G V [34] explained in their paper some effects of turbulence on bluff bodies. The bluff bodies included square and rectangular prisms.

Leutheusser J [37] made wind tunnel tests on scale models of typical building configurations. The experiment was conducted on four models each with different height and cross section. He found out the static wind loading on each of the buildings in freestanding condition and as a member of a group of building. He concluded that the wind loading of a building was less severe when it formed a part of a group than when it was free standing.

Koeing K and Roshiko A [32] described in their paper an experimental investigation of the shielding effects of various disks placed co-axially upstream of an axisymmetric flat faced cylinder. For certain combinations of the diameter and gap ratios they observed a considerable decrease in the drag of such a system. By flow visualization technique they showed that for such optimum shielding the upstream surface, which separated from the disk reattached smoothly onto the front edge on the downstream cylinder.

Islam T [27] conducted experiments on the wind effect on the rectangular cylinders. The rectangular cylinders had side ratios of H/D= 1.25, 1.5, 1.75 and 2.0 where D is section width normal to flow direction and H is section depth along the flow direction. The flow had a turbulence intensity of 0.33% and a constant free stream velocity of 18.3 m/s was used for the purpose. He measured mean pressure distributions around each of the cylinders for different angles of attack. He found that the form drag on the rectangular cylinder with its axis normal to the approaching flow increased with rise of the value of side ratio up to about 0.6 then decreased with the further increase in the side ratio. It was also observed that the drag on an isolated cylinder was higher in general than that on the same cylinder while it becomes part of a group. The rectangular cylinder with the highest

side ratio experienced minimum drag for all conditions of spacing.

Bearman P W and Wadcock A J [8] presented in their paper how the flows around two circular cylinders, displaced in a plane normal to the free stream, interact as the two bodies are brought close together. Surface pressure measurements at a Reynolds number of 25000 based on the diameter (d) of a single cylinder, showed the presence of a mean repulsive force between the cylinders. At gaps between 0.1d and 1d a marked asymmetry in the flow was observed with the two cylinders experiencing different drags and base pressures. The base pressure was found to change from one steady value to another or simply fluctuate between the two extremes. They also showed how mutual interference influenced the formation of vortex streets from the two cylinders.

Besides these models scale and full-scale measurements of the wind loads on buildings have been performed by different authors as mentioned in the references [15], [17], [18] and [60].

CHAPTER-3

EXPERIMENTAL SET-UP

The investigation of wind load on the square cylinders with rounded facet has been performed with the help of a subsonic open circuit Wind Tunnel. Five sets of square cylinders with rounded facet have been taken into consideration in the investigation. An inclined multi-manometer is used to measure the static pressure distribution around the cylinders placed normal to the approaching uniform flow. This chapter also provides with a brief idea about the wind tunnel and its proper utilization.

3.1 Measurement of Wind Characteristics

In the early days of aeronautics the characteristics of aerofoils, the drag of bodies and later the stability of aircraft configurations were required. The simplifications introduced by measuring forces, moments and stability on a stationary body past which wind was blown, rather than by trying to measure these quantities as the body moved through still air were released. Stanton at the National Physical Laboratory in UK built one of the first wind tunnels in 1903 and the Wright Brothers used wind tunnel results consistently.

Over the years wind tunnel design was improved and wind tunnels become more sophisticated. Their use was applied almost exclusively to aeronautical problems and the air streams became smoother with smaller velocity profiles or distortions and the levels of turbulence were reduced to confirm with the smooth flow [26].

When wind loads were first considered, a few investigations were conducted in aeronautical wind tunnels and the results were found to bear little relation to the scanty full-scale measurements available and the use of wind tunnels were filled with work on aircraft and little effort was available for a study to try to understand the causes of the differences [3]. One exception was a study by Franks in Denmark. The volume of aeronautical work in low-speed wind tunnels decreased at the end of the 1950s and in the 1960s several wind tunnel technologists turned their full-time attention to the earlier discrepancies. Davenport set up the boundary layer wind tunnel

at the University of Western Ontario, Canada. Baines [6] presented a notable paper in which he explained the part played by the shear in the wind on the flow over the front face of a bluff body, while Davenport discussed the importance of turbulence.

After all, wind is a random natural phenomenon. It can only be understood by detailed laborious measurements. Many measurement techniques in wind engineering are available. The meteorologists have been measuring the wind velocity and direction for many years. In building aerodynamics there are measurement techniques for pressure on buildings, and also on a small scale in wind tunnels. The instrumentation on these techniques is steel being improved with the developments of electronics. On the other hand, many comparisons in the study of the wind environment have been made and the criteria established in their forms mirror the full-scale measurements made. Melbourne [43] compares the criteria of different workers and mentions the various technologies used. Several straight comparisons between wind tunnel and full-scale measurements have been made, for example the measurements made in the Commerce Court Plaza [28]. The measurements can be divided into full scale and wind tunnel scale. A survey of possible measuring equipment is shown in the following Table-3.1.

Table-3.1: A List of Different Measuring Equipment

Parameter	Full Scale	Wind Tunnel Scale
Wind Velocity	Cup or propeller type, anemometer, Pitot tube	Pitot tube, Hot wire Anemometer.
Wind Direction	Vane	Vane, Wool thread
Static Pressure	Static holes, Barometer	Static holes
Pressure on structure	Pressure transducers, membranes, and Strain gauge based equipment.	Membranes, Water tubes, Capacitor microphones
Force	Pressure Vessel, Strain Gauge, Inductive strain measurement equipment.	Strain gauge, Aerodynamic balance.
Movements	Deflection measuring equipment, Accelerometers.	Accelerometers.

Most of the apparatus mentioned above transform the required quantity into an electric current that can be recorded and transformed into the desired data. The electrical information can be collected by a digital computer system and transformed into the required statistical data. However, in the present investigation, wind velocity was measured with help of a digital Anemometer and by the help of an inclined manometer using water in the manometric liquid measured the static pressure distribution.

3.2 Types of Wind Tunnel

Knowledge of the types of wind tunnel might be helpful when talking to wind tunnel aerodynamicists [40]. All wind tunnels used in the study of industrial aerodynamics are "low speed wind tunnel" whose top wind speed will probably be less than 30 m/s although most investigations are carried out at much lower wind speeds.

Two types of wind tunnel (i) Straight through or open return type is a simpler form of wind tunnel which has an inlet, contraction, working section, fan, diffuser and outlet. Open return types are usually better control but higher running costs. It has a definite advantage when studying dynamic models, (ii) Closed return type or return type wind tunnel has continuous return. These types of wind tunnels have solid walls for their working sections. The side walls of the working section have boundary layers [31] which exercise a small effect on the flow in the main part of the working section and allowance for this presence is made by the use of blockage corrections.

3.3 Specification of the Wind Tunnel

The schematic diagram of the experimental set-up of the present investigation has been shown in Figure 3.1. The cylinders were positioned at the exit end of the wind tunnel in the downstream. Open circuit subsonic type wind tunnel is used to develop the required flow. The tunnel is 5.93 meter long with a test section of 460 mm x 460 mm cross-section. In order to smoothen the flow a honeycomb is fixed near the end of the wind tunnel. There is a converging bell mouth shaped entry. To generate the wind velocity, two axial flow fans are used. Each of the fans is connected with the motor of 2.25 kilowatt and 2900 rpm. There is a butterfly valve to control the wind speed. There is a silencer just after the butterfly valve as shown in the figure.

The central longitudinal axis of the wind tunnel is maintained at a constant height of 990 mm from the floor. The axis of the model coincides with that of the wind tunnel. The converging mouth entry is incorporated in the wind tunnel for smooth entry of air into the tunnel and to maintain uniform flow into the duct free from outside disturbances. The induced flow through the wind tunnel is produced by a two-stage rotating axial flow fan of capacity 18.16 m^3/s at the head of 152.4 mm of water and 1475 rpm.

A butterfly valve, actuated by a screw thread mechanism, is placed behind the fan and used to control the flow. A silencer is fitted at the end of the flow controlling section in order to reduce the noise of the system. This section is incorporated with a honeycomb. The diverging and converging section of the wind tunnel is 1550 mm long and made of 16 SWG black sheets. The angle of divergence and convergence is 7, which has been done with a view to minimizing expansion and contraction loss and reducing the possibility of flow separation.

In each case of the tests, wind velocity is measured directly with the help of a digital anemometer. The flow velocity in the test section is maintained at 14.2 m/s approximately. The measured velocity distribution is uniform almost throughout in the upstream side of the models in the tunnel test section.

3.4 Test Section:

The test is done at the exit end of the wind tunnel (Figure 3.1) in the open air. In order to fix the cylinder a steel frame is manufactured, the top floor of which is at the same level of the wind tunnel at the exit end. Two side walls are attached to the steel frame at the two sides by the help of nut and bolt, so that the distance between them is equal to the distance of the side walls of the wind tunnel exit end. This distance is 460 mm. The top of the test section is kept open and at the bottom no cover plate is used. The cylinders are attached to the side walls. The side walls are made of plywood. In one side wall the cylinder is fastened by the help of nut and bolt. The bolt is fixed with one end of the cylinder. Through the other end of the cylinder, the plastic tubes are taken out in order to connect them with the inclined manometer. This end is supported in the groove of the side wall of the test section, which is compatible with the square end of the cylinder. The cylinder is so positioned and fastened so that the flow

24

direction remains parallel to its sides and the face A remains perpendicular to the flow direction.

To test in a group, for fixing the two cylinders one at the upstream and the other at the downstream along the free stream direction, compatible grooves are made on the side walls of the test section. The inter-space between the two cylinders is varied at 1D, 2D, 4D, 6D and 8D. With a view to achieving this, several groups are made on the side walls of the test section. When the test is conducted the unnecessary grooves are closed. The cylinders are fixed at one end by the help of bolt and nut and the other end is kept fixed in groove, which in attached with the square cylinder. Through the groove as in the single cylinder the plastic tubes are taken out. They are connected to the inclined manometer. During fixing the cylinders, it is carefully checked whether the sides of the cylinders remain parallel to the free stream velocity direction and the downstream cylinder is just behind the upstream cylinder. Leveling of the testing cylinder is always checked and balanced by a standard spirit level.

3.5 Constructional Details of Cylinder

For the experimental investigation ten (five pairs) wooden square cylinders are constructed. Of them the two (one pair) are made with side dimensions of 60 mm × 60 mm (D = 60 mm, H = 60 mm). The rest eight cylinders (four pairs) are made with side dimensions of 60 mm × 60 mm (D = 60 mm and H = 60 mm) having the rounded facets of different widths. The various sections of the square cylinder and that with rounded facet are shown in Figure 3.2. The widths at the mid-point of the rounded facet (one pair) are considered as h = D/2 = 30 mm, h = 3D/8 = 22.50 mm, h = D/4 = 15 mm and h = D/8 = 7.50 mm, where D is the side dimension of the cylinder. The respective diameters of the rounded facets (one pair) are 1.000D = 60 mm, 1.042D = 62.50 mm, 1.250D = 75 mm and 2.125D = 127.50 mm. The square cylinder with flat facet of diameter is infinity.

Section view of a specimen square cylinder is shown in Figure 3.3. About one third of the cylinder is kept solid while the rest two-third is made hollow. A bolt is welded to a steel plate, which is attached with the solid end of the square cylinder by the help of screw. The plastic tubes, which are connected with the pressure tapings, are allowed to pass through the hollow end of the cylinder. They are finally connected with the

inclined manometer.

Taping points on the plane and curved surface are shown in Figure 3.4 and 3.5. To measure pressure distribution tapings are made on adjacent sides of the cylinder as shown in the Figure. Six pressure tapings are made on each side of the cylinder. It was not possible to accommodate all the tapings along the direction perpendicular to the axis of the cylinder because of space limitation. Since the side dimension of the cylinder is 60 mm, the centre to centre distance between the consecutive tapings is made 10 mm. Each corner tapping is located at a distance of 5 mm from the near edge of the cylinder. The cylinders are made of seasoned teak wood in order to avoid buckling, expansion and contraction due to change of temperature and humidity.

To make the pressure tapings, first 1.70 mm holes are made on each surface of the cylinder, and then approximately 10 mm length copper tubes of 1.71 mm outside diameter were press fitted to the above holes from inside, keeping the upper surface smooth as far as possible. The entire outer surface of the cylinder is made polished very carefully to avoid any error in measurements due to surface irregularities. From the end of the copper tube flexible plastic tube of 1.70 mm inner diameter was press fitted. Water is used as the manometric liquid.

3.6 Experimental Procedure

The experiment is conducted in two phases. In the first phase, measurements of pressure distribution on single cylinder and single cylinder with rounded facet are taken. Pressure distributions on the cylinders are recorded for angles of attack varying from 0^0 to 90^0 in 10^0 steps. In the second phase, either two square cylinders or two square cylinders with rounded facet of identical dimension are mounted horizontally in the group form. One cylinder is placed centrally in the upstream side and the other cylinder is placed symmetrically in the downstream side with respect to tunnel axis. Pressure distributions around the cylinders are measured for various longitudinal spacing of the cylinders. The flow velocity in the test section is kept constant at 13.6 m/s. The Reynolds number based on the side dimension of D = 60 mm is 5.4 $\times 10^4$. The turbulence intensity of the flow is very small, hence the flow is considered as the smooth flow.

In the experiment, before measuring the pressure distribution, first the mean velocity was measured in a vertical 400 mm upstream from the cylinders. This is done by means of a pitot static tube, which is connected to an inclined manometer filled with water. It is clear to from Figure 3.6 that the measured velocity distribution was almost uniform along the height of test section.

3.6.1 Test of the Single Cylinder

In the first phase of the experimental investigation, the single cylinder is taken into consideration. The location of the cylinder is shown in tunnel test section in Figure 3.7. The cylinders with side dimensions of D = 60 mm and H = 60 mm and the widths at the mid-point of the rounded facet of 0 mm (flat), 7.50 mm, 15 mm, 22.50 mm and 30 mm are used in this phase. The respective diameters of the rounded facets are infinity (i.e. flat), 127.50 mm, 75 mm, 62.50 mm, and 60 mm.

First, the cylinder with side dimensions of D = 60 mm and H = 60 mm and the widths at the mid-point of the rounded facet of 0 mm (flat) is placed centrally at the downstream side of the exit end of the wind tunnel. The diameter of the rounded facet is infinity for this cylinder with flat facet. The bolt fixed with the cylinder is fitted with an attachment graduated from 0^0 to 360^0 and with its rotation; the cylinder is positioned at different angles of attack with the flow direction. The velocity at the upstream side of the cylinder is maintained at 13.6 m/s. The velocity is measured by the help of a digital anemometer. The upstream velocity is assumed to be uniform. The face A (D = 60 mm) of the cylinder is oriented towards the flow direction and the face B or face D (H = 60 mm) is parallel to the flow direction. In this position the angle of attack is 0°. Then the static pressure distributions on the surfaces are measured by means of manometer. The static pressure distributions are also measured at angles of attack 10^0 to 90^0, increasing by 10^0 at each step.

The same test procedure is repeated to measure the static pressure distributions for the cylinders with side dimensions of D = 60 mm and H = 60 mm and the widths at the mid-point of the rounded facet of 7.50 mm, 15 mm, 22.50 mm, 30 mm. The respective diameters of the rounded facets are 127.50 mm, 75 mm, 62.50 mm, and 60 mm.

3.6.2 Test of the cylinder in Group

In the second phase of the experimental investigation two cylinders are used, one is at the upstream and the other is at the downstream side (Figure 3.8). They are placed centrally along the flow direction. In this phase also cylinders with side dimensions of $D = 60$ mm and $H = 60$ mm and the widths at the mid-point of the rounded facet of 0 mm, 7.50 mm, 15 mm, 22.50 mm and 30 mm are used. For widths at the mid-point of the rounded facet of 0 mm, 7.50 mm, 15 mm, 22.50 mm and 30 mm, the respective diameters of the rounded facets are infinity (i.e. flat), 127.50 mm, 75 mm, 62.50 mm, and 60 mm. First of all, the cylinder with widths at the mid-point of the rounded facet of 0 mm is used. The angle of attack is kept at 0°. The Reynolds number based on face A of the cylinder ($D = 60$ mm) is 5.4×10^4. The inter-space between the upstream cylinder and the downstream cylinder is taken 1D i.e. 60mm. Then pressure distributions are measured on the upstream and the downstream cylinders. Keeping everything identical the inter-space is changed to 2D and the procedure is repeated. Next the inter-space varied to 4D, 6D and 8D and in each case the static pressure distributions on both the upstream and the downstream cylinders are taken. The same test procedure is repeated to measure the static pressure distributions for the cylinders with side dimensions of $D = 60$ mm and $H = 60$ mm and the widths at the mid-point of the rounded facet of 7.50 mm, 15 mm, 22.50 mm, 30 mm.

Converging Inlet

Fan

Butterfly Valve

Silencer
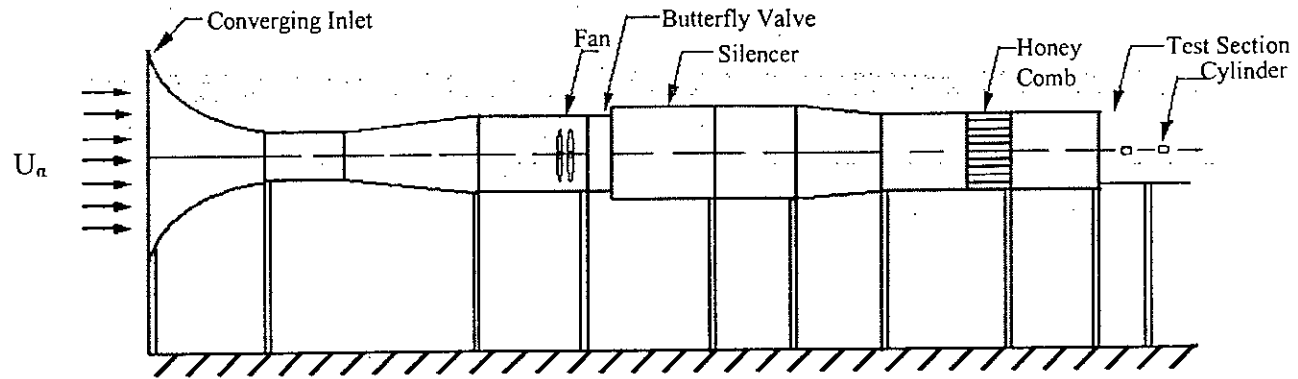
Honey
Comb

Test Section

Cylinder

U_α

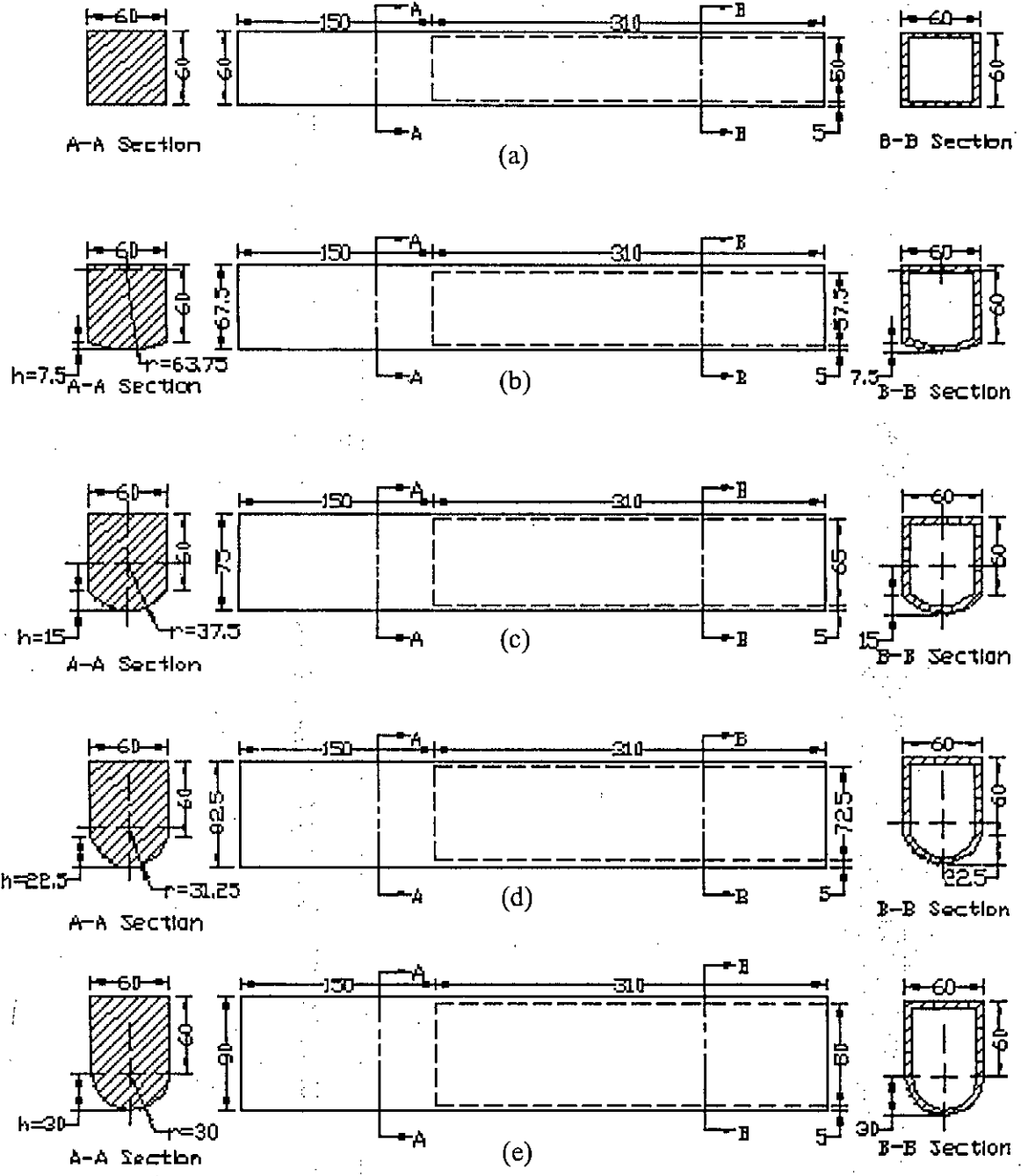Figure 3.1: Schematic Diagram of Wind Tunnel

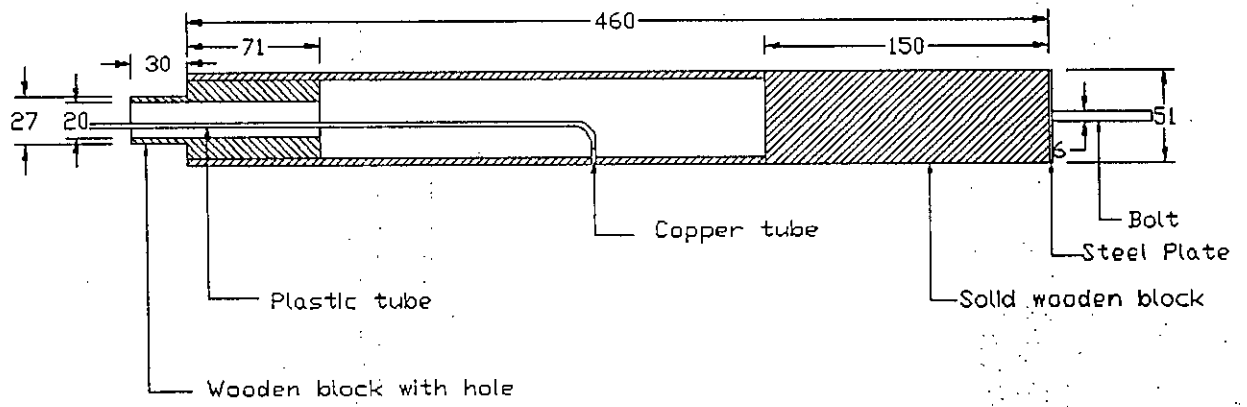Figure 3.2: Sections of Square Cylinder and That With Rounded Facet.

Figure 3.3: Sectional View of a Specimen Square Cylinder
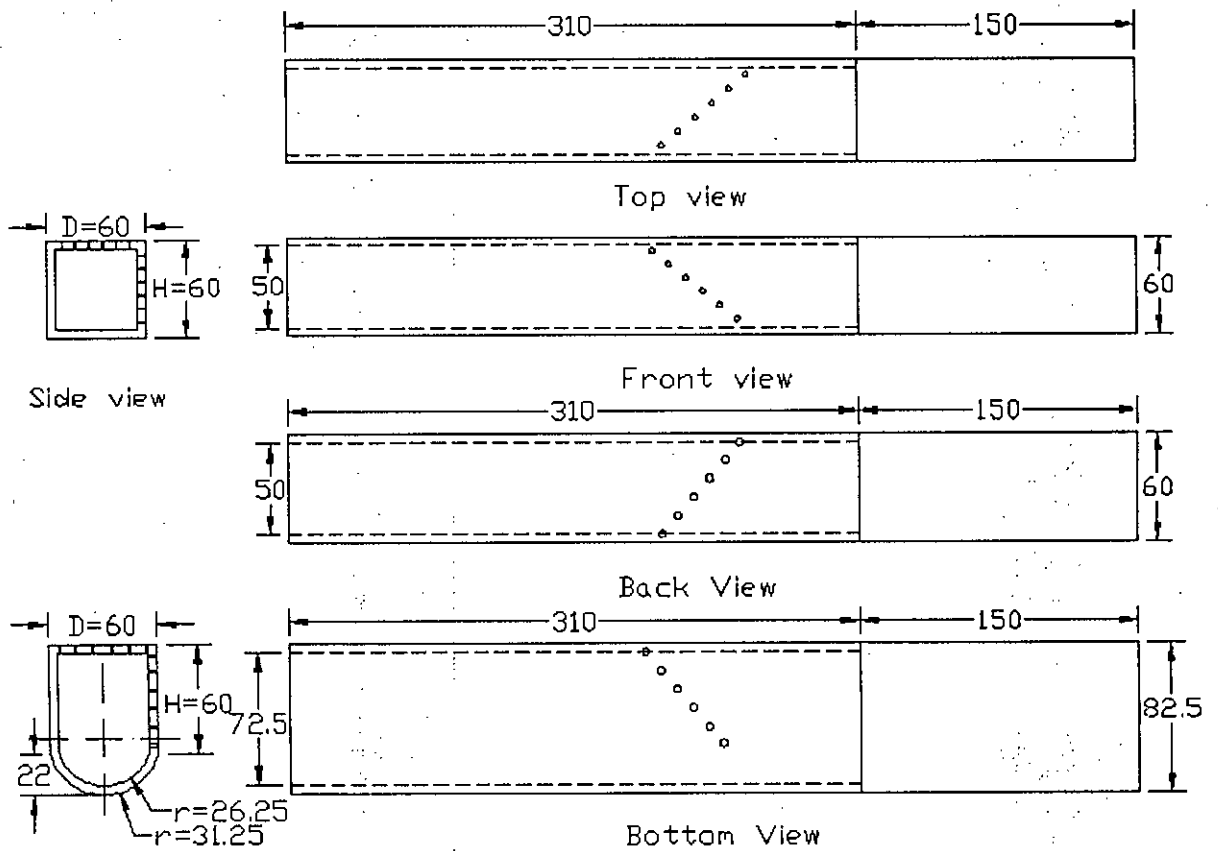
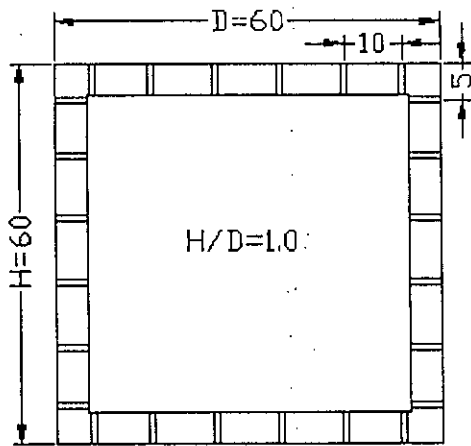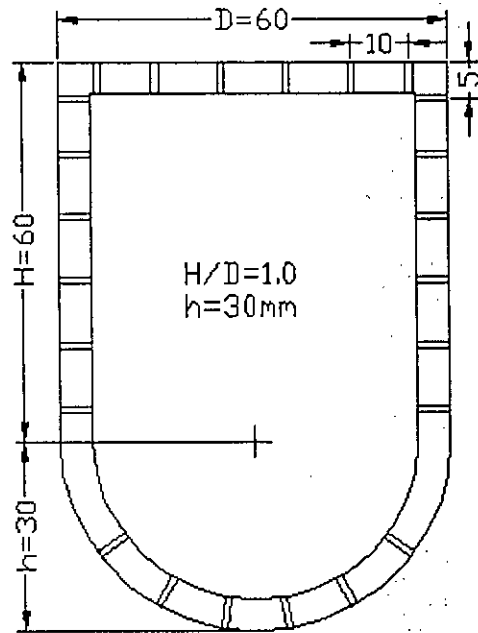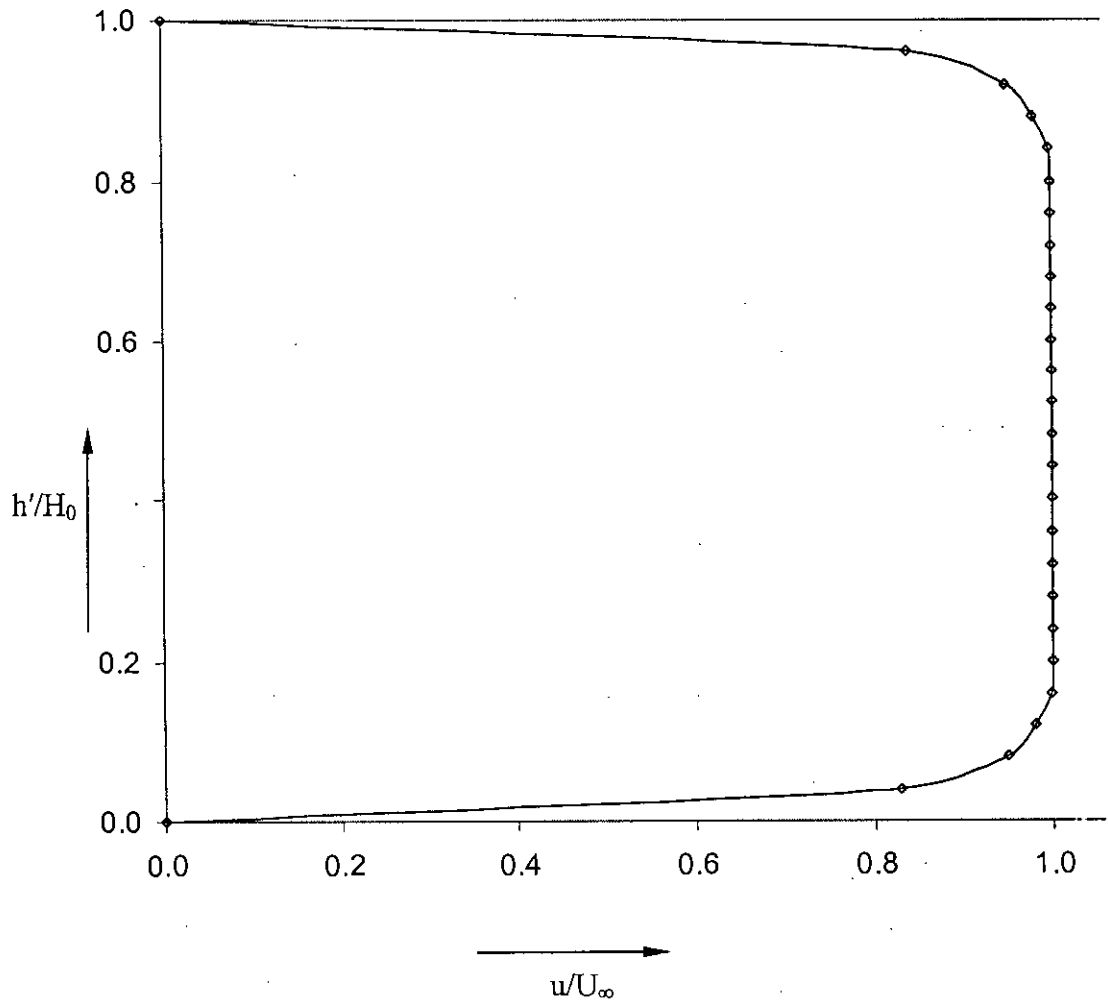Figure 3.4: Tapping Points on Adjacent Sides of Cylinder

Figure 3.5: Tapping Position on Cross-Section of Square cylinder and That With
        Rounded Facet

Figure 3.6: Velocity Distribution Along Height of Test Section.
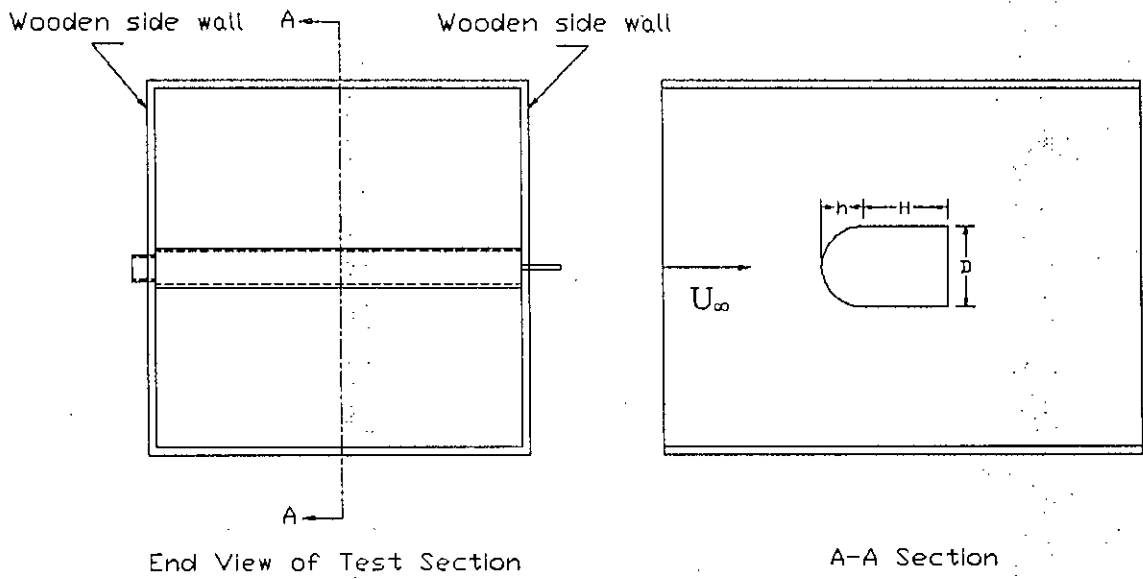
34

Figure 3.7: Tunnel Test Section Showing Position of Single Cylinder with Rounded Facet
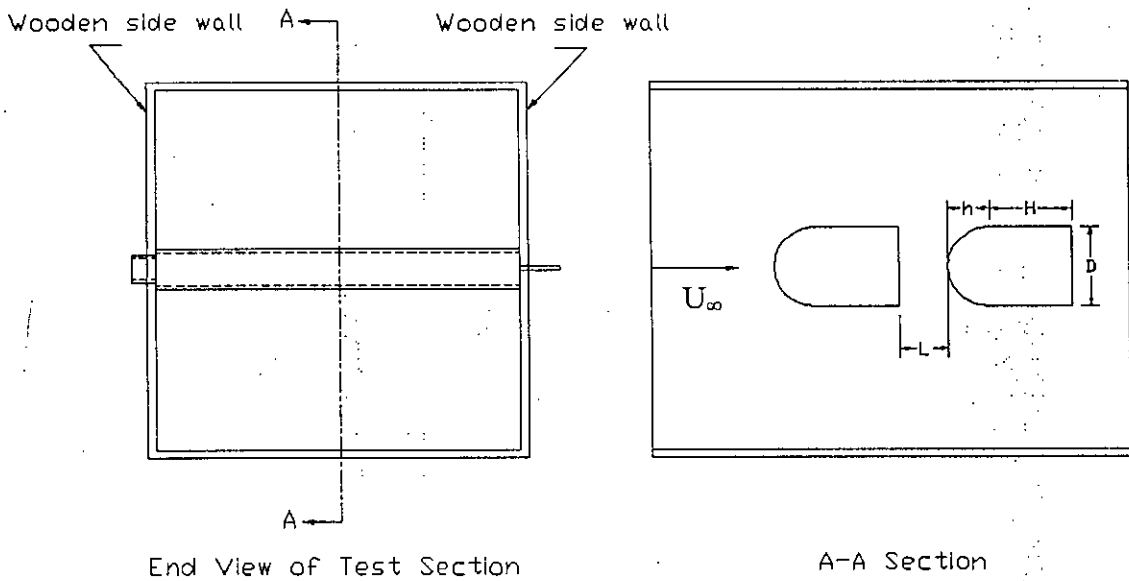
Figure 3.8: Tunnel Test Section Showing Position of the Group of Cylinders with Rounded Facet.

CHAPTER-4

MATHEMATICAL MODEL

In this chapter the calculation procedure of finding pressure coefficients and drag coefficients has been described in brief. The pressure coefficients and the drag coefficients are obtained with the help of numerical method. Using the measured values of the pressure coefficients at the different tapping points, the expression of the pressure and the drag coefficients values are established.

4.1 Calculation Procedure

In Figure 4.1, a cross-section of the cylinder is shown. The cylinder is oriented in such a manner that at zero degree angle of attack (i.e. $\alpha = 0^0$), the face A is the windward face, which occurs along the flow direction; the faces B and D remain parallel to the flow direction and the rear face C is perpendicular to the flow direction, which is called leeward face.

Figure 4.1: Section of a Cylinder Showing Pressure Tapping Points and Forces Acting on Each Strip

The section has been divided both horizontally and vertically. In the horizontal direction, the cross-section of the cylinder has been divided into six equal strips of width Δd. Along the horizontal 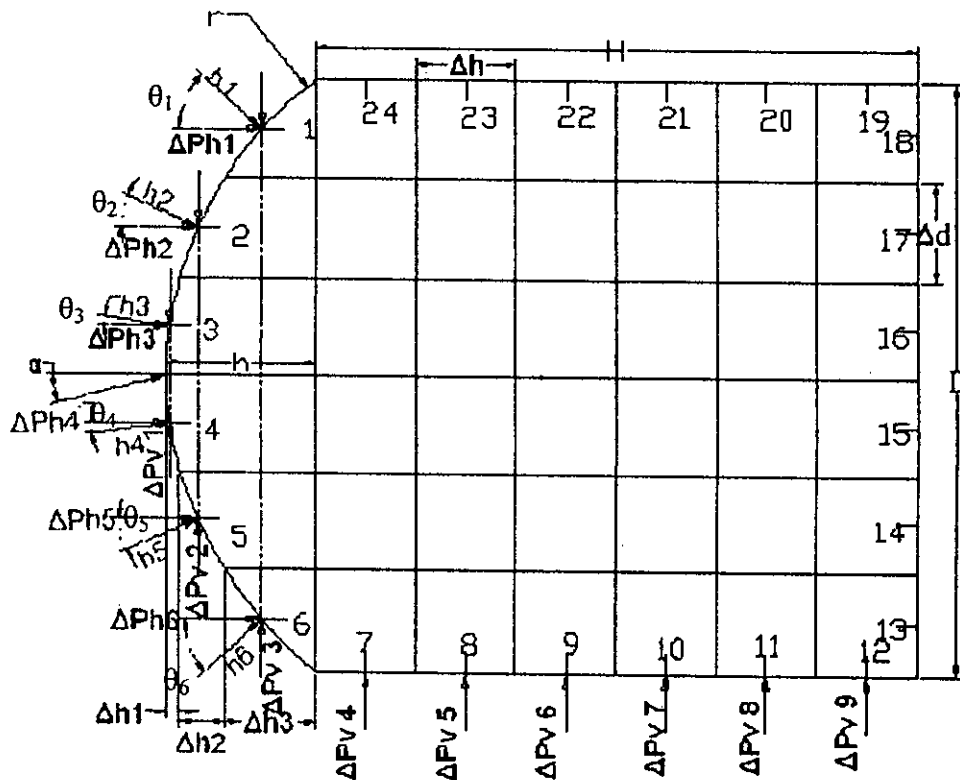direction there are nine divisions of them the width of the six divisions are equal and is denoted by Δh. The other three unequal widths are denoted by Δh_1, Δh_2 and Δh_3. It is assumed that this will make negligible error in the overall values of the pressure and drag coefficients.

Let ΔP_{h1}, ΔP_{h2}, ΔP_{h3}, ΔP_{h4}, ΔP_{h5}, and ΔP_{h6} are respectively the pressure differences along the horizontal division between the opposite sides of each horizontal strip and ΔP_{v1}, ΔP_{v2}, ΔP_{v3}, ΔP_{v4}, ΔP_{v5}, ΔP_{v6}, ΔP_{v7}, ΔP_{v8} and ΔP_{v9} are the pressure differences in the vertical division between the opposite sides of each vertical strip. Based on the unit length of the cylinder the area under each strip along the horizontal division is $\Delta d \times 1$ while along the vertical direction it is $\Delta h \times 1$ for strips of equal width. However, in order to take the contribution in the vertical direction from the front face, the projected areas are taken and they are of unequal sizes, which are denoted by Δh_1, Δh_2 and Δh_3 as shown in Figure 4.1. The pressure difference along the horizontal strips in the face A are obtained from,

$$\Delta P_{h1} = h_1 \cos\theta_1 - h_{18} \qquad \Delta P_{h2} = h_2 \cos\theta_2 - h_{17}$$
$$\Delta P_{h3} = h_3 \cos\theta_3 - h_{16} \qquad \Delta P_{h4} = h_4 \cos\theta_4 - h_{15}$$
$$\Delta P_{h5} = h_5 \cos\theta_5 - h_{14} \qquad \Delta P_{h6} = h_6 \cos\theta_6 - h_{13}$$

The pressure difference along the vertical strips in the face A are obtained as,

$$\Delta P_{v1} = h_4 \sin\theta_4 - h_3 \sin\theta_3 \qquad \Delta P_{v2} = h_5 \sin\theta_5 - h_2 \sin\theta_2$$
$$\Delta P_{v3} = h_6 \sin\theta_6 - h_1 \sin\theta_1$$

where, θ_1, θ_2, θ_3 θ_4, θ_5 and θ_6 are the angles between the horizontal and normal to the surface.

The vertical projected width can be expressed as,

$$\Delta h_1 = a\ \Delta h, \quad \Delta h_2 = b\ \Delta h \quad \text{and} \quad \Delta h_3 = c\ \Delta h$$

where a, b and c are the constants and they are dependent on the value of the width h of the face A i.e. facet. The values of the constants are given in the following Table-4.1

37

Table-4.1: Values of angle between resultant and horizontal forces and constant

Tapping Point	Model	M#01 (Deg)	M#02 (Deg)	M#03 (Deg)	M#04 (Deg)	M#05 (Deg)
7	Angle between resultant and horizontal forces		23	42	54	58
8			14	24	29	30
9			5	8	9	10
10			5	8	9	10
11			14	24	29	30
12			23	42	54	58
Unequal size	Δh_1		0.39	0.68	0.82	0.86
	Δh_2		1.21	2.21	2.80	2.96
	Δh_3		2.14	4.61	7.63	11.18
Constant	a	0	0.078	0.136	0.164	0.172
	b	0	0.242	0.442	0.56	0.592
	c	0	0.428	0.922	1.526	2.236

The pressure differences along the other strips in the vertical directions are obtained as,

$$\Delta P_{v4} = (h_7 - h_{24}) \qquad \Delta P_{v5} = (h_8 - h_{23})$$

$$\Delta P_{v6} = (h_9 - h_{22}) \qquad \Delta P_{v7} = (h_{10} - h_{21})$$

$$\Delta P_{v8} = (h_{11} - h_{20}) \qquad \Delta P_{v9} = (h_{12} - h_{19})$$

Now adding all the components of forces in the horizontal direction the drag forces is obtained as,

$$F_d = [\, \Delta P_{h1} \times \gamma_w \times \Delta d \times 1 + \Delta P_{h2} \times \gamma_w \times \Delta d \times 1 + \Delta P_{h3} \times \gamma_w \times \Delta d \times 1 + \Delta P_{h4} \times$$
$$\gamma_w \times \Delta d \times 1 + \Delta P_{h5} \times \gamma_w \times \Delta d \times 1 + \Delta P_{h6} \times \gamma_w \times \Delta d \times 1\,] \times g \cos\alpha +$$
$$[\, \Delta P_{v1} \times \gamma_w \times \Delta h_1 \times 1 + \Delta P_{v2} \times \gamma_w \times \Delta h_2 \times 1 + \Delta P_{v3} \times \gamma_w \times \Delta h_3 \times 1 +$$
$$\Delta P_{v4} \times \gamma_w \times \Delta h \times 1 + \Delta P_{v5} \times \gamma_w \times \Delta h \times 1 + \Delta P_{v6} \times \gamma_w \times \Delta h \times 1 + \Delta P_{v7} \times$$
$$\gamma_w \times \Delta h \times 1 + \Delta P_{v8} \times \gamma_w \times \Delta h \times 1 + \Delta P_{v9} \times \gamma_w \times \Delta h \times 1\,] \times g \sin\alpha \qquad (1)$$

where γ_w is the specific weight of manometric fluid

The lift force is determined from,

$$F_l = [\Delta P_{h1} \times \gamma_w \times \Delta d \times 1 + \Delta P_{h2} \times \gamma_w \times \Delta d \times 1 + \Delta P_{h3} \times \gamma_w \times \Delta d \times 1 + \Delta P_{h4} \times$$
$$\gamma_w \times \Delta d \times 1 + \Delta P_{h5} \times \gamma_w \times \Delta d \times 1 + \Delta P_{h6} \times \gamma_w \times \Delta d \times 1] \times g \sin\alpha +$$
$$[\Delta P_{v1} \times \gamma_w \times \Delta h_1 \times 1 + \Delta P_{v2} \times \gamma_w \times \Delta h_2 \times 1 + \Delta P_{v3} \times \gamma_w \times \Delta h_3 \times 1 +$$
$$\Delta P_{v4} \times \gamma_w \times \Delta h \times 1 + \Delta P_{v5} \times \gamma_w \times \Delta h \times 1 + \Delta P_{v6} \times \gamma_w \times \Delta h \times 1 + \Delta P_{v7} \times$$
$$\gamma_w \times \Delta h \times 1 + \Delta P_{v8} \times \gamma_w \times \Delta h \times 1 + \Delta P_{v9} \times \gamma_w \times \Delta h \times 1\,] \times g \cos\alpha \qquad (2)$$

Equation (1) may be written as

$$F_d = \gamma_w \times \Delta d \times 1 \times g [\Delta P_{h1} + \Delta P_{h2} + \Delta P_{h3} + \Delta P_{h4} + \Delta P_{h5} + \Delta P_{h6}] \cos \alpha + \gamma_w \times \Delta h$$
$$\times 1 \times g [a \times \Delta P_{v1} + b \times \Delta P_{v2} + c \times \Delta P_{v3} + \Delta P_{v4} + \Delta P_{v5} + \Delta P_{v6} + \Delta P_{v7} + \Delta P_{v8} +$$
$$\Delta P_{v9}] \times g \sin \alpha \tag{3}$$

This can be expressed as,

$$F_d = \gamma_w \times 1 \times g [\Delta d \times \Delta P_h \times \cos \alpha + \Delta h \times \Delta P_v \times \sin \alpha] \tag{4}$$

where, $\Delta P_h = \Delta P_{h1} + \Delta P_{h2} + \Delta P_{h3} + \Delta P_{h4} + \Delta P_{h5} + \Delta P_{h6}$ $\qquad$ (5)

$$\Delta P_v = a \times \Delta P_{v1} + b \times \Delta P_{v2} + c \times \Delta P_{v3} + \Delta P_{v4} + \Delta P_{v5} + \Delta P_{v6} + \Delta P_{v7} + \Delta P_{v8} + \Delta P_{v9} \tag{6}$$

Writing $\Delta d = \Delta L$ and $\Delta h = \Delta L$ and substituting in equation (4), drag force can be expressed as,

$$F_d = \gamma_w \times \Delta L \times 1 \times g [\Delta P_h \cos \alpha + \Delta P_v \sin \alpha] \tag{7}$$

This can be written as,

$$F_d = \gamma_w \times \Delta L \times 1 \times g [\Delta P_d] \tag{8}$$

where, $\Delta P_d = \Delta P_h \cos \alpha + \Delta P_v \sin \alpha$ $\qquad$ (9)

When the value of angle of attack becomes zero, the ΔP_d is obtained from,

$$\Delta P_d = \Delta P_h \tag{10}$$

In the same way, the expansion of the lift force F_l is found as,

$$F_l = \gamma_w \times \Delta L \times 1 \times g [\Delta P_l] \tag{11}$$

Where, $\Delta P_L = \Delta P_h \sin \alpha + \Delta P_v \cos \alpha$ $\qquad$ (12)

When the angle of attack becomes zero, the ΔP_l is reduced to,

$$\Delta P_l = \Delta P_v \tag{13}$$

Drag co-efficient is defined as, $C_d = \dfrac{F_d}{\frac{1}{2} \rho A U_\infty^2}$ $\qquad$ (14)

where, U_∞ is the free stream velocity, ρ is the density and A is the frontal area of the cylinder

Substituting the value of F_d from equation (8), equation (14) may be written as

$$C_d = \dfrac{\gamma_w \times \Delta L \times 1 \times g \times \Delta P_d}{\frac{1}{2} \rho \times 6 \Delta L \times 1 \times U_\infty^2} \tag{15}$$

The lift coefficient is defined as, $C_l = \dfrac{F_l}{\frac{1}{2} \rho A U_\infty^2}$ $\qquad$ (16)

39

This can be written as, substituting the value of F_l from equation (11)

$$C_l = \frac{\gamma_w \times \Delta L \times 1 \times g \times \Delta P_l}{\frac{1}{2}\rho \times 6\Delta L \times 1 \times U_\infty^2} \tag{17}$$

Equation (15) and (17) are reduced to the form,

$$C_d = \frac{\gamma_w \times g \times \Delta P_d}{3 \times \rho \times U_\infty^2} \tag{18}$$

and $C_l = \dfrac{\gamma_w \times g \times \Delta P_l}{3 \times \rho \times U_\infty^2}$ $\tag{19}$

Pressure co-efficient is defined as,

$$C_p = \frac{P - P_0}{\frac{1}{2}\rho U_\infty^2} \tag{20}$$

where, P_0 is the ambient pressure

P is the static pressure on the surface of the cylinder.

ρ is the density of the air

Equation (20) may be rewritten in the form,

$$C_p = \frac{\Delta P}{\frac{1}{2}\rho U_\infty^2} \tag{21}$$

The value of ΔP is obtained from

$\Delta P = K \times \Delta h \times \gamma_w \times g$

where, Δh is the manometer reading.

K is a constant.

4.2 Sample Calculation

The coefficient of pressure (C_p) can be calculated as,

$$C_p = \frac{\Delta P}{\frac{1}{2}\rho U_\infty^2}$$

$$= \frac{\frac{\Delta h \times 25.4}{1000} \times 1000 \times 9.81}{\frac{1}{2} \times 1.22 \times U_\infty^2}$$

$$= \frac{25.4 \times 9.81 \times 2}{1.22}\left(\frac{\Delta h}{U_\infty^2}\right); \text{ where } \Delta h = \text{inch of water and } U_\infty = \text{Velocity of air (m/s)}$$

$$= 408.482 \left(\frac{\Delta h}{U_\infty^2}\right)$$

The coefficient of drag (C_d) can be calculated from

$$C_d = \frac{\gamma_w \times g \times \Delta P_d}{3 \times \rho \times U_\infty^2}$$

$$= \frac{\frac{\Delta P_d \times 25.4}{1000} \times 1000 \times 9.81}{3 \times 1.22 \times U_\infty^2}$$

$$= 68.081 \left(\frac{\Delta P_d}{U_\infty^2}\right); \text{ where } \Delta P_d = \text{inch of water and } U_\infty = \text{Velocity of air (m/s)}$$

$\Delta P_d = \Delta P_h \cos\alpha + \Delta P_v \sin\alpha$

$= (\Delta P_{h1} + \Delta P_{h2} + \Delta P_{h3} + \Delta P_{h4} + \Delta P_{h5} + \Delta P_{h6}) \cos\alpha + (a \times \Delta P_{v1} + b \times \Delta P_{v2} + c \times \Delta P_{v3} + \Delta P_{v4} + \Delta P_{v5} + \Delta P_{v6} + \Delta P_{v7} + \Delta P_{v8} + \Delta P_{v9}) \sin\alpha$

$= [(h_1 \times \cos\theta_1 - h_{18}) + (h_2 \times \cos\theta_2 - h_{17}) + (h_3 \times \cos\theta_3 - h_{16}) + (h_4 \times \cos\theta_4 - h_{15}) + (h_5 \times \cos\theta_5 - h_{14}) + (h_6 \times \cos\theta_6 - h_{13})] \cos\alpha + [a \times (h_4 \sin\theta_4 - h_3 \sin\theta_3) + b \times (h_5 \sin\theta_5 - h_2 \sin\theta_2) + c \times (h_6 \sin\theta_6 - h_1 \sin\theta_1) + (h_7 - h_{24}) + (h_8 - h_{23}) + (h_9 - h_{22}) + (h_{10} - h_{21}) + (h_{11} - h_{20}) + (h_{11} - h_{20})] \sin\alpha$

$= \text{inch of water}$

41

The coefficient of lift (C_d) can be calculated from

$$C_l = \frac{\gamma_w \times g \times \Delta P_l}{3 \times \rho \times U_\infty^2}$$

$$= \frac{\dfrac{\Delta P_l \times 25.4}{1000} \times 1000 \times 9.81}{3 \times 1.22 \times U_\infty^2}$$

$$= 68.081 \left(\frac{\Delta P_l}{U_\infty^2} \right); \text{ where } \Delta P_l = \text{inch of water and } U_\infty = \text{Velocity of air (m/s)}$$

$\Delta P_l = \Delta P_h \sin \alpha + \Delta P_v \cos \alpha$

$\quad = (\Delta P_{h1} + \Delta P_{h2} + \Delta P_{h3} + \Delta P_{h4} + \Delta P_{h5} + \Delta P_{h6}) \sin \alpha + (a \times \Delta P_{v1} + b \times \Delta P_{v2} + c \times$

$\quad \Delta P_{v3} + \Delta P_{v4} + \Delta P_{v5} + \Delta P_{v6} + \Delta P_{v7} + \Delta P_{v8} + \Delta P_{v9}) \cos \alpha$

$\quad = [(h_1 \times \cos\theta_1 - h_{18}) + (h_2 \times \cos\theta_2 - h_{17}) + (h_3 \times \cos\theta_3 - h_{16}) + (h_4 \times \cos\theta_4 -$

$\quad h_{15}) + (h_5 \times \cos\theta_5 - h_{14}) + (h_6 \times \cos\theta_6 - h_{13})] \sin \alpha + [a \times (h_4 \sin\theta_4 - h_3$

$\quad \sin\theta_3) + b \times (h_5 \sin\theta_5 - h_2 \sin\theta_2) + c \times (h_6 \sin\theta_6 - h_1 \sin\theta_1) + (h_7 - h_{24}) + (h_8 -$

$\quad h_{23}) + (h_9 - h_{22}) + (h_{10} - h_{21}) + (h_{11} - h_{20}) + (h_{11} - h_{20})] \cos \alpha$

$\quad = \text{inch of water}$

When the value of angle of attack is maintained at zero and the cylinder is so arranged that the static pressure on the top and the bottom surfaces are symmetric, then the net lift force for that case is zero.

CHAPTER-5

RESULTS AND DISCUSSION

In this chapter the results of the experimental investigation in regard to distributions of static pressure coefficients on the square cylinder and cylinders with rounded facet have been discussed. First of all the distributions of the static pressure coefficients around a single square cylinder and that with rounded facets at different widths and different angles of attack are taken into consideration. Then the distributions of the static pressure coefficients around the cylinders in a group are considered. The results based on the various inter-space (longitudinal spacing) of the cylinders in the group are discussed elaborately. The calculated drag and lift coefficients from the measured static pressures for both the single cylinder and the cylinders in the group are also discussed. The results of the present research works have been compared with those of the existing research works.

5.1 Single Cylinder

In this section distributions of the static pressure coefficients, the drag and lift coefficients have been taken into consideration for discussion. The static pressure coefficients are obtained from the measured static pressures. The drag and lift coefficients, which are calculated from the pressure coefficients, are also discussed.

It would be relevant to show the typical flow pattern around a square cylinder before discussing the results of the experimental investigation. The typical nature of the flow pattern around a square cylinder at zero angle of attack, at about 15^0 angle of attack and at an angle of 45^0 is shown in Figures 5.1(a), 5.1(b) and 5.1(c) respectively. For the flow over the cylinder with rounded facet there is no fixed separation point as in the case of a cylinder with the sharp edge, where the separation point is fixed and it occurs just at the sharp edge. For the cylinder with rounded facet the separation point proceeds towards the downstream side. A pair of vortices is generated at the downstream side of the square cylinder as shown in figure. One rotates in the clockwise direction and the other rotates in the anti-clockwise direction. The distance of the pair of the vortices from the rear side of the cylinder depends on the orientation

(angle of attack) of the cylinder, which can be observed from this figure. It can be further noticed from this figure that the lateral distance of the two vortices also depends on the orientation. The location of the separation point and the distance of the pair of the vortices are the controlling factor of the values of the pressures on the face B, face D and face C of the cylinder. The pressure developed on the back surface depends on the distance of vortices. While the distance of vortices from the body is longer, the back pressure is higher and vice versa. For this reason pressure increases at the face C of the cylinder in small range of angle of attack but decreases in the higher range of angle of attack.

5.1.1 Pressure Distribution on Single Cylinder

The distribution of mean pressure coefficients around the square cylinder with angle of attack varying from 0^0 to 45^0 have been presented in Figure 5.2. From this figure, it is evident that C_P-distribution is a function of α. The test results are obtained for two dimensional uniform flows. The turbulence intensity and scale are not measured. The turbulence intensity in the test section is 0.4% as supplied by manufacturer of the tunnel. The side dimension of the cylinder perpendicular to the flow direction is 60 mm. Based on this side dimension the Reynolds number is 5.40 x 10^4. The C_P-distributions on the face A of the cylinder with side ratio of 1.0 reveal that a stagnation point is developed at the mid point of the surface for angle of attack of 0^0. This stagnation point is shifted towards the corner of the face D with increasing angle of attack.

From the C_P-distributions on the face D, it is seen that at $\alpha = 0^0$, almost constant values of C_P exist throughout the surface along the flow direction, because separation starts at the corner of the face A with no pressure recovery. In the range of small angles of attack, pressure recovery is seen to be there at the face C at a slow rate. As the angle of attack is increased further ($\geq 20^0$), the location of highest pressure recovery gradually shifts toward the corner of the face A, with increasing magnitude. Near the corner of the face C as the angle of attack is increased ($\geq 20^0$), the value of C_P increases slowly. At $\alpha = 45^0$, the C_P-distributions on face A and face D are almost identical; however, there is minor variation.

On the face B, the variation of C_P-distributions with angle of attack is small and for each angle of attack C_P-distributions is almost uniform throughout the surface. There is no pressure recovery in the face B. Now observing the C_P-distributions on the face C it is seen that the values of C_P are found to increase up to 10^0 and with onward increase of α, these values decrease up to 45^0. One may observe that the pressure distributions on face B and face C reveal similar trend.

The distribution of pressure coefficients around the cylinder with facet width of 7.50 mm at the mid point has been presented in Figure 5.3 with angle of attack varying from 0^0 to 90^0. From this figure, it is evident that C_P-distribution is a function of α. One can observe from the pressure coefficients distribution on the face A at $\alpha = 0^0$, the values of the pressure coefficients in the middle is almost unity whereas with the further increase of the angle of attack by 10^0, stagnation point is shifted towards the corner of the face D. The C_P-distributions on the face D of the cylinder at $\alpha = 0^0$ is almost uniform throughout the surface. At angle of attack 10^0, there appears slight pressure recovery at the rear side of the face D. However, as the angle of attack is increased further, the location of the highest pressure gradually shifts towards the corner of the face A with increasing magnitude. At $\alpha = 90^0$, the C_P-distribution on the face D and at $\alpha = 0^0$, the C_P-distribution on the face A are almost identical which is similar. On the face B, variation of C_P-distributions with angle of attack is small and for each angle of attack C_P-distribution is almost uniform throughout the surface. Now observing the C_P-distributions on the face C it is seen that the values of C_P distributions on the face C reveal a similar trend.

The distribution of pressure coefficients around the cylinder with facet width of 15.00 mm at the midpoint and the diameters of the rounded facets of 75 mm with angle of attack varying from 0^0 to 90^0 is shown in Figure 5.4. From this figure, it is seen that C_P-distribution is a function of α. One can observe from the pressure distribution on the face A at $\alpha = 0^0$, the values of the pressure coefficients in the middle is almost unity whereas with the further increase of the angle of attack, stagnation point is shifted towards the corner of the face D. The C_P-distributions on the face D of the cylinder at $\alpha = 0^0$ is almost uniform throughout the surface. At the angle of attack 10^0, there occurs further drop of pressure near the face A. The Figure shows that as the angle of attack is increased further, the location of the highest pressure gradually

45

shifts towards the corner of the face A with increasing magnitude. At $\alpha = 90^0$, the C_P-distribution on the face D and at $\alpha = 0^0$, the C_P-distribution on the face A are almost identical. On the face B, variation of C_P-distributions with angle of attack is small and for each angle of attack C_P-distribution is almost uniform throughout the surface. Now observing the C_P-distributions on the face C it is seen that the values of C_P distributions on the face C reveal a similar trend like those of the face B.

The distribution of pressure coefficients around the cylinder with facet widths of 22.50 mm and 30.00 mm have been presented in Figures 5.5 and 5.6 respectively with angle of attack varying from 0^0 to 90^0. From these figures, it is found that they show almost the similar trend as for the cylinder with facet width of 15.0 mm presented in Figure 5.4.

5.1.2 Variation of Drag Coefficients

The variation of drag co-efficient (C_d) for side ratios H/D = 1.0 with angle of attack from 0^0 to 45^0 is shown in the Figure 5.7. It can be seen from this figure that the general trend of drag variation occur in such a way that with the increase of angle of attack the drag coefficient falls and becomes minimum in the region of angle of attack 12^0 and subsequently with further increase of angle of attack its value rises sharply up to the angle of attack of 45^0. It is already mentioned that as the angle of attack increases the vortex formation occurs at larger distance thereby creating higher back pressure, which is mainly the cause of lower drag with increased value of angle of attack. For further increase of angle of attack vortex formation appear closer to the face C of the body making the back pressure lower which is mainly the reason of higher drag for increased value of angle of attack in the higher range.

Comparison is also made in Figure 5.7 with the experimental results presented by Mandal [38] for a square cylinder placed in a uniform flow with a turbulence intensity of 0.4%. It is seen that the drag coefficients follow the same pattern and are reasonably close with each other. The variation of drag coefficient with angle of attack in this study is also compared with that presented by Lee [36] and it is seen that the present results agree well with that of Lee.

The variation of drag co-efficient (C_d) for the cylinder with facet width of 7.50 mm with angle of attack varying from 0^0 to 90^0 has been presented in Figure 5.8. It can be seen from this figure that the general trend of drag variation occur in such a way that with the increase of angle of attack the drag coefficient falls up to 13^0 and then increases up to 20^0 and again decreases gradually up to 65^0 and then increases gradually up to 90^0. The value of the drag coefficient is close to unity which is significantly below from that for square cylinder as shown in Figure 5.7. It indicates that for making the round facet drag value has been dropped tremendously, which the designer can notice.

The variation of drag co-efficient (C_d) for cylinder with facet width of 15.00 mm with angle of attack varying from 0^0 to 90^0 has been presented in Figure 5.9. It can be seen from this figure that the general trend of drag variation occur in such a way that with the increase of angle of attack the drag coefficient falls up to 30^0 and then increases gradually. Still the maximum drag coefficient is lower than that for the square cylinder. Comparing the drag values in Figure 5.8 and 5.9, it can be conducted that cylinder with facet width of 7.5 mm better.

The variation of drag co-efficient (C_d) for the cylinder with facet width of 22.50 mm with angle of attack varying from 0^0 to 90^0 has been shown in Figure 5.10. It can be seen from this figure that the general trend of drag variation occurs in such a way that with the increase of angle of attack the drag coefficient increases gradually.

The variation of drag co-efficient (C_d) for the cylinder with facet width of 30.00 mm with angle of attack varying from 0^0 to 90^0 has been shown in Figure 5.11. It can be seen from this figure that the general trend of drag variation occurs in such a way that with the increase of angle of attack the drag coefficient increases gradually. The trend for both the facet widths of 22.50 mm and 30.00 mm are similar. However, for the cylinder with facet width of 30.00 mm the drag coefficient becomes close to that for the square cylinder with facet width of 22.50 mm.

The variation of drag co-efficient (C_d) with angle of attack for different facet widths has been shown in Figure 5.12. It can be observed from this figure that there is significant effect of facet width on the drag coefficient. As the facet width increases, drag coefficient decreases and at a maximum value of facet width, the drag coefficient

minimum up to a certain angle of attack. However, there is small effect of angle of attack in the value of the drag coefficient.

5.1.3 Variation of lift Coefficients

The variation of lift coefficient (C_l) with angle of attack for square cylinder is shown in Figure 5.13. The general trend in the variation of lift is similar to that of drag with angle of attack. The variation of lift coefficient with angle of attack is compared with that of Mandal [38] and it is seen that they are almost same up to certain angle of attack but at higher angle of attack, small difference is observed. The variation of lift coefficient presented by Lee [36] is also shown in this figure, which follows a similar trend. The high negative lift at small angle of attack is associated with the formation of large enclosed separation bubble on the face D of the cylinder, which caused higher local suctions than those on the face B.

The variation of lift coefficient (C_l) for cylinder with facet width of 7.50 mm with angle of attack varying from 0^0 to 90^0 has been presented in Figure 5.14. It can be seen from this figure that the general trend of lift variation occurs in such a way that with the increase of angle of attack the lift coefficient decreases gradually up to 45^0 (magnitude of lift coefficient increases) and then increases gradually.

The variation of lift coefficient (C_l) for cylinder with facet width of 15.00 mm with angle of attack varying from 0^0 to 90^0 has been presented in Figure 5.15. It is observed from this figure that the general trend of lift variation occurs in such a way that with the increase of angle of attack the lift coefficient decreases gradually up to 50^0 (magnitude of lift coefficient increases) and then increases gradually.

The variation of lift coefficient (C_l) for cylinder with facet width of 22.50 mm with angle of attack varying from 0^0 to 90^0 has been presented in Figure 5.16. It can be seen from this figure that the variation almost follows the similar trend as for that with facet width of 15.00 mm. However, the magnitude of lift coefficient becomes maximum at about 55^0 angle of attack

The variation of lift coefficient (C_l) for cylinder with facet width of 30.00 mm with angle of attack varying from 0^0 to 90^0 has been presented in Figure 5.17. It is seen from this figure that the variation follows almost the similar trend as the prior ones.

However, the magnitude of the lift coefficient is maximum at about 45^0 angle of attack.

The variation of lift co-efficient (C_l) with angle of attack for different facet widths has been shown in Figure 5.18. It can be observed from this figure that there is significant effect of facet width on the lift coefficient. As the facet width increases, lift coefficient decreases and at a maximum value of facet, the lift coefficient is minimum. However, there is small effect of angle of attack in the value of the lift coefficient.

5.2 Group of Cylinders

In this section the distributions of mean pressure coefficients on the cylinder in a group are discussed. The group consists of two cylinders, one at the upstream and the other at the downstream side just behind the upstream cylinder along the flow direction. The drag coefficients on the cylinder are also discussed. The effect of the inter-space of the two cylinders on the static pressure coefficients and the drag coefficients has been discussed elaborately.

5.2.1 Pressure Distribution on Upstream Cylinder

The distribution of static pressure coefficients on the upstream cylinder in a group is shown in Figures 5.19 to 5.23. In Figure 5.19 distributions of static pressure coefficients on the upstream square cylinder have been presented. The pressure coefficients at the different inter-space (longitudinal spacing) of L = 1D, 2D, 4D, 6D and 8D between the upstream and the downstream cylinders are given in this figure. The Reynolds number based on the size of face A of the cylinder is 5.40×10^4 and the angle of attack is 0°. One can observe from the pressure coefficients distribution on the face A that the values of the pressure coefficients in the middle are almost unity.

It is seen from this figure that on the face B and face D the pressure coefficients values are almost identical due to the symmetry of the flow. In general the values of the pressure coefficients increase by some amount with the increase of the inter-space on the face B, face D and the face C of the cylinder. Comparing the pressure coefficients from Figures 5.2 and 5.19 it is evident that due to the presence of the

cylinder at the downstream side the back pressure of the upstream cylinder in the group increases in respect to that for the single cylinder. The recovery of the pressure occurs due to the presence of the downstream cylinder. The flow at the downstream of the upstream cylinder is influenced for the presence of the downstream cylinder. The flow at the downstream of the upstream cylinder becomes more turbulent resulting relatively more mass and momentum transfer, which creates pressure recovery on the face B, face D and the face C of the upstream cylinder.

The distributions of the pressure coefficients on upstream cylinder of the group with facet width of 7.50 mm at various inter-spaces of L = 1D, 2D, 4D, 6D and 8D have been presented in Figure 5.20. One can observe from the pressure coefficients distribution on the face A that the values of the pressure coefficients in the middle are almost unity. Comparing the pressure coefficients from the Figures 5.3 and 5.18 it is evident that due to the presence of the cylinder at the downstream side the back pressure of the upstream cylinder in the group increases compared to that for the single cylinder. Comparing the pressure distributions on the face B, face D and the face C from the Figures 5.19 and 5.20 it is seen that the pressures as shown in Figure 5.20 is higher than that of Figure 5.19. However, the pressure distribution on the face A is very close to each other.

The distributions of the pressure coefficients on upstream cylinder of the group with facet width of 15.00 mm at various inter-spaces of L = 1D, 2D, 4D, 6D and 8D have been presented in Figure 5.21. One can observe from the pressure coefficients distribution on the face A that the pressure coefficients in the middle are almost unity for all inter-spaces. Comparing the pressure coefficients from the Figures 5.4 and 5.19 it is evident that due to the presence of the cylinder at the downstream side the back pressure of the upstream cylinder in the group increases compared to that for the single cylinder. Comparing the pressure distributions on the face A, face B, face D and the face C from the Figures 5.18 and 5.19 it is seen that they are very close to each other.

The distributions of the pressure coefficients on upstream cylinder of the group with facet width of 22.50 mm at various inter-spaces of L = 1D, 2D, 4D, 6D and 8D have been presented in Figure 5.22. One can observe from the pressure coefficients distribution on the face A that the values of the pressure coefficients in the middle are

almost unity for all inter-space values. Comparing the pressure coefficients from the Figures 5.5 and 5.22 it is evident that due to the presence of the cylinder at the downstream side the back pressure of the upstream cylinder in the group increases compared to that for the single cylinder. Comparing the pressure distributions on the face A, face B, face D and the face C from the Figures 5.19 and 5.20 it is seen that they are very close to each other.

The distributions of the pressure coefficients on upstream cylinder of the group with facet width of 30.00 mm at various inter-spaces of L = 1D, 2D, 4D, 6D and 8D have been presented in Figure 5.23. One can observe from the pressure coefficients distribution on the face A that the values of the pressure coefficients in the middle are almost unity for all inter-space values. Comparing the pressure coefficients from the Figures 5.6 and 5.23 it is clear that due to the presence of the cylinder at the downstream side the back pressure of the upstream cylinder in the group increases compared to that for the single cylinder. Comparing the pressure distributions on the face A, face B, face D and the face C from the Figures 5.20 and 5.21 it is seen that they are very close to each other.

Moreover, it can be seen from this Figures 5.19 to 5.23 that at the different inter-spaces the values of the pressure coefficients for the face A, face B, face D and the face C are very close to each other respectively.

5.2.2 Variation of Drag on Upstream Cylinder

The variation of drag coefficient (C_d) on the upstream cylinder (F) in a group with rounded facet at different inter-spaces (longitudinal spacing) is shown in Figures 5.24 to 5.29. In Figure 5.24, variation of drag coefficients on the square cylinder has been presented. The drag coefficients at various inter-spaces of L = 1D, 2D, 4D, 6D and 8D between the upstream and the downstream cylinders are given in this figure. It is seen from this Figure 5.24 that with the increase of the inter-space the drag coefficient decreases gradually. Since the back pressure increases on the upstream cylinder with the increase of the inter-space, which can be seen from Figure 5.19, the drag coefficient decreases.

In Figure 5.25, variation of drag coefficients on square cylinder with facet width of 7.50 mm has been presented. The drag coefficients at the different inter-spaces of L =

1D, 2D, 4D, 6D and 8D between the upstream and the downstream cylinders are given in this figure. It is seen from this figure that with the increase of the inter-space the drag coefficient decreases gradually up to L = 6D and then increases with the increase of the inter-space. However it can be further noticed from this figure that the drag coefficient is lower than that on the square cylinder as shown in Figure 5.24.

In Figure 5.26, variation of drag coefficients on square cylinder with facet width of 15.00 mm has been shown. The drag coefficients at the various inter-spaces of L = 1D, 2D, 4D, 6D and 8D between the upstream and the downstream cylinders are provided in this figure. It is reveled from this figure that with the increase of the inter-space the drag coefficient decreases gradually up to L = 5D and then increases with the increase of the inter-space. It gives the similar trend as for the cylinder with facet width of 7.50 mm shown in Figure 5.25.

In Figure 5.27, variation of drag coefficients on square cylinder with facet width of 22.50 mm has been presented. The drag coefficients at the various inter-spaces of L = 1D, 2D, 4D, 6D and 8D between the upstream and the downstream cylinders are shown in this figure. It is observed from this figure that with the increase of the inter-space the drag coefficient decreases slightly up to L = 2D and then increases with the increase of the inter-space.

Finally in Figure 5.28, variation of drag coefficients on square cylinder with facet width of 30.00 mm has been shown. The drag coefficients at the various inter-spaces of L = 1D, 2D, 4D, 6D and 8D between the upstream and the downstream cylinders are provided in this figure. It is seen from this figure that with the increase of the inter-space the drag coefficient decreases slightly up to L = 1.5D and then increases with the increase of the inter-space. However, it is seen from this figure that the drag coefficient value is significantly lower than on the upstream square cylinder as shown in Figure 5.24

In Figure 5.29, variation of drag coefficient with interspace on front cylinder in a group for various facet widths has been presented. It can be observed from this figure that there is significant effect of facet width on the drag coefficient. As the facet width increases, drag coefficient decreases and at a maximum value of facet width, the drag

coefficient is minimum. However, there is small effect of the interspace in the value of the drag coefficient.

5.2.3 Pressure Distribution on Downstream Cylinder

The distribution of static pressure coefficients on the downstream cylinder in a group is shown in Figures 5.30 to 5.34. In Figure 5.30, the distribution of the static pressure coefficients on the downstream square cylinder has been presented. It is observed from this figure that, when the longitudinal spacing is small i.e. L = 1D, 2D and 4D the pressure distributions on the face A are negative, but for large longitudinal spacings i.e. L = 6D and 8D, the pressure distributions become positive. Pressure values for L = 8D are higher than those for the other longitudinal spacing. Even though at L = 8D, the pressure values are lower than those of the single cylinder. There is a wake region in front of the face A of the downstream cylinder produced by the upstream cylinder. When spacing is small, relatively larger may be produced. The flow on this face never becomes potential whereas it is potential for the single cylinder. The velocity on the face A of the single cylinder is higher than that of the face A of the downstream cylinder, because the mean velocity in the wake is less than the free stream velocity. For this reason, the pressure distribution on the face A is quite different than those produced on the face A of the single cylinder, at $\alpha = 0^0$.

On the face C of this cylinder the pressure distribution curves are almost uniform throughout the surface and do not vary a lot for different longitudinal spacings (L). Again, these pressures are higher i.e. less negative, than those of single cylinder on the subsequent surface. This is may be due to high turbulence for which this nature of pressure distribution occurs.

The pressure distribution curves of the face B and face D are identical because of symmetry. On the face B and face D, at longitudinal spacings of L = 1D, 2D and 4D, the pressure distribution curves are nearly close together and at longitudinal spacings of L = 6D and 8D, the pressure distribution curves are nearly close together. Again, these pressures are higher i.e. less negative, than those of single cylinder on the subsequent surface. This nature of pressure distribution may be due to the high turbulent behavior which is created by the upstream cylinder in the group.

53

The distributions of pressure coefficients on the downstream cylinder of the group with facet width of 7.50 mm at various inter-spaces of L = 1D, 2D, 4D, 6D and 8D have been shown in Figure 5.31. It is observed from this figure that, when the longitudinal spacing is small i.e. L = 1D, 2D and 4D the pressure distributions on the face A are negative, but for high longitudinal spacing i.e. L = 6D and 8D, the pressure distributions become positive. The values of pressure for L = 8D is higher than those of the other longitudinal spacings. On the face C of this cylinder the pressure distribution curves are almost uniform throughout the surface and do not vary a lot for different longitudinal spacings. Again, these pressures are higher i.e. less negative, than those of single cylinder on the subsequent surface. On the other hand pressure distribution curves on the face B and the face D are same because of symmetry. On the face B and the face D, at longitudinal spacings of L = 1D, 2D and 4D, the pressure distribution curves are nearly close and at longitudinal spacings of L = 6D and 8D, the pressure distribution curves are nearly close. Again, these pressures are higher i.e. less negative, than those of single cylinder on the subsequent surface. Comparing the pressure distributions on the face A, face B, face D and the face C from the figures 5.30 and 5.31 they appear to be closer.

The distributions of pressure coefficients on the downstream cylinder of the group with facet width of 15.00 mm at various inter-spaces of L = 1D, 2D, 4D, 6D and 8D have been shown in Figure 5.32. It is revealed from this figure that, when the longitudinal spacing is small i.e. L = 1D, 2D and 4D the pressure distributions on the face A are negative, but for high longitudinal spacing i.e. L = 6D and 8D, the pressure distributions become positive. On the face C of this cylinder the pressure distribution curves are almost uniform throughout the surface and do not vary a lot for different longitudinal spacings. Again, these pressures are higher i.e. less negative, than those of single cylinder on the subsequent surface. On the other hand pressure distribution curves of the face B and the face D are identical because of symmetry. On the face B and the face D, at longitudinal spacings of L = 1D, 2D, 4D, 6D and 8D the pressure distribution curves are nearly close. Again, these pressures are higher i.e. less negative, than those of single cylinder on the subsequent face.

The distributions of pressure coefficients on the downstream cylinder of the group with facet width of 22.50 mm at various inter-spaces of L = 1D, 2D, 4D, 6D and 8D

54

have been shown in Figure 5.33. On the face A, a unusual character of pressure dissimilar is observed. At small interspacings of L = 1D, 2D, the pressure distribution shows the uniform nature approximately. On the face C of this cylinder the pressure distribution curves are almost uniform throughout the surface and do not vary a lot for different longitudinal spacings. Again, these pressures are higher i.e. less negative, than those of single cylinder on the subsequent surface. On the other hand pressure distribution curves on the face B and the face D are same because of symmetry. On the face B and the face D, at longitudinal spacings of L = 1D, 2D, 4D, 6D and 8D the pressure distribution curves are nearly close. Again, these pressures are higher i.e. less negative, than those of single cylinder on the subsequent face.

The distributions of pressure coefficients on the downstream cylinder of the group with facet width of 30.0 mm at various inter-spaces of L = 1D, 2D, 4D, 6D and 8D have been shown in Figure 5.34. On the face A, at small interspacing values i.e. L = 1D, 2D, the pressure distribution curves show the oscillating nature and the values are close to zero and they are close to each other. On the face C of this cylinder the pressure distribution curves are almost uniform throughout the surface and do not vary a lot for different longitudinal spacings. Again, these pressures are higher i.e. less negative, than those of single cylinder on the subsequent surface. On the other hand pressure distribution curves on the face B and the face D are identical because of symmetry. On the face B and the face D, at longitudinal spacings of L = 1D, 2D, 4D, 6D and 8D the pressure distribution curves are nearly close. Again, these pressures are higher i.e. less negative, than those of single cylinder on the subsequent surface.

5.2.4 Variation of Drag for Downstream Cylinder

The variation of drag coefficient (C_d) on downstream cylinder (R) in a group at different longitudinal spacings (L) is shown in Figures 5.35 to 5.40. In Figure 5.35, variation of drag coefficients on the square cylinder has been presented. The drag coefficients at the different inter-spaces of L = 1D, 2D, 4D, 6D and 8D between the upstream and the downstream cylinders are given in this figure. It is seen from this figure that at small inter-space values negative drag is developed while at large inter-space values positive drag is found but they are significantly lower than that on the single cylinder. The presence of the upstream cylinder reduces the drag significantly

on the downstream cylinder. It can be explained from the pressure distributions on this cylinder.

In Figure 5.36, variation of drag coefficients on square cylinder with facet width of 7.50 mm has been presented. The drag coefficients at the different inter-spaces of L = 1D, 2D, 4D, 6D and 8D between the upstream and the downstream cylinders is provided in this figure. It is observed from this figure that at small inter-space values negative drag is developed while at large inter-space values positive drag is obtained. The values of drag coefficient are much lower than that on the single cylinder. The presence of the upstream cylinder reduces the drag significantly on the downstream cylinder. It can be explained from the pressure distributions on this cylinder.

In Figure 5.37, variation of drag coefficients on square cylinder with facet width of 15.00 mm has been shown. The drag coefficients at the various inter-spaces of L = 1D, 2D, 4D, 6D and 8D is provided in this figure. At small value of inter-space negative drag coefficient is found. On the other hand at large values of inter-space positive values are obtained. The values are remarkably lower than those for the single cylinder. The presence of the upstream cylinder reduces the drag significantly on the downstream cylinder. It can be explained from the pressure distributions on this cylinder.

In Figure 5.38, variation of drag coefficients on square cylinder with facet width of 22.50 mm is shown. The variation of drag coefficients at the various inter-spaces of L = 1D, 2D, 4D, 6D and 8D is given in this figure. With the increase of inter-space value drag coefficient increases then it begin to fall with further increase in the inter-space value. However, all values are positive and much lower than that on the single cylinder. The presence of the upstream cylinder reduces the drag significantly on the downstream cylinder. It can be explained from the pressure distributions on this cylinder.

In Figure 5.39, variation of drag coefficients on cylinder with facet width of 30.00 mm has been presented. The variation of drag coefficients at the various inter-spaces of L = 1D, 2D, 4D, 6D and 8D is provided in this figure. It can be noticed from this figure that at small inter-space value, the drag coefficient increases then begin to fall with further increase of inter-space. However, the values of drag coefficient are

remarkably lower than that on the single cylinder. The presence of the upstream cylinder reduces the drag significantly on the downstream cylinder. It can be explained from the pressure distributions on this cylinder.

Finally, in Figure 5.40, variation of drag coefficient with interspace on downstream cylinder in a group for various facet widths has been presented. It can be observed from this figure that there is reasonable effect of facet width on the drag coefficient. As the facet width increases, drag coefficient increases up to a certain interspace and then decreases width further increase of interspace. However, there is small effect of the interspace in the value of the drag coefficient.

5.3   Observation of Pressure Fluctuations

The pressure data are recorded at steady state condition. During recording of the pressure data, fluctuation of liquid in the manometer limbs is always observed due to separated flow and interference of the flows (in staggered form). This fluctuation is very low for the test on a single cylinder at an angle of attack, $\alpha = 0^0$. Whereas, in the higher range of angle of attack fluctuation of pressure slightly increased, especially on the face D; but the difference between the maximum and minimum liquid column observed in the manometer limb never exceeds 7mm. When two cylinders are considered, fluctuations increased appreciably on the downstream cylinder and the maximum fluctuation observed is of the order of 10 mm. However, for this test, always mean pressure is recorded with careful observation.

(a)

(b)

(c)

$\beta_3 > \beta_2 > \beta_1$
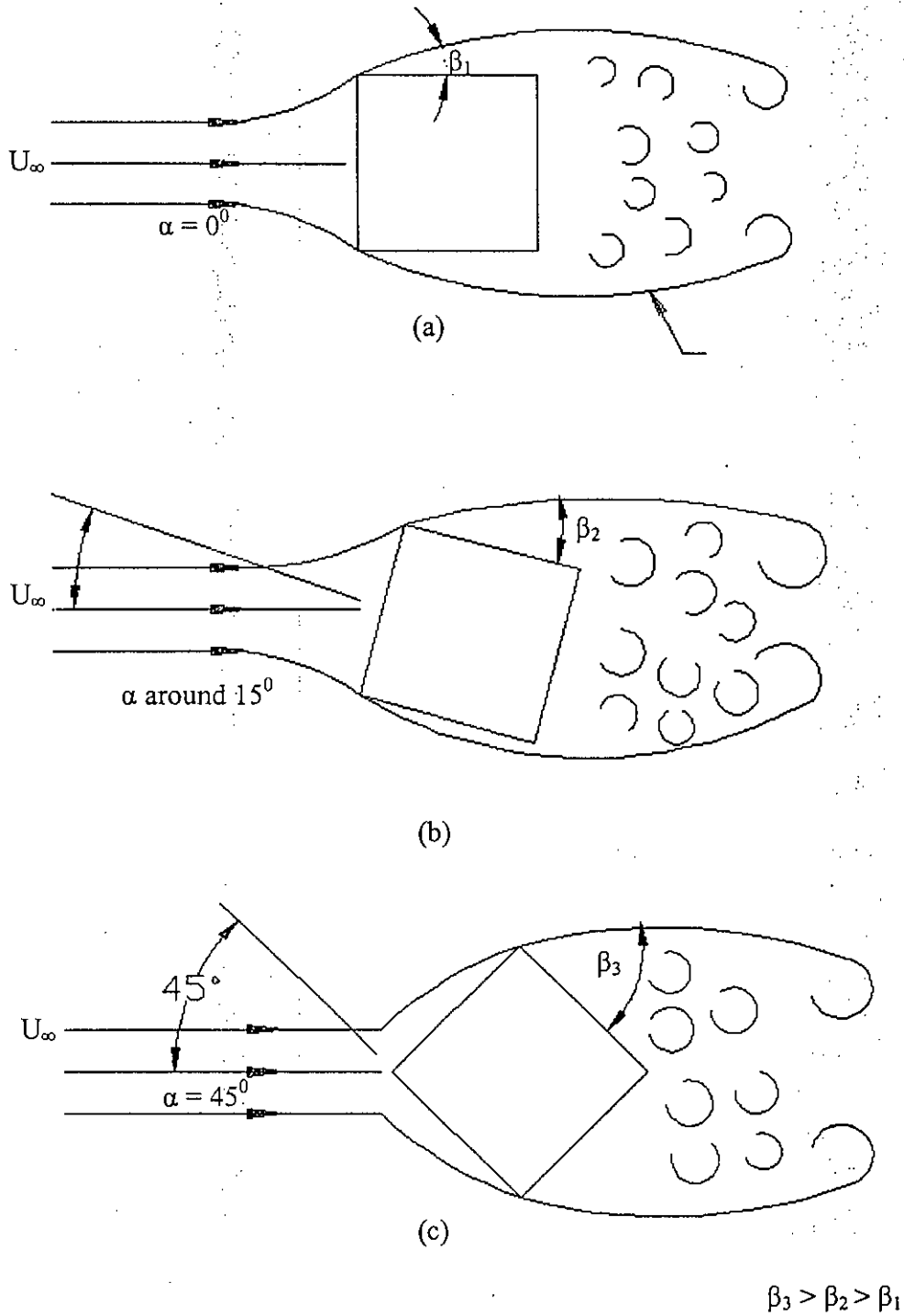
Figure 5.1: Square Cylinder in Flow Field showing Typical Nature of Vortex

58
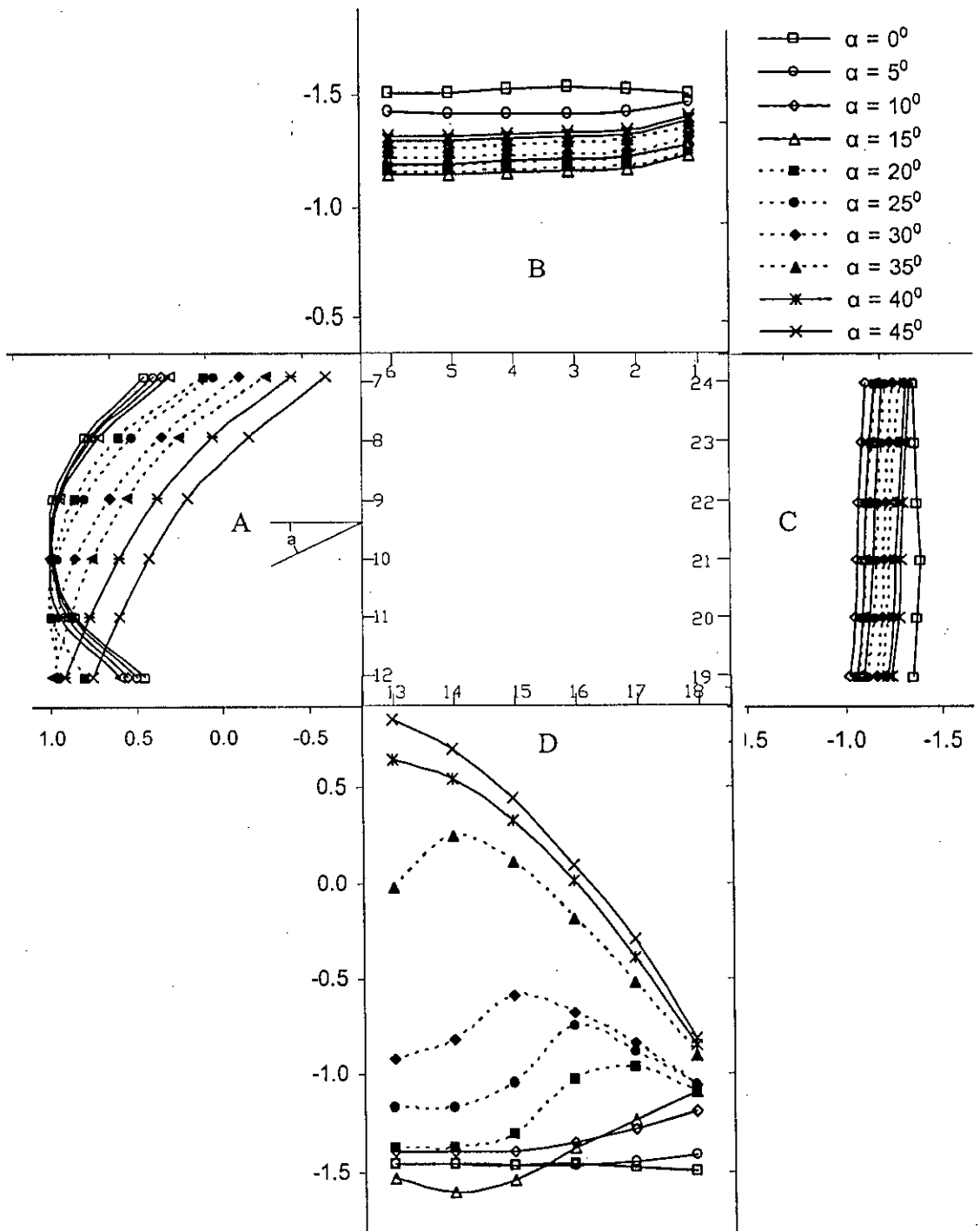
Figure 5.2: Pressure Coefficients at Various Angles of Attack for Cylinder with Facet Width of 0.0mm (i.e. flat).

59
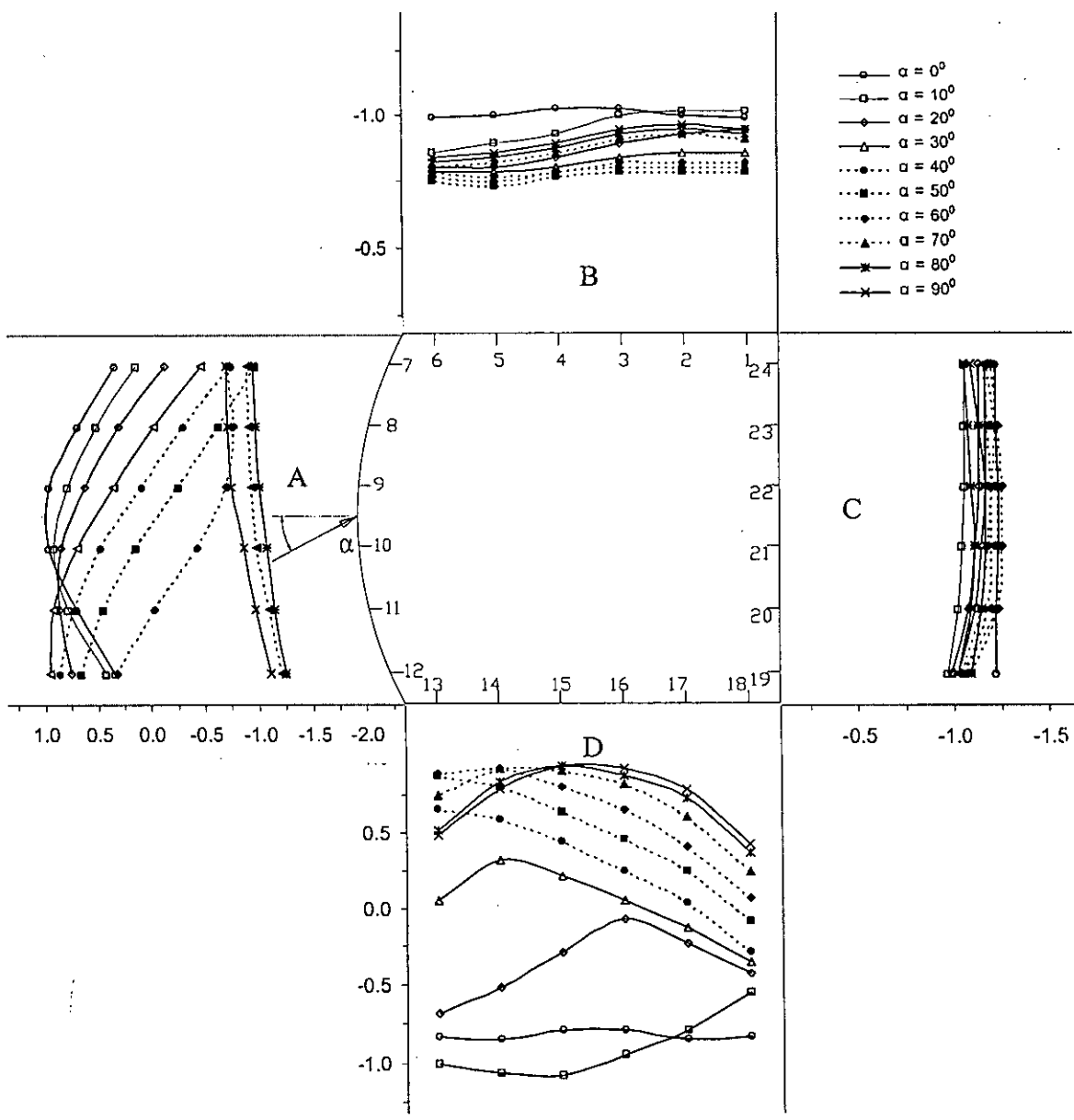
Figure 5.3: Pressure Coefficients at Various Angles of Attack for Cylinder with Facet Width of 7.50mm.
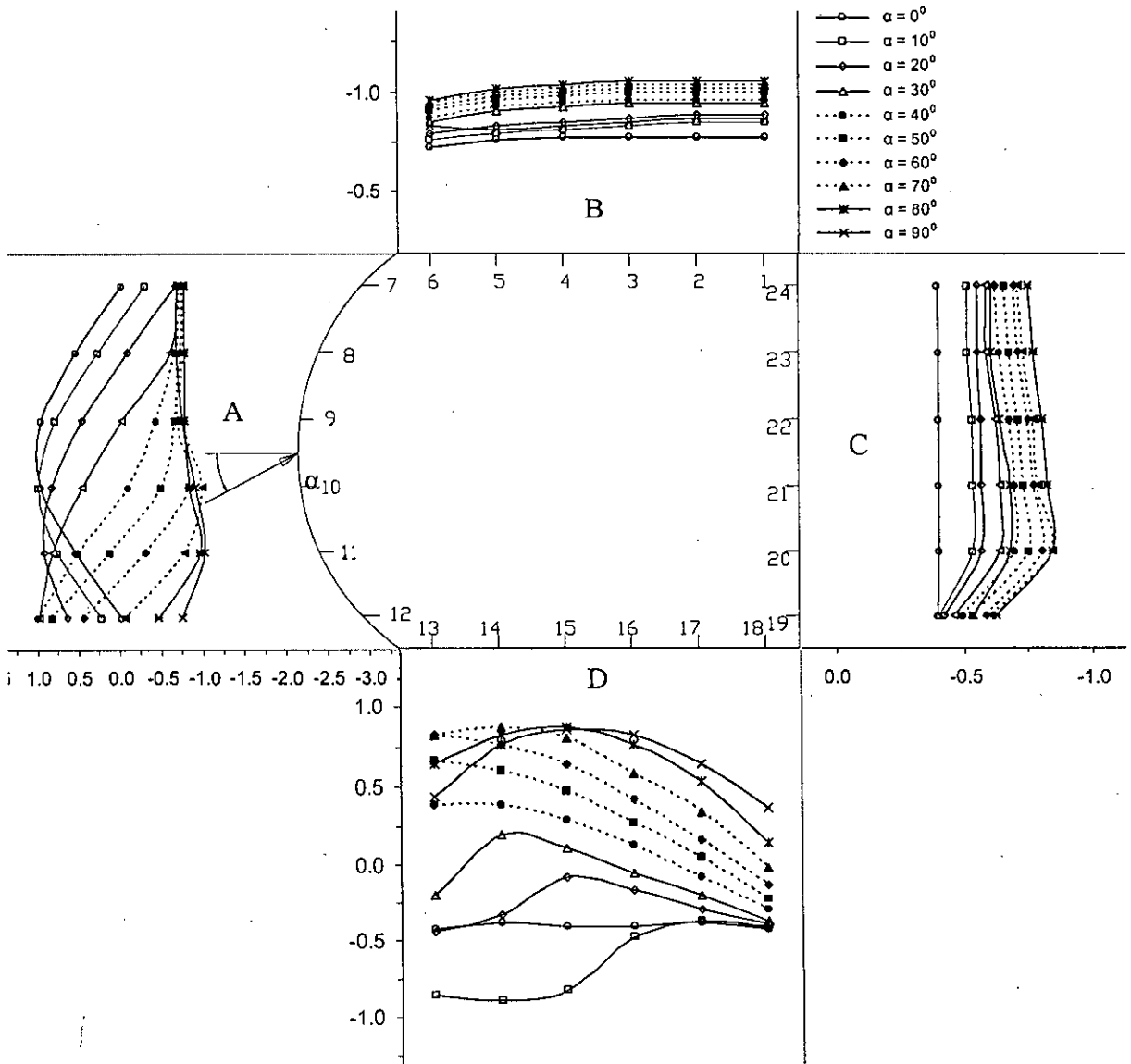
Figure 5.4: Pressure Coefficients at Various Angles of Attack for Cylinder with Facet Width of 15.00mm.
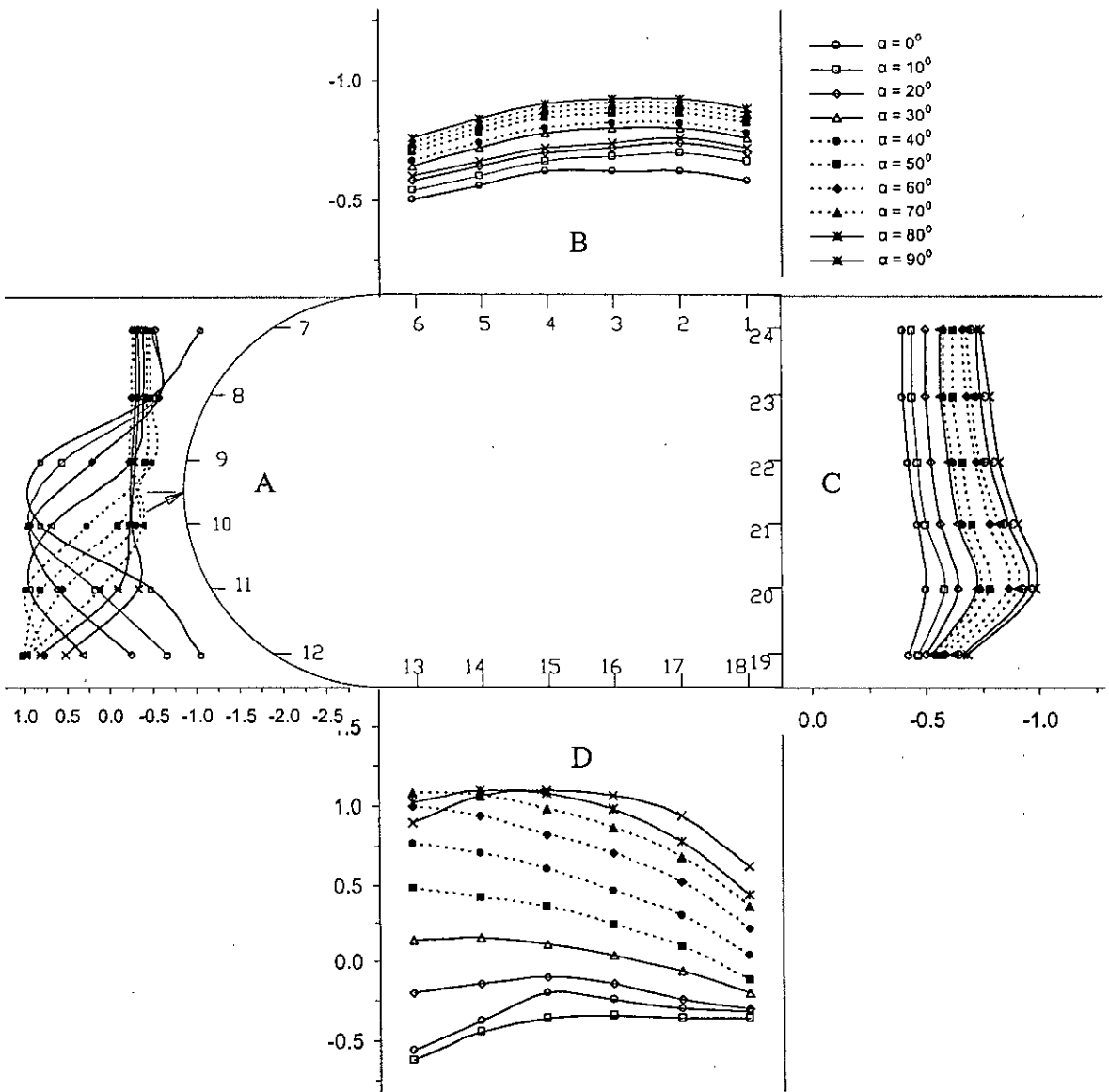
Figure 5.6: Pressure Coefficients at Various Angles of Attack for Cylinder with Facet Width of 30.00mm
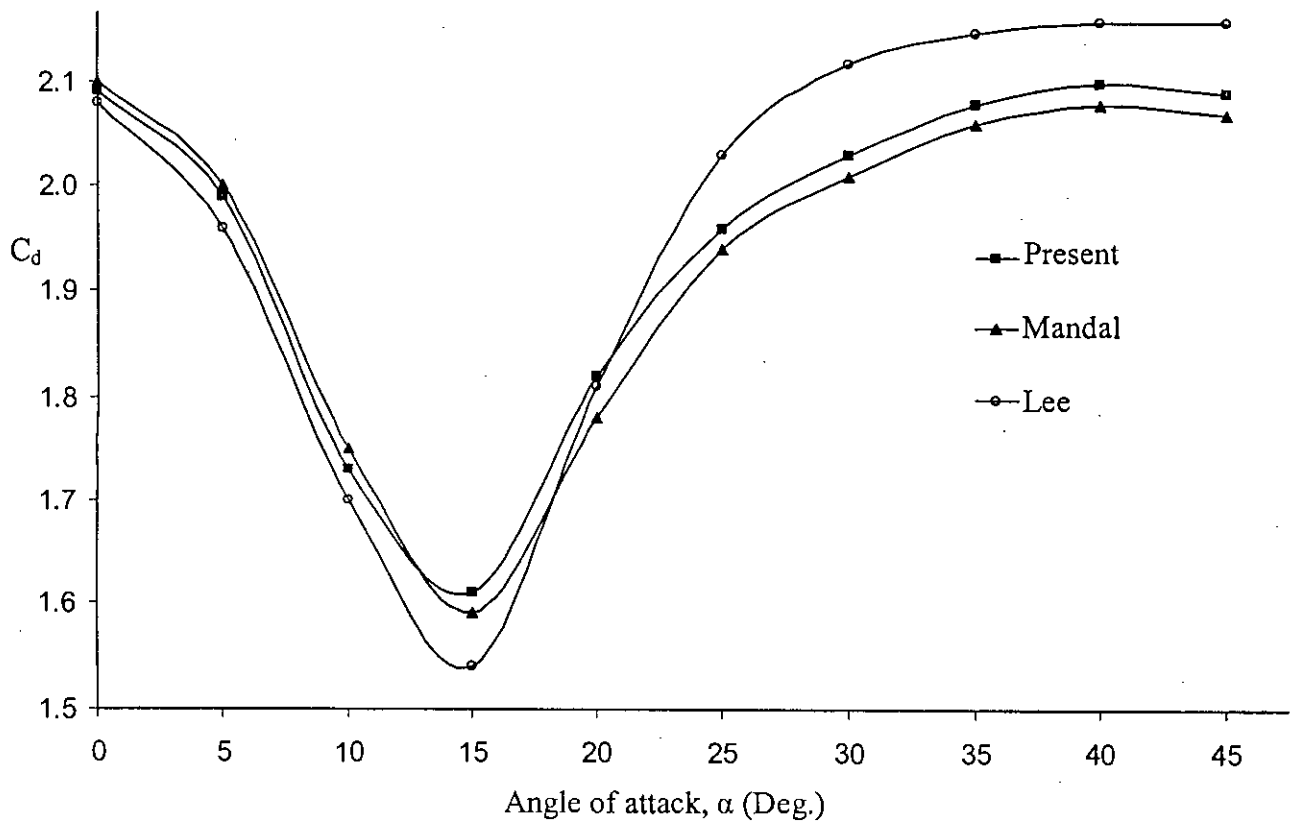
Figure 5.7: Variation of Drag Coefficient (C_d) with Angle of Attack (α) for Square Cylinder.
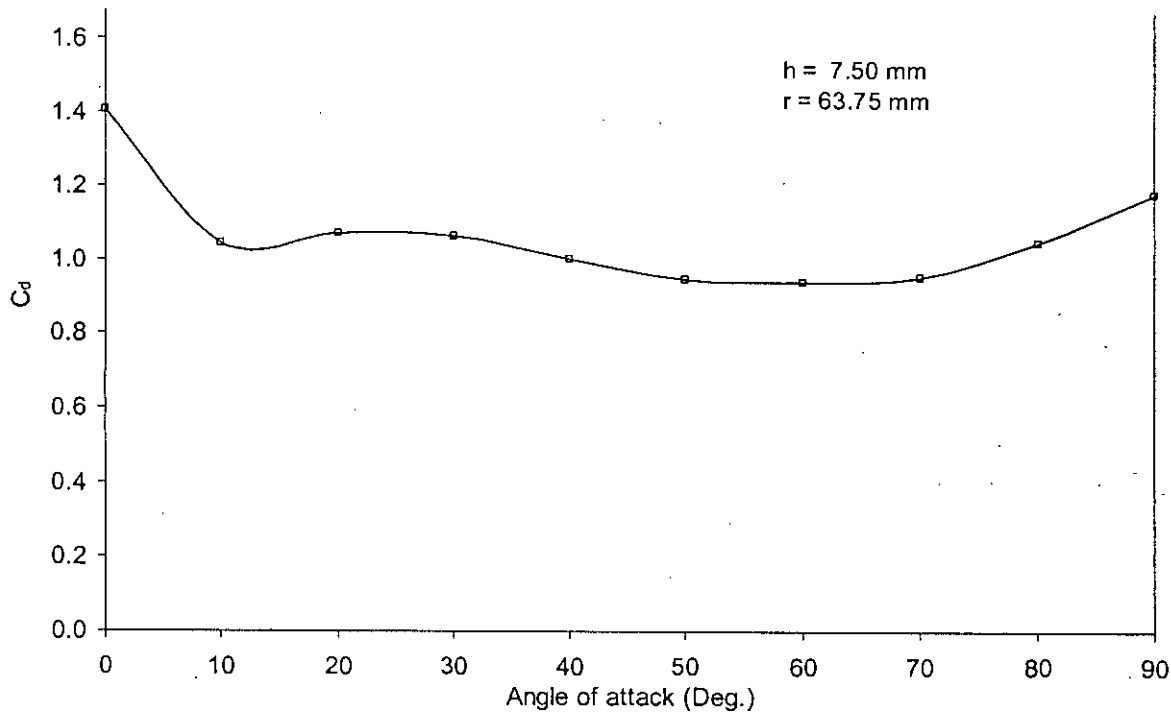
Figure 5.8: Variation of Drag Coefficient (C_d) with Angle of Attack (α) for Cylinder with Facet Width of 7.50mm.
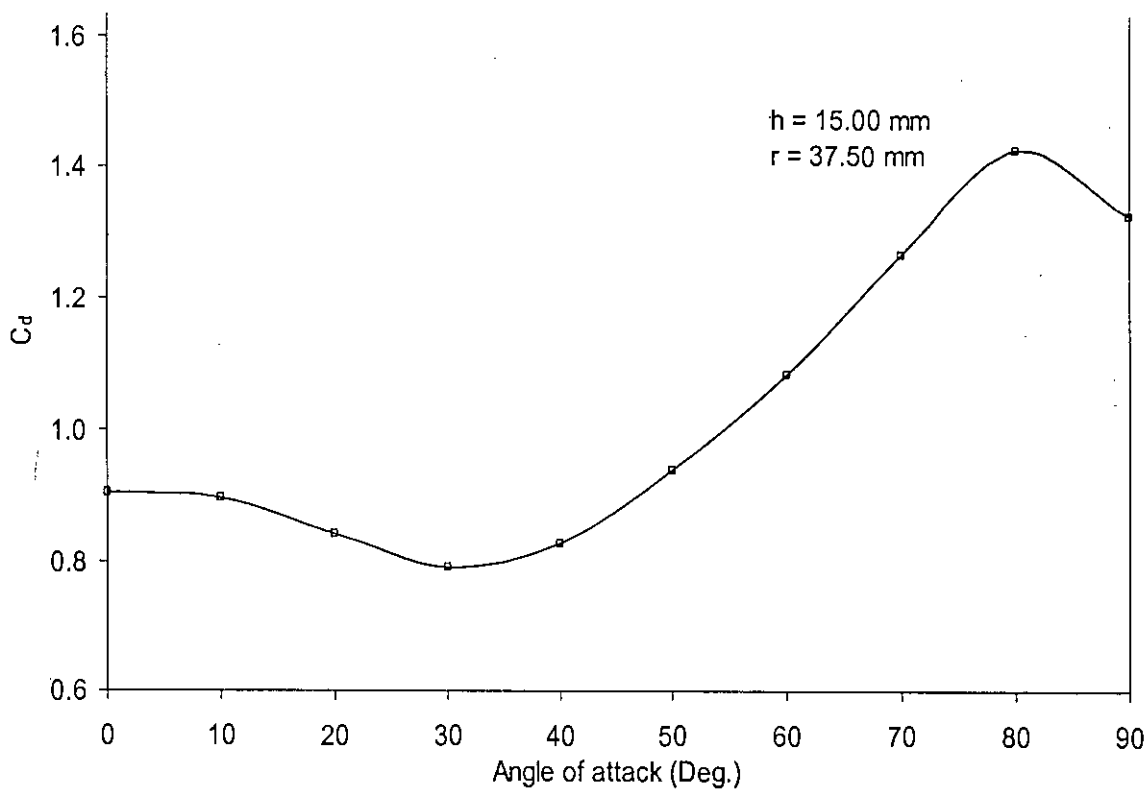
Figure 5.9: Variation of Drag Coefficient (C_d) with Angle of Attack (α) for Cylinder with Facet Width of 15.00mm.
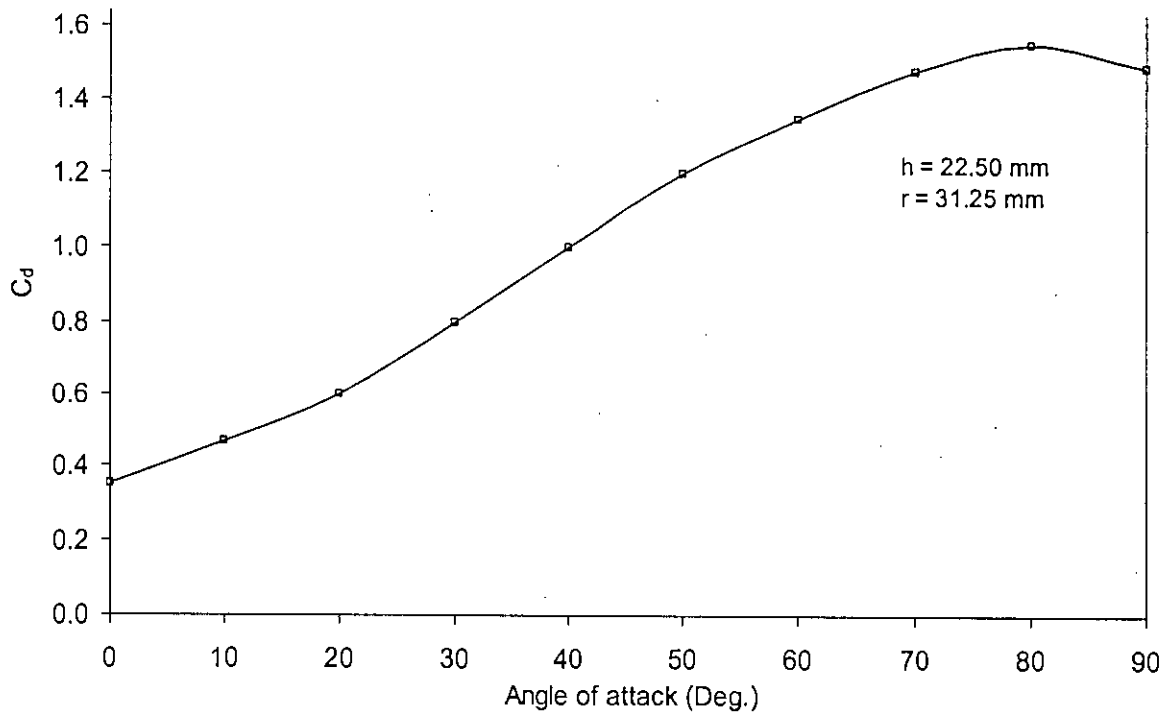
Figure 5.10: Variation of Drag Coefficient (C_d) with Angle of Attack (α) for Cylinder with Facet Width of 22.50mm.
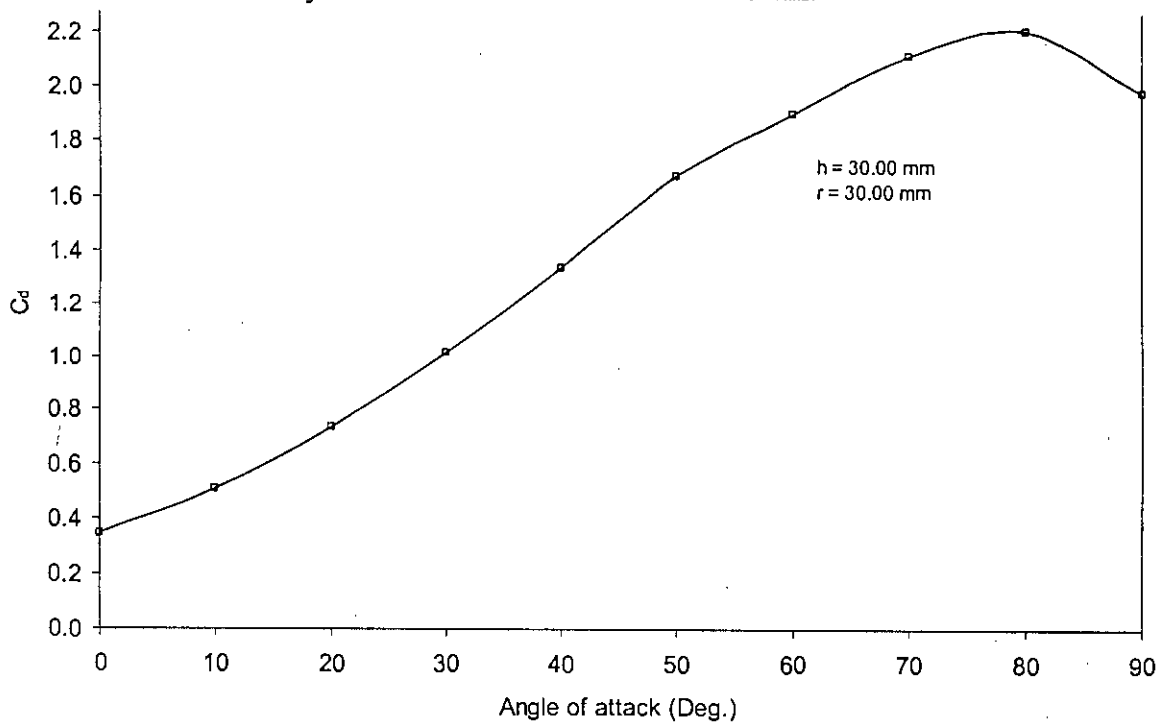
Figure 5.11: Variation of Drag Coefficient (C_d) with Angle of Attack (α) for Cylinder with Facet Width of 30.00

66
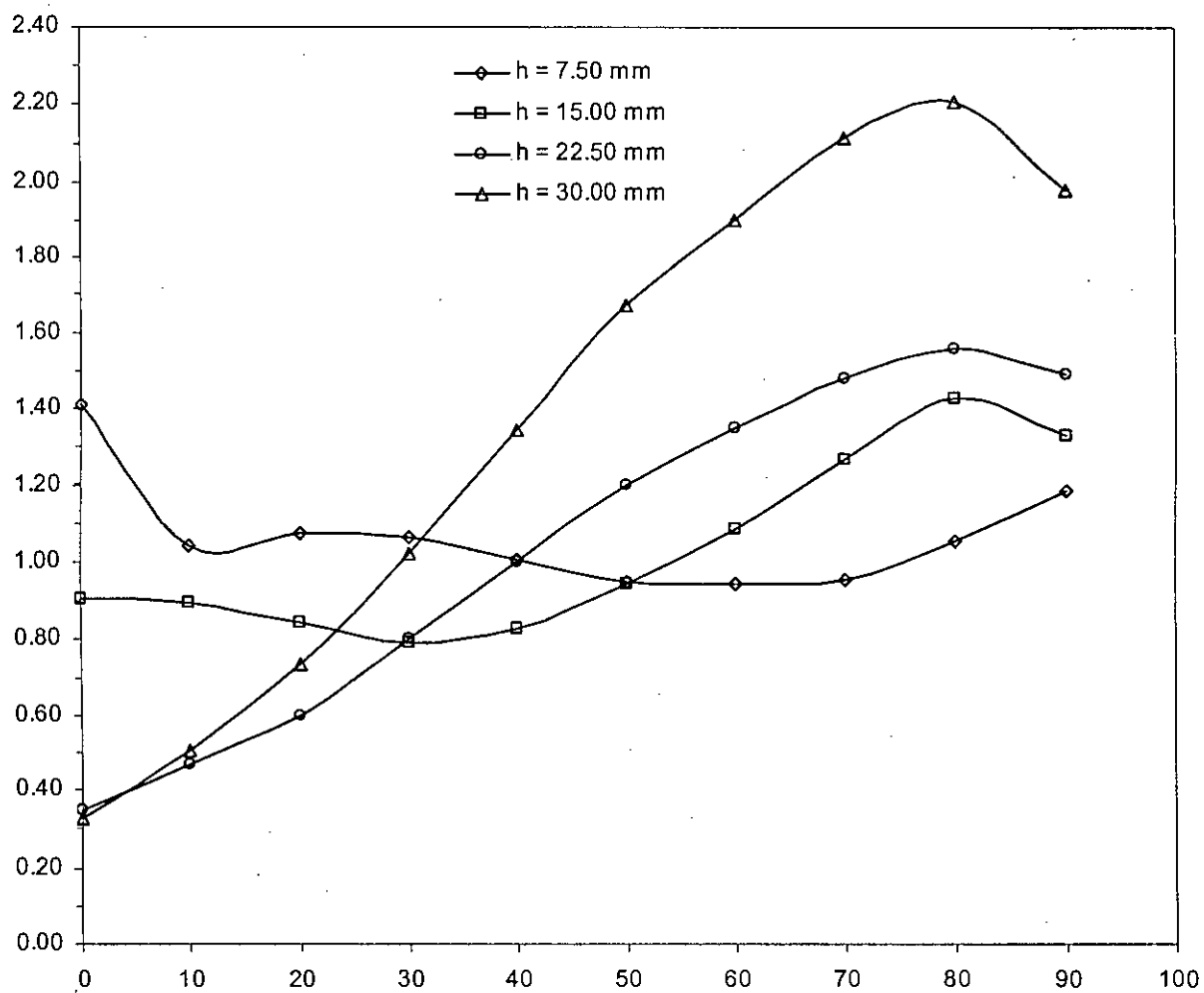
Figure 5.12: Variation of Drag Coefficient (C_d) with Angle of Attack (α) for Cylinder with Different Facet Widths
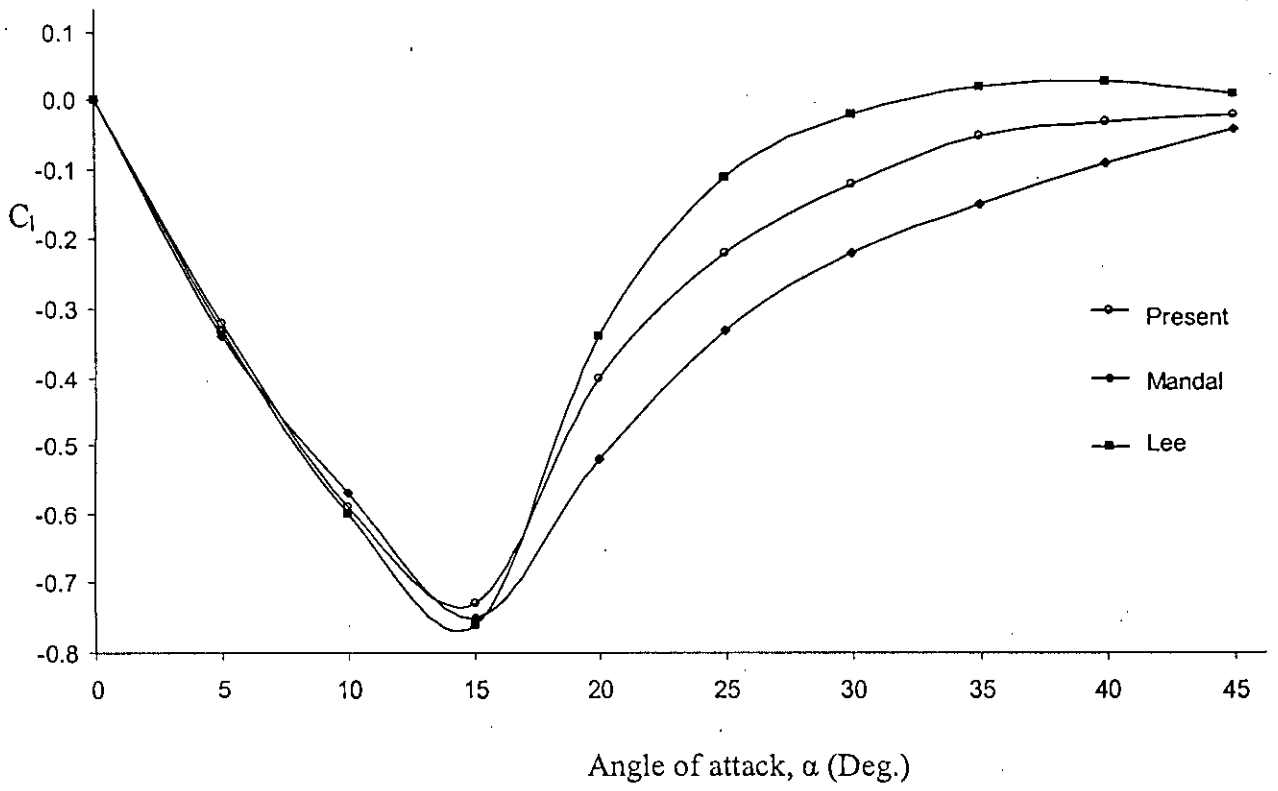
Figure 5.13: Variation of Lift Coefficient (C_l) with Angle of Attack (α) for Square Cylinder.
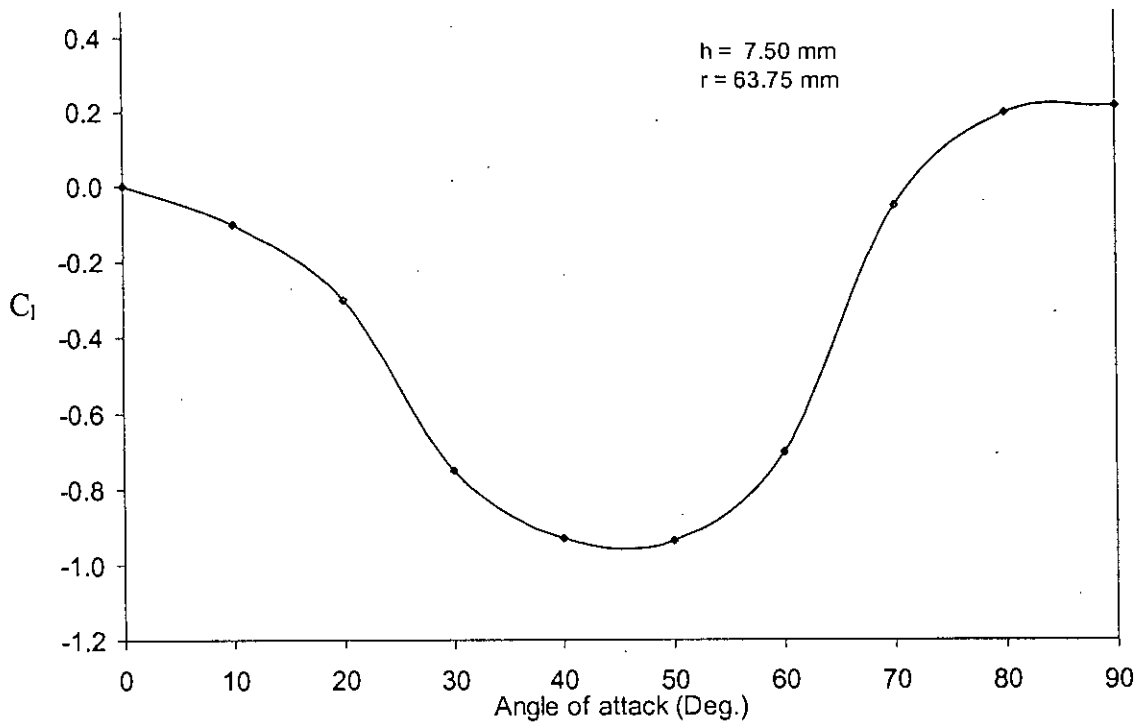
Figure 5.14: Variation of Lift Coefficient (C_l) with Angle of Attack (α) for Cylinder with Facet Width of 7.50mm.
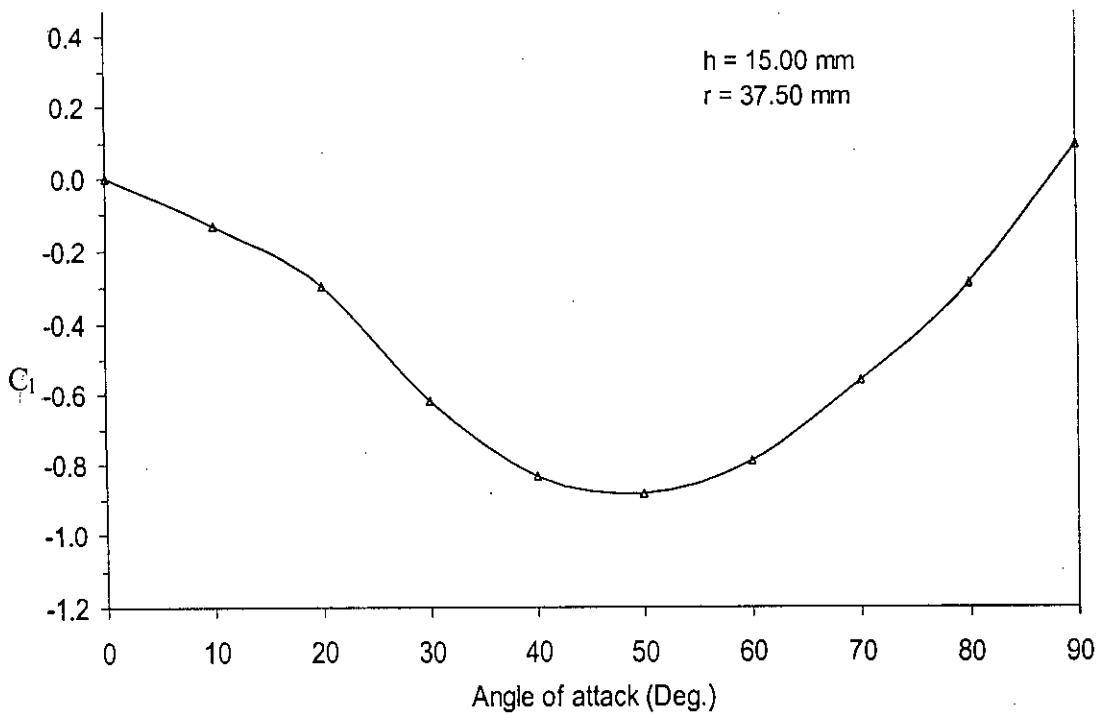
Figure 5.15: Variation of Lift Coefficient (C_l) with Angle of Attack (α) for Cylinder with Facet Width of 15.00mm.
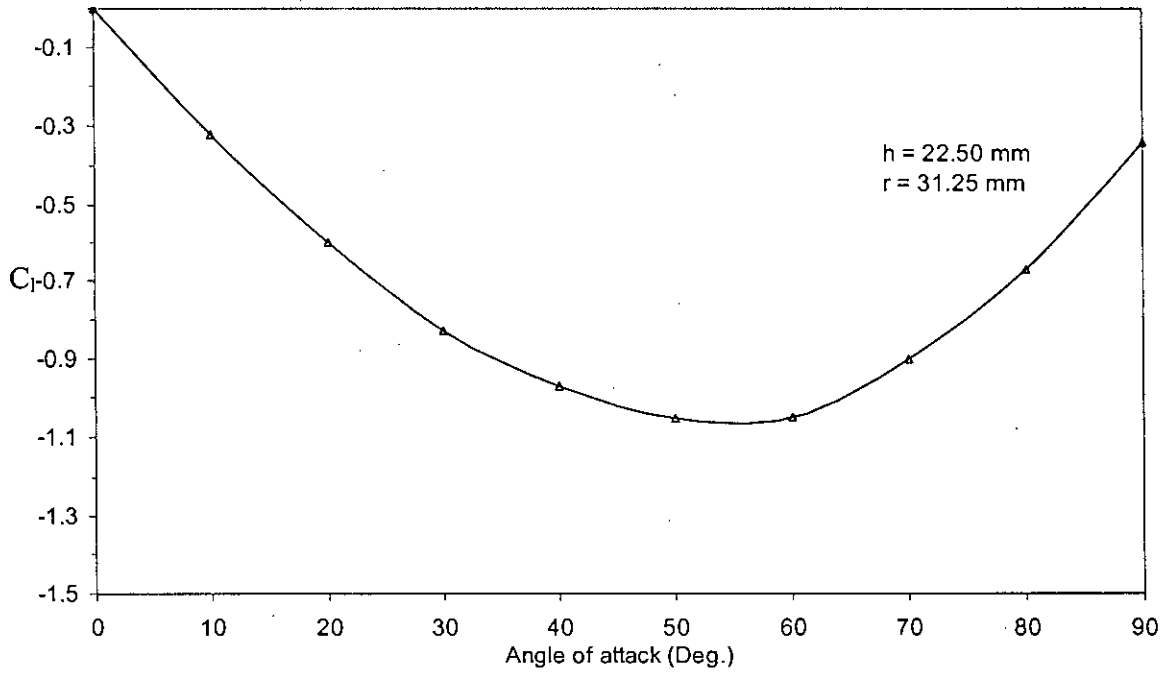
Figure 5.16:Variation of Lift Coefficient (C_l) with Angle of Attack (α) for Cylinder with Facet Width of 22.50mm.
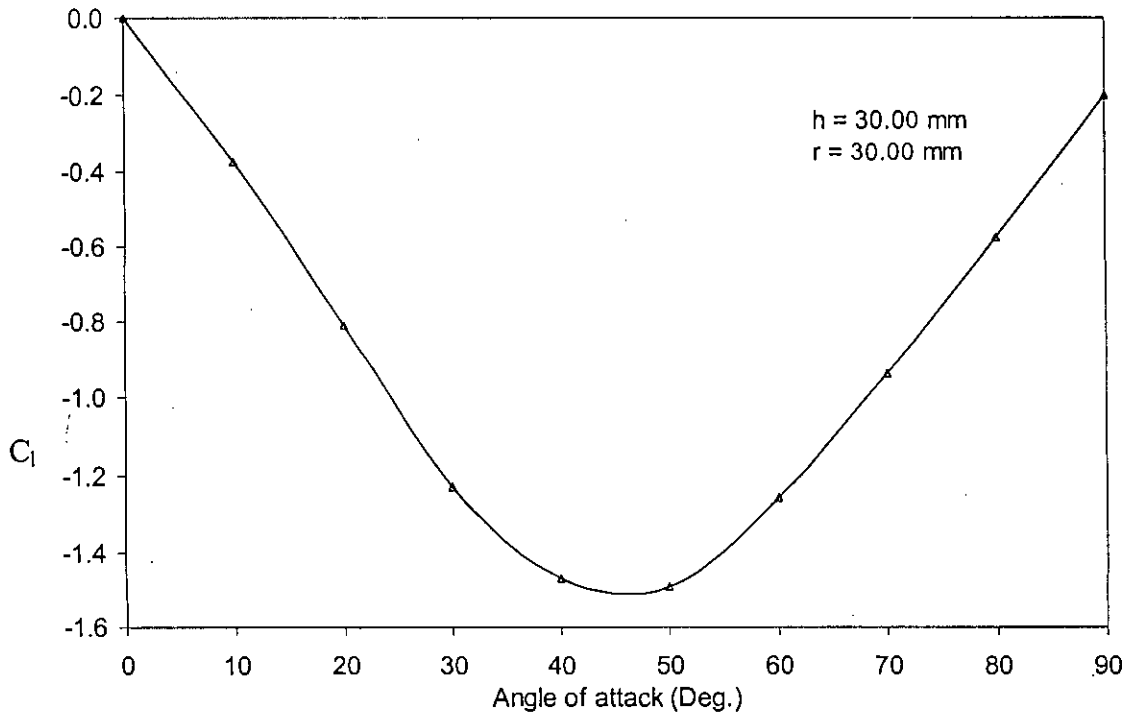
Figure 5.17: Variation of Lift Coefficient (C_l) with Angle of Attack (α) for Cylinder with Facet Width of 30.00mm.

70
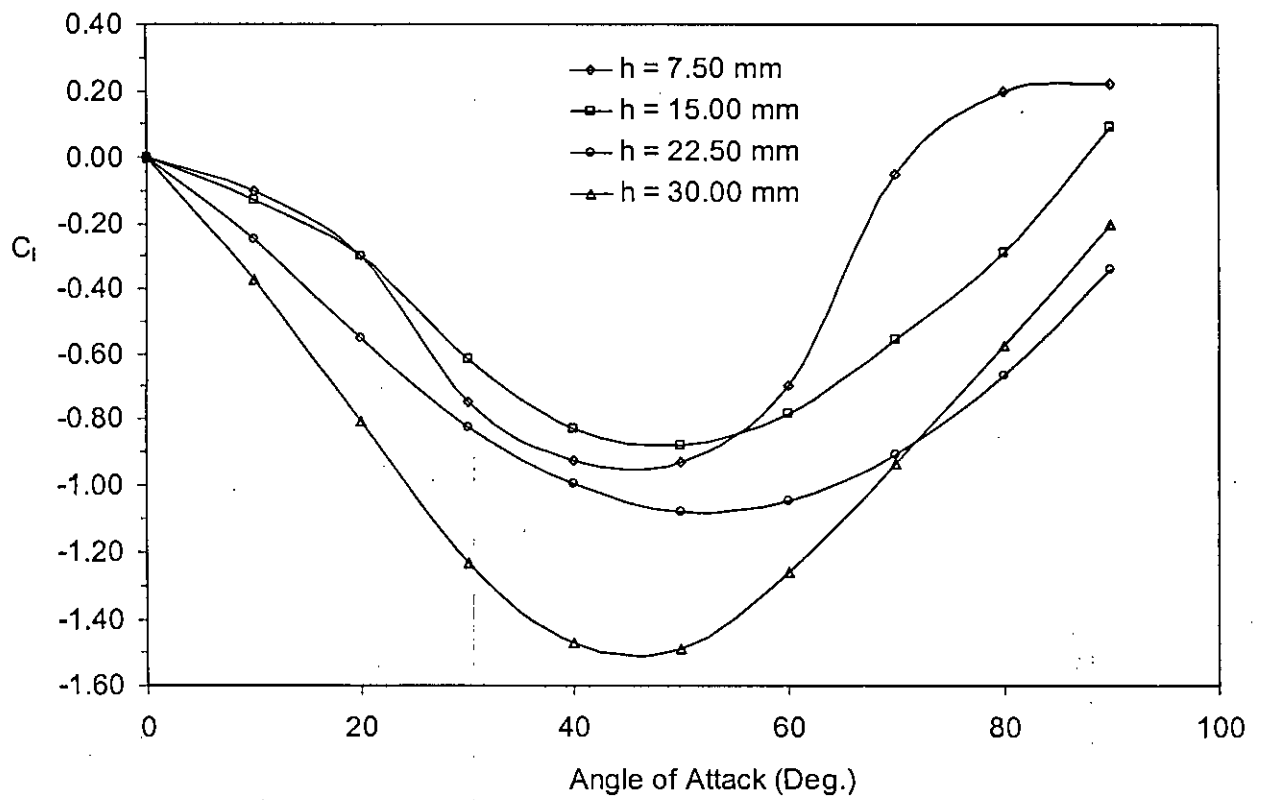
Figure 5.18: Variation of Lift Coefficient (C_l) with Angle of Attack (α) for Cylinder with Different Facet Widths
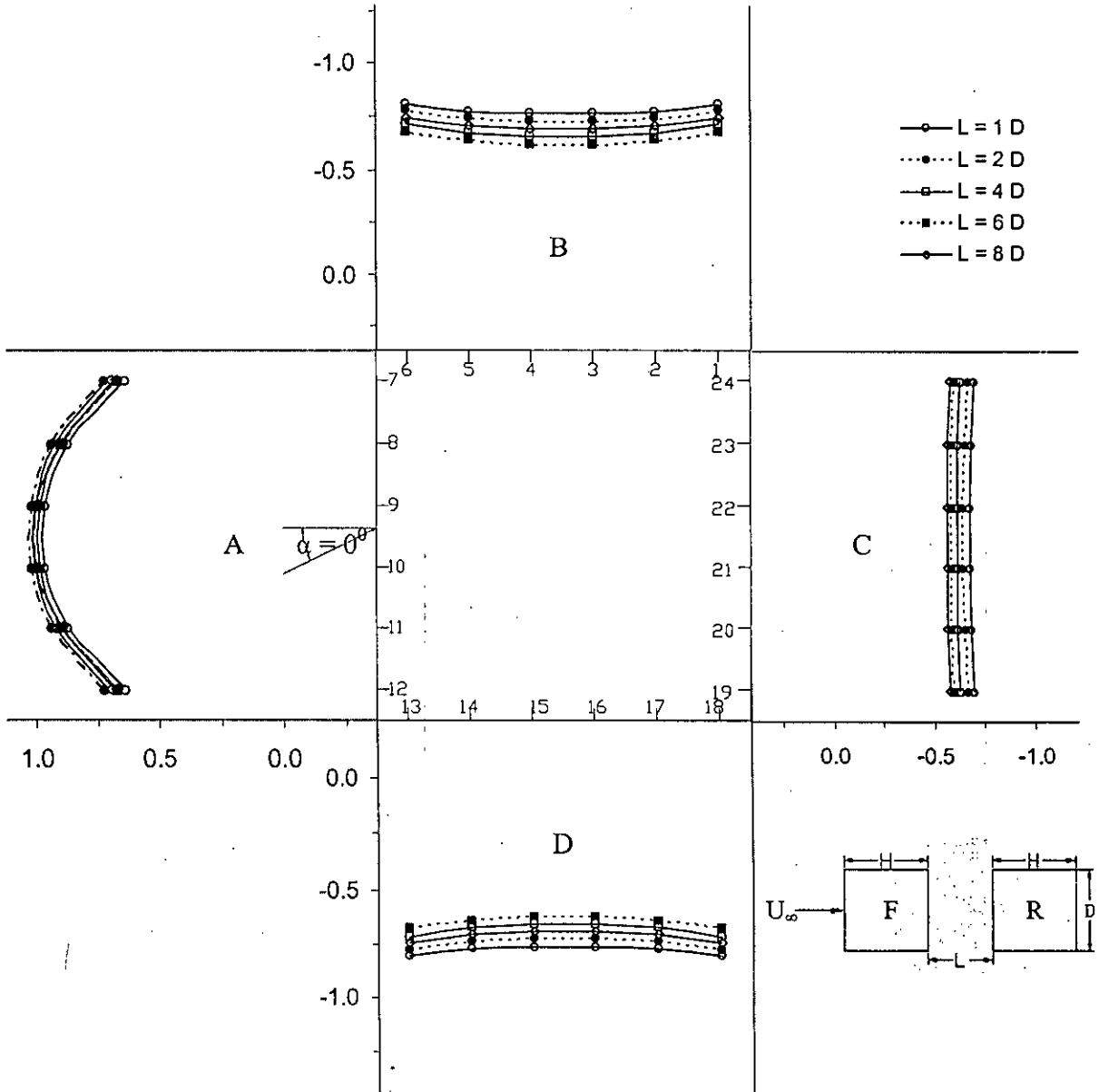
Figure 5.19: Static Pressure Distribution on Front Cylinder in a Group with Facet Width of 0.00 mm (i.e. flat) for Various Longitudinal Spacings.
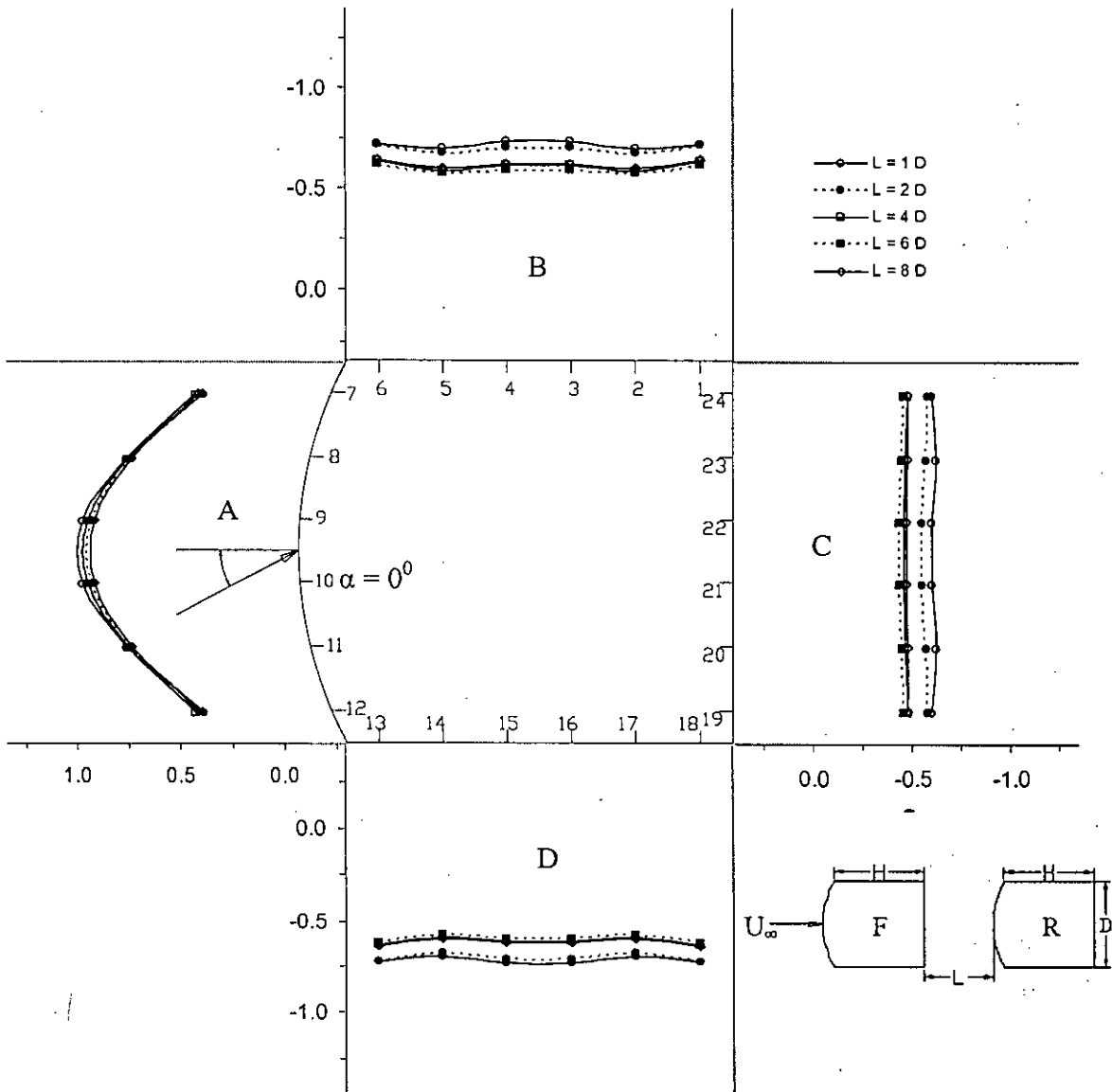
Figure 5.20: Static Pressure Distribution on Front Cylinder in a Group with Facet Width of 7.50 mm for Various Longitudinal Spacings.
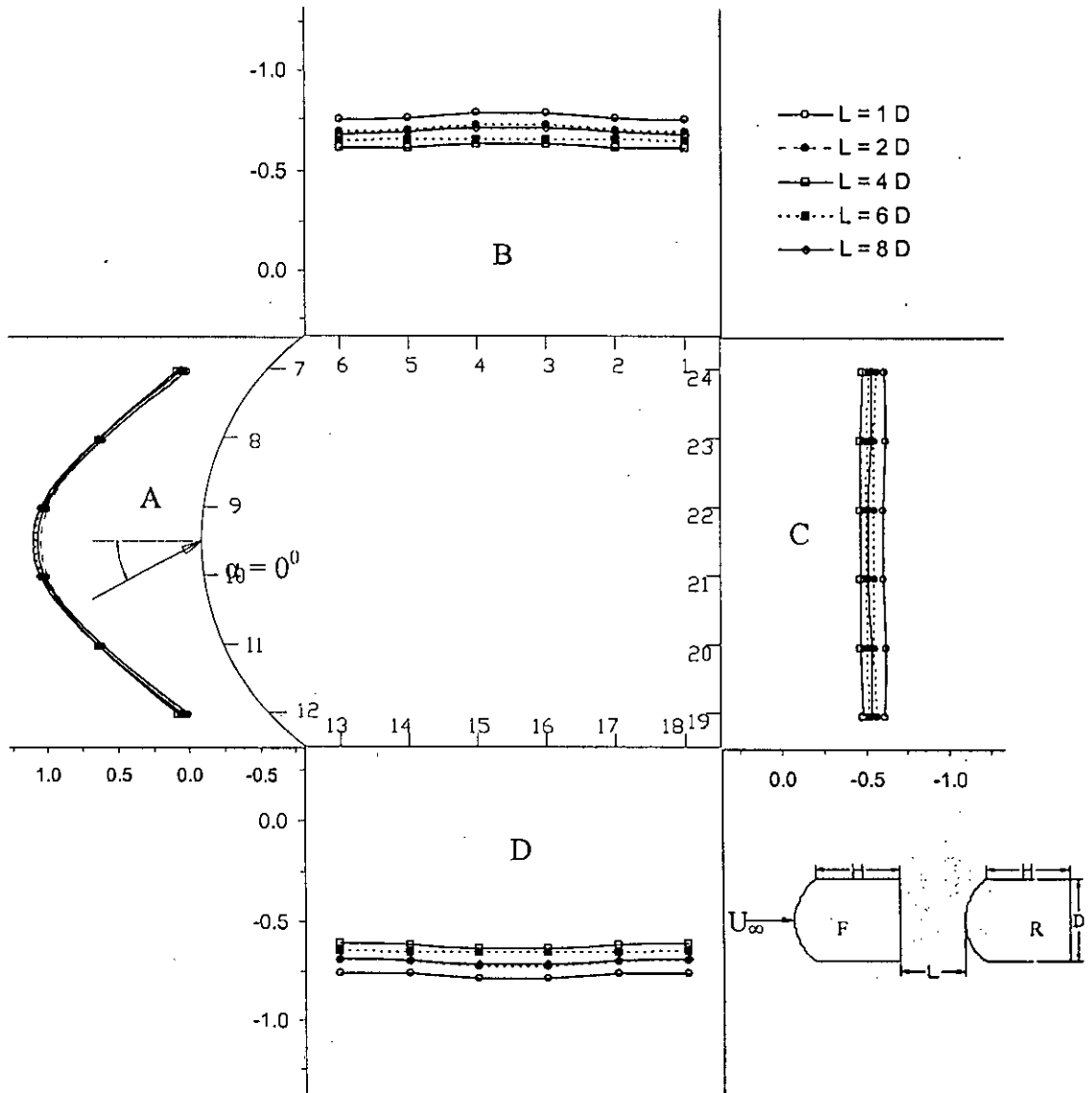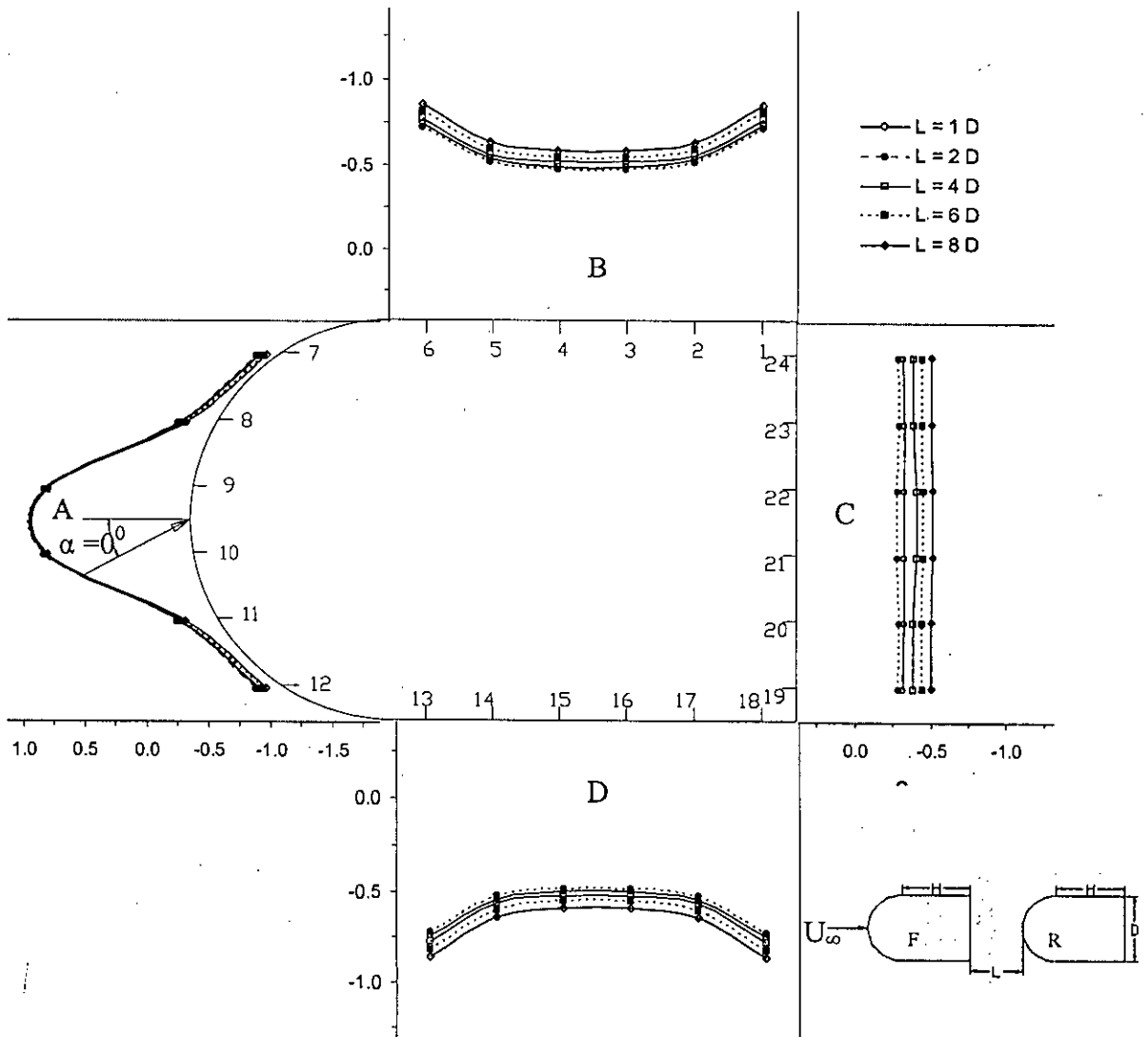
Figure 5.21: Static Pressure Distribution on Front Cylinder in a Group with Facet Width of 15.00 mm for Various Longitudinal Spacings.
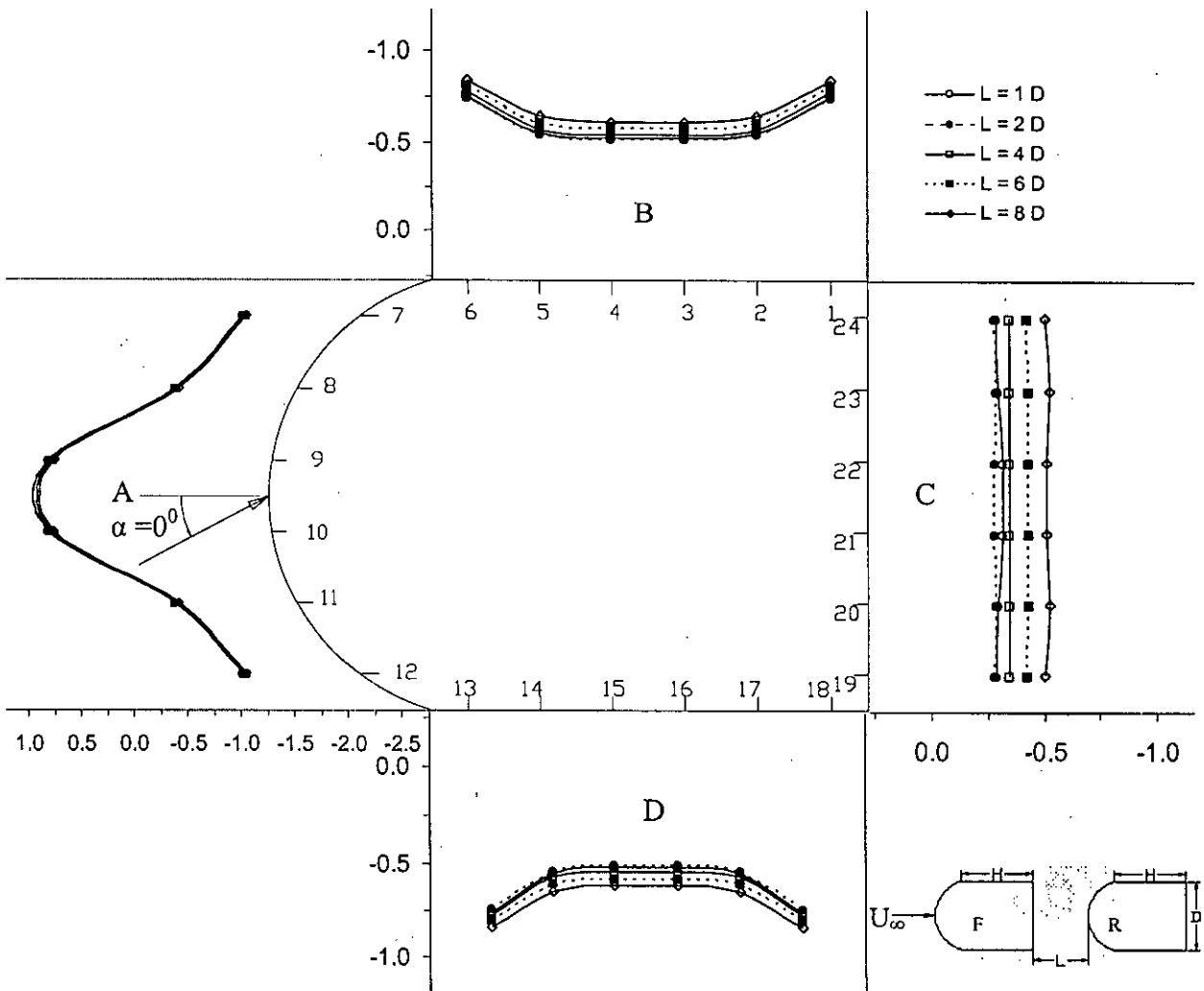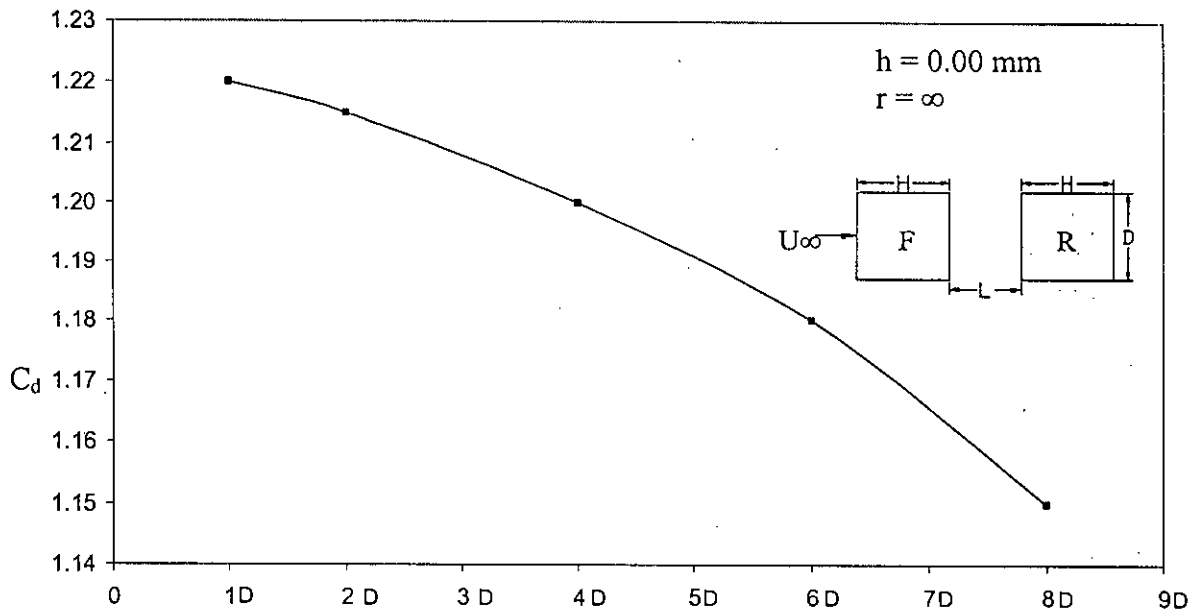
Figure 5.22: Static Pressure Distribution on Front Cylinder in a Group with Facet Width of 22.50 mm for Various Longitudinal Spacings.

Figure 5.23: Static Pressure Distribution on Front Cylinder in a Group with Facet Width of 30.00 mm for Various Longitudinal Spacings.

Figure 5.24: Variation of Drag Coefficient (C_d) with Inter Spaces on Front Square
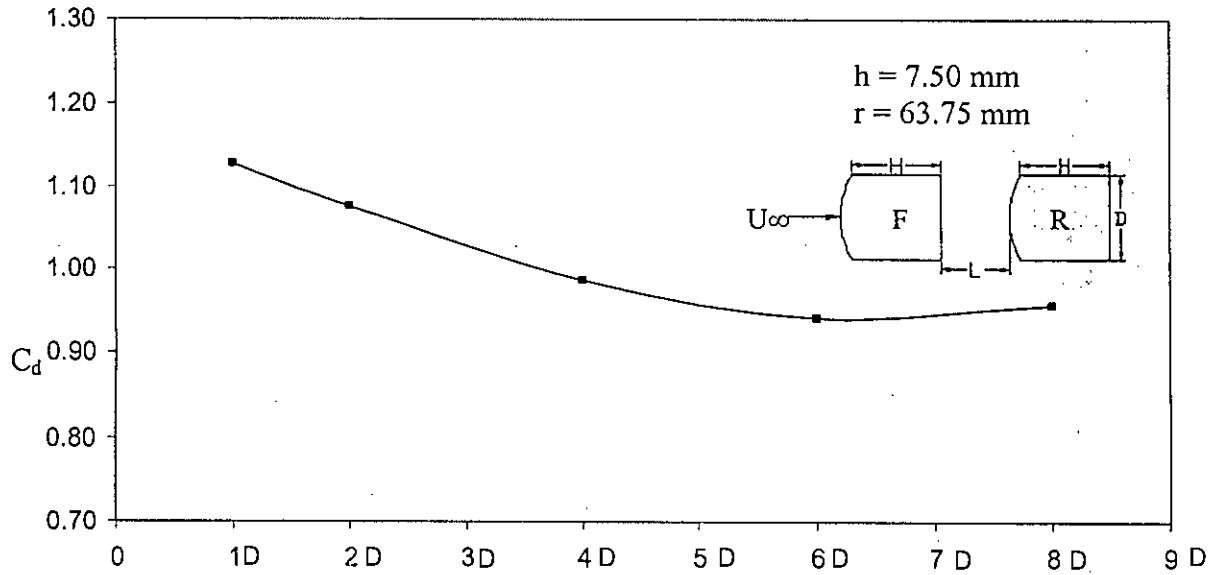Cylinder in a Group

Figure 5.25: Variation of Drag Coefficient (C_d) with Inter Spaces on Front
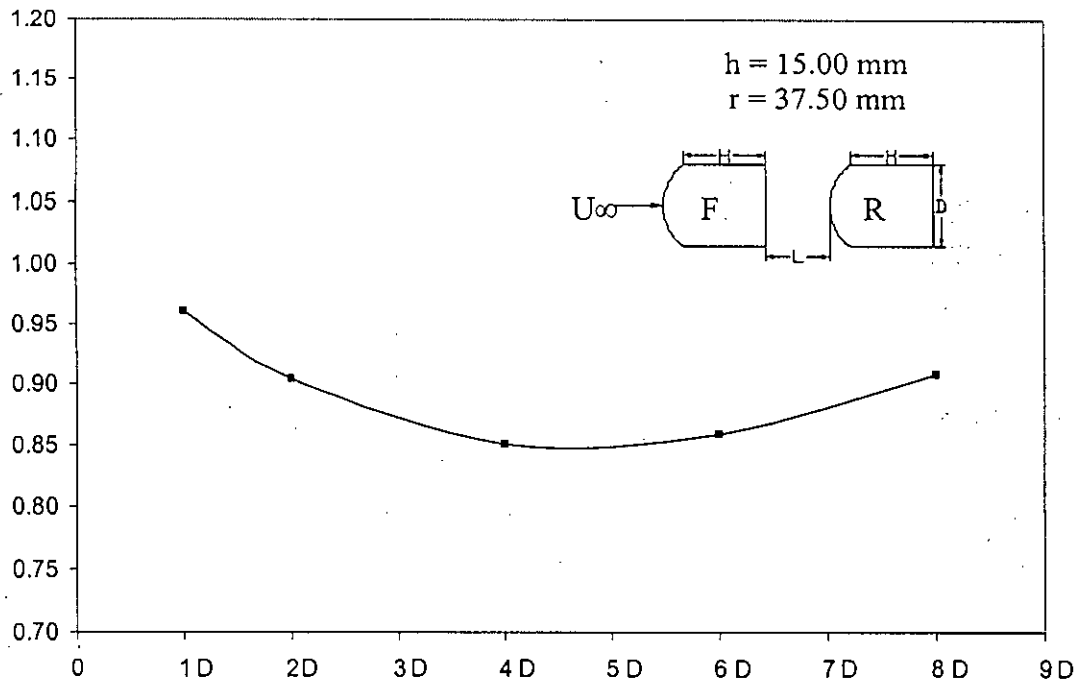Cylinder with Facet Width of 7.50mm in a Group

77

Figure 5.26: Variation of Drag Coefficient (C_d) with Inter Spaces on Front Cylinder with Facet Width of 15.000mm in a Group
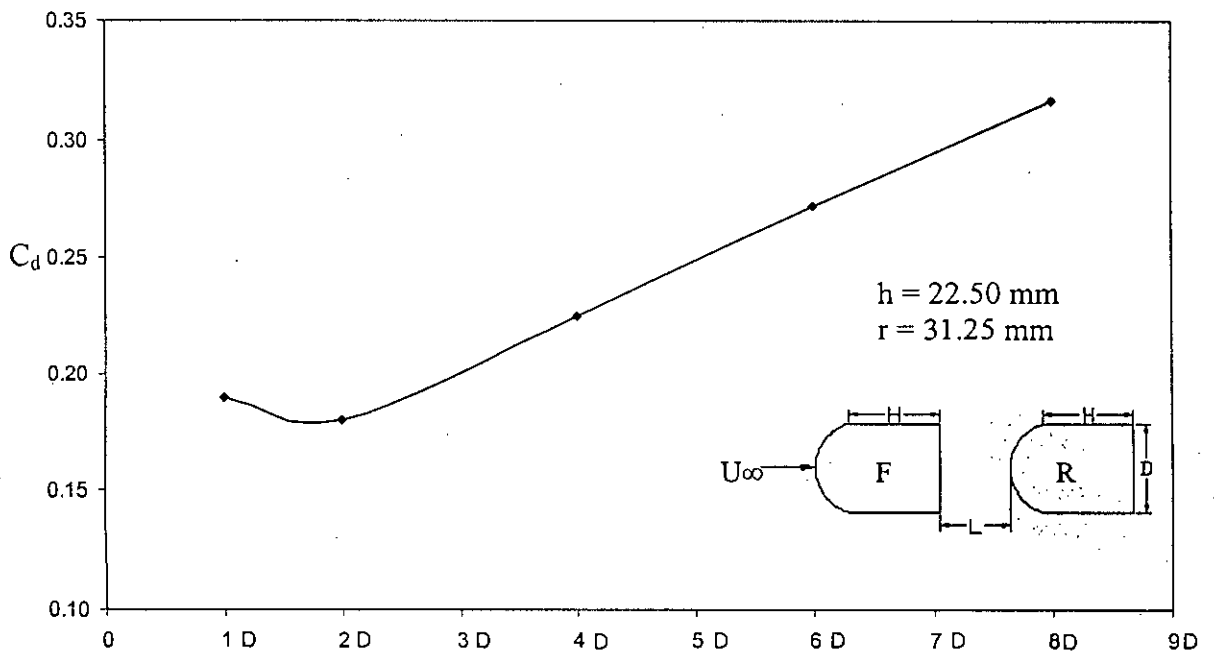

Figure 5.27: Variation of Drag Coefficient (C_d) with Inter Spaces on Front Cylinder with Facet Width of 22.50mm in a Group
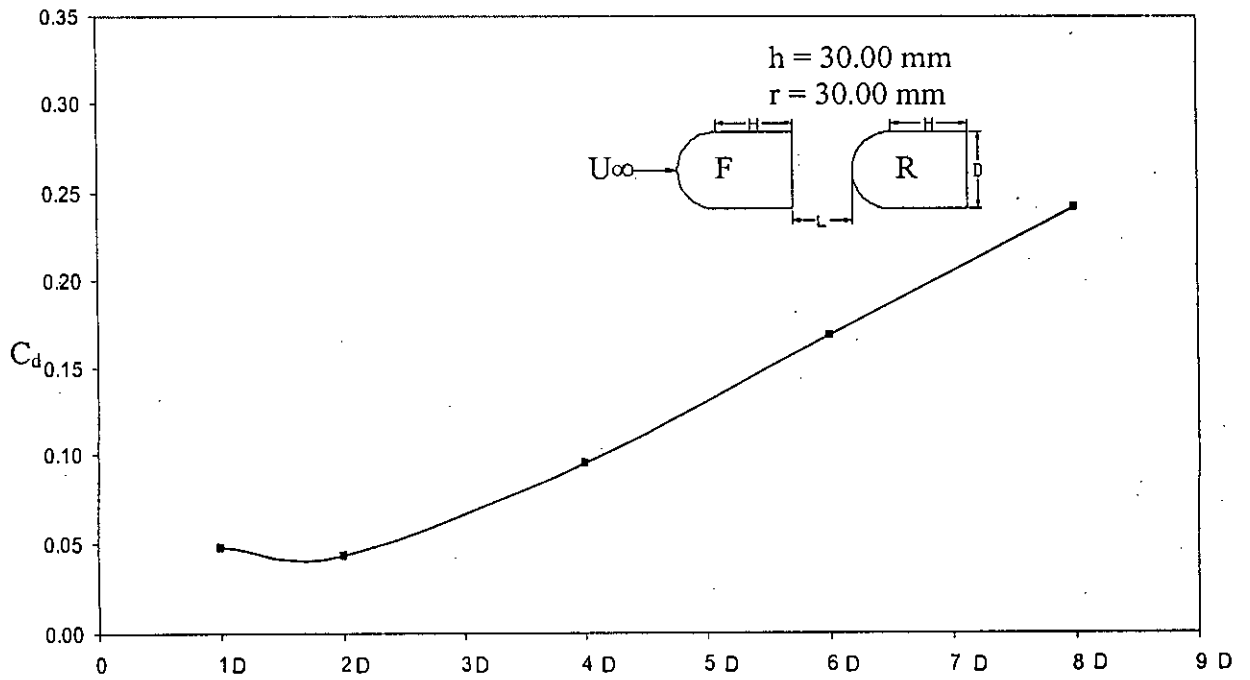
78

Figure 5.28: Variation of Drag Coefficient (C_d) with Inter Spaces on Front Cylinder with Facet Width of 30.00mm in a Group.
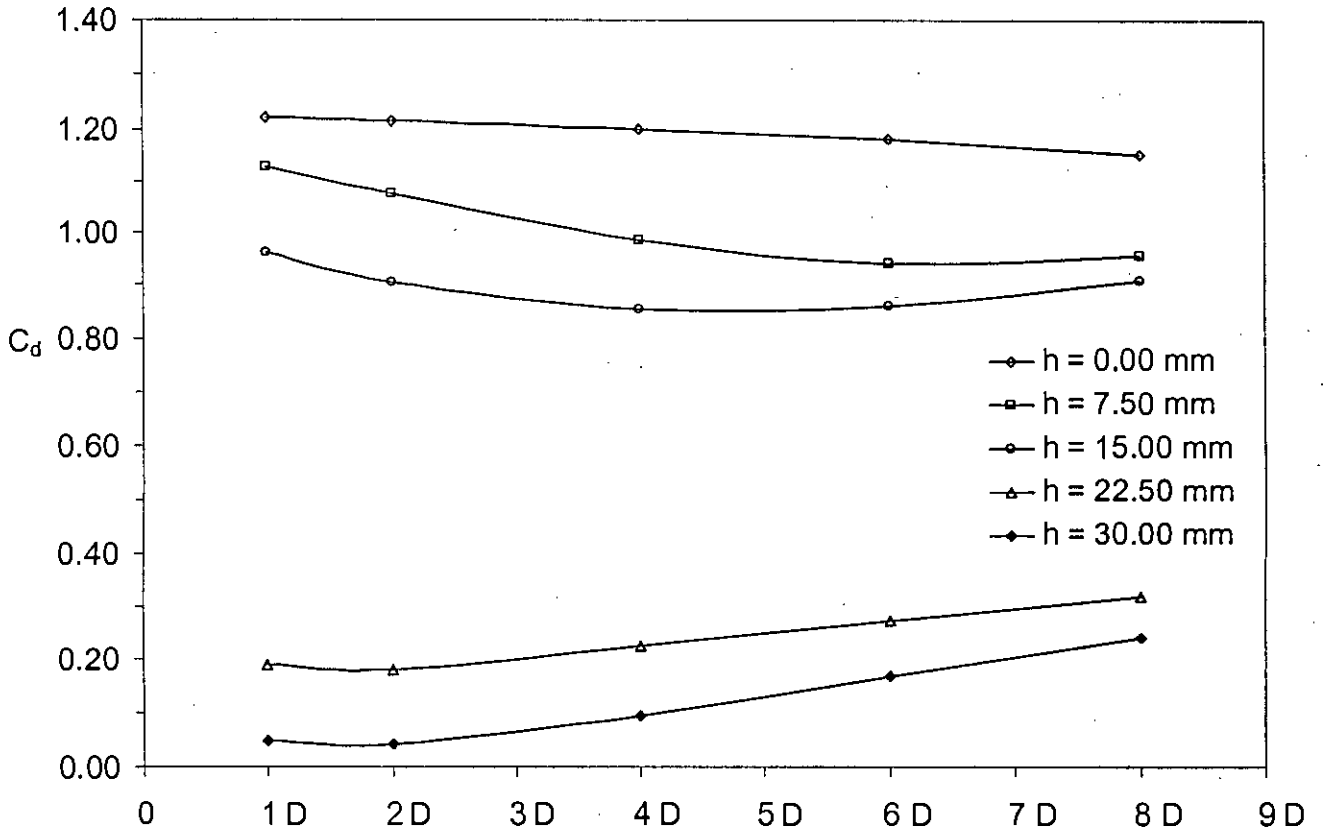
Figure 5.29: Variation of Drag Coefficient (C_d) with Inter Spaces on Front Cylinder with Different Facet Widths in a Group.
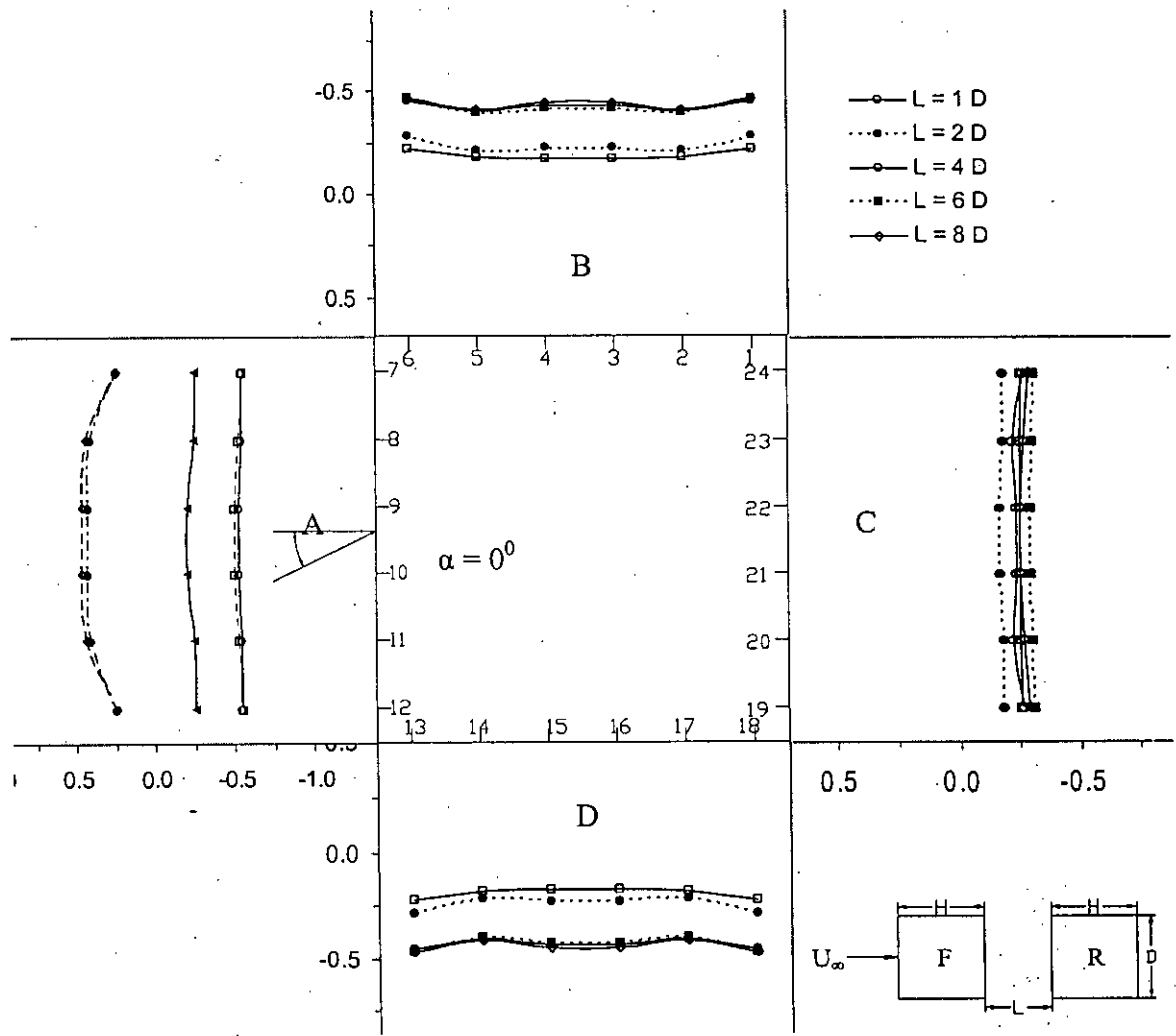
Figure 5.30: Static Pressure Distribution on Rear Square Cylinder in a Group with for Various Longitudinal Spacings.

Figure 5.31: Static Pressure Distribution on Rear Cylinder in a Group with Facet Width of 7.50mm for Various Longitudinal Spacings.

Figure 5.32: Static Pressure Distribution on Rear Cylinder in a Group with Facet Width of 15.00mm for Various Longitudinal Spacings.
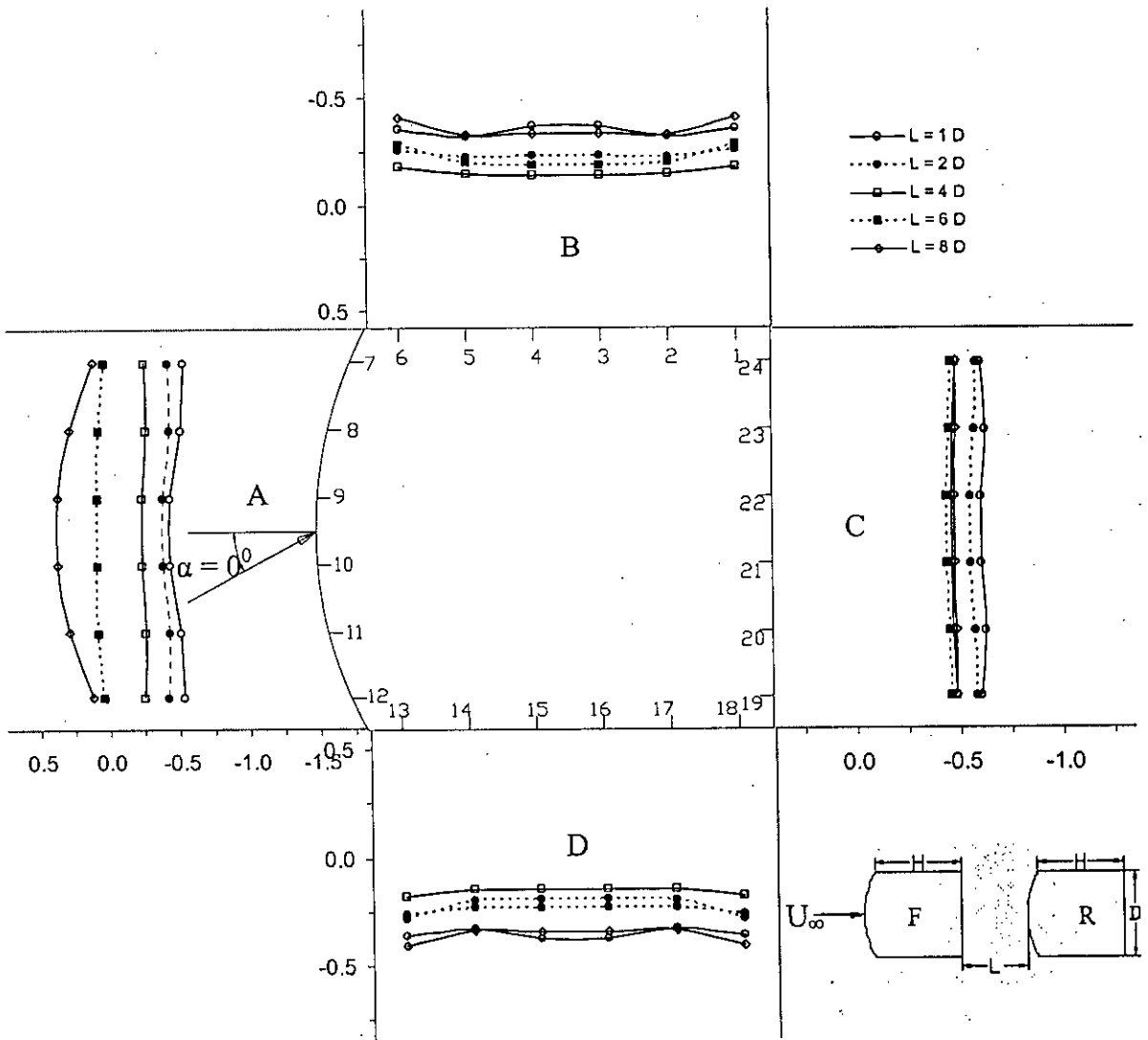
Figure 5.33: Static Pressure Distribution on Rear Cylinder in a Group with Facet Width of 22.50mm for Various Longitudinal Spacings.
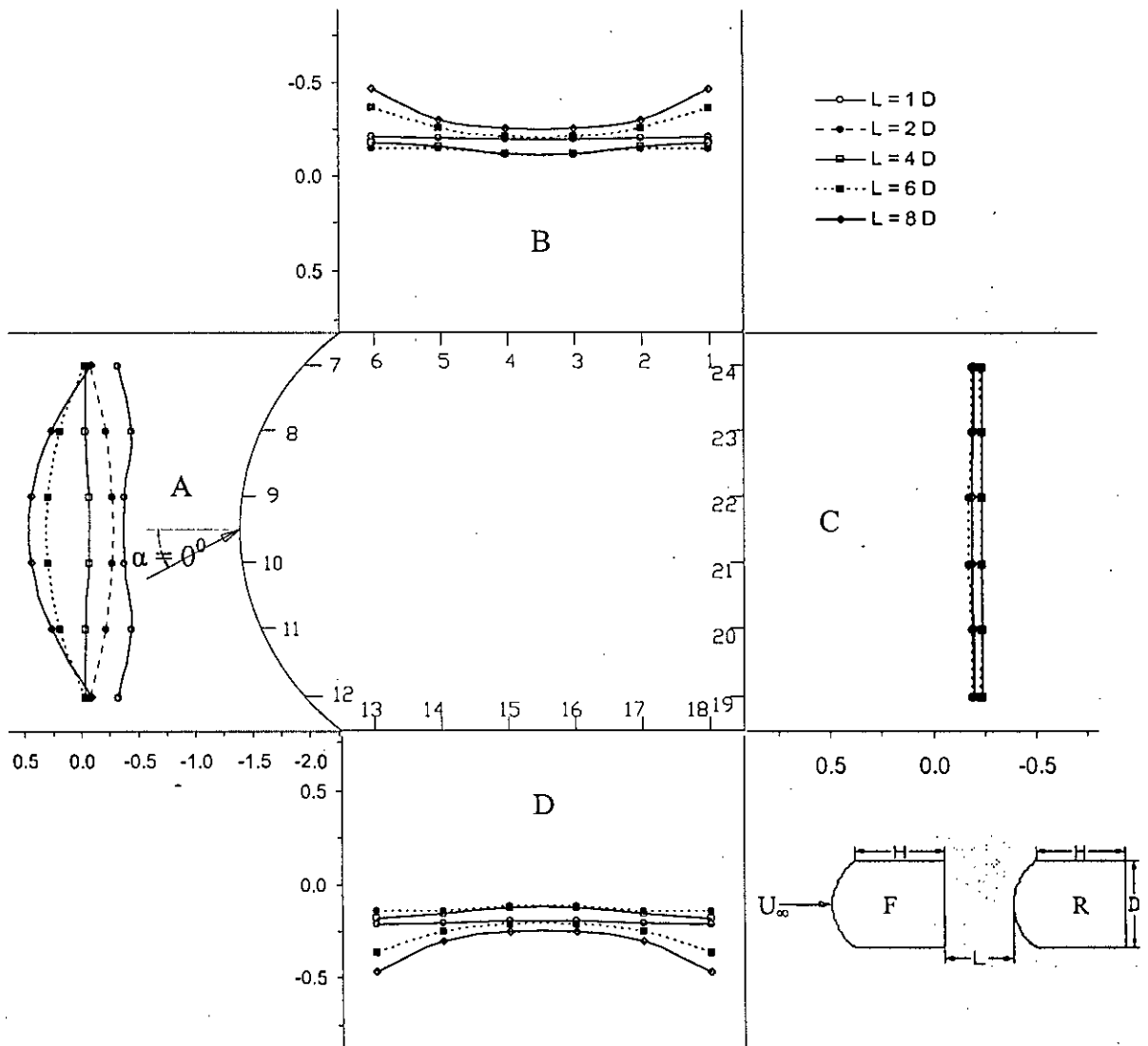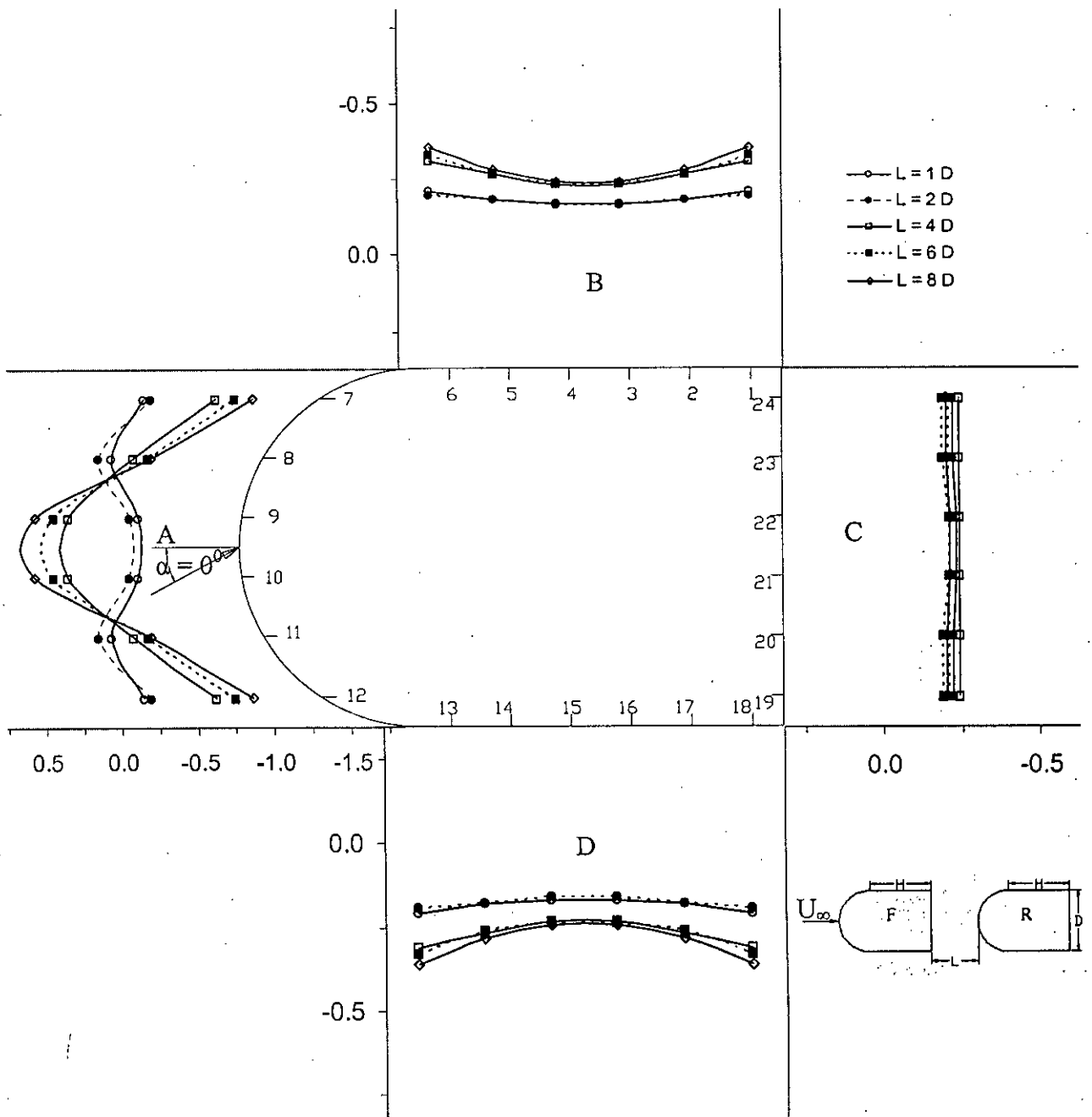
Figure 5.34: Static Pressure Distribution on Rear Cylinder in a Group with Facet Width of 30.00mm for Various Longitudinal Spacings.
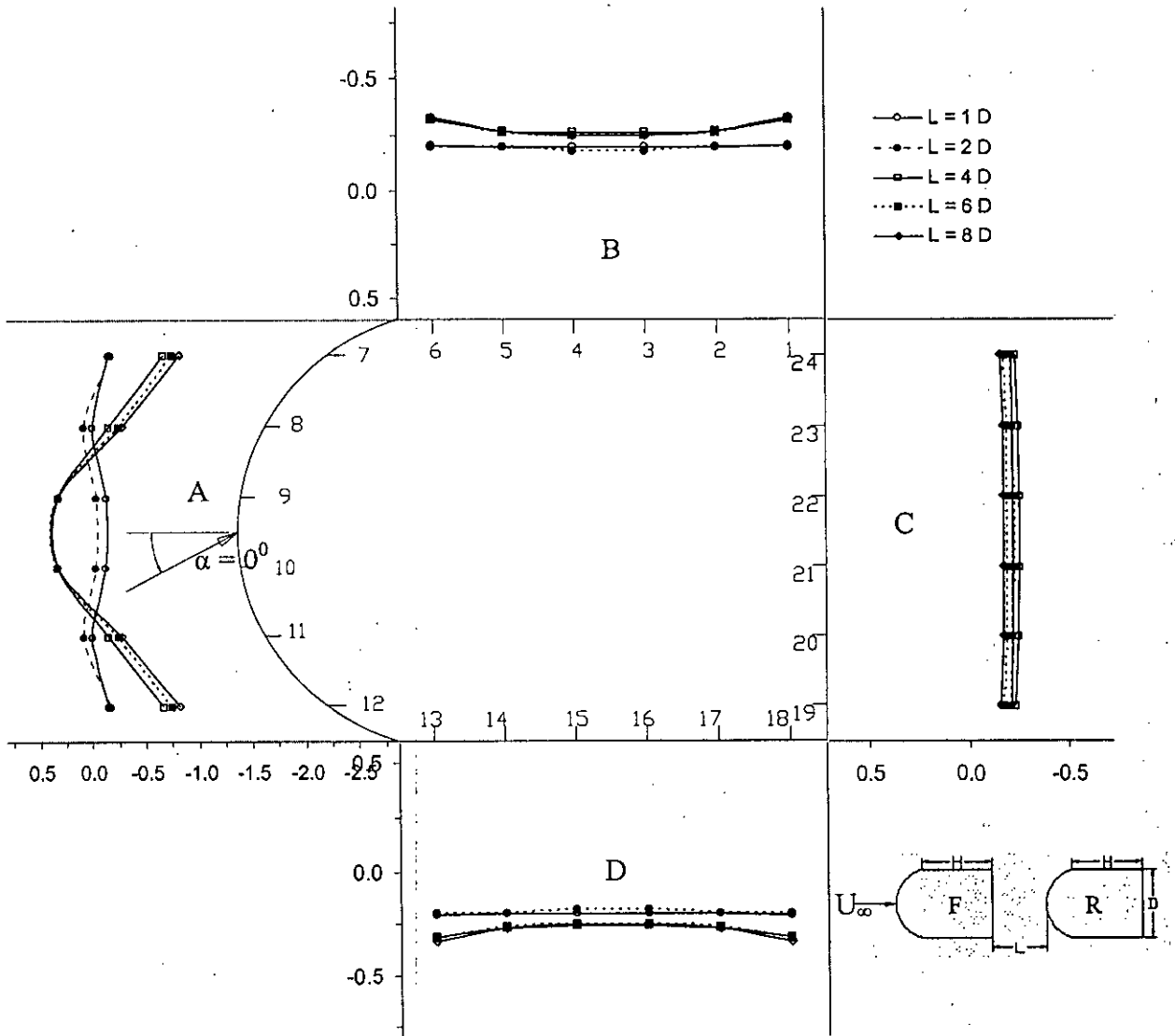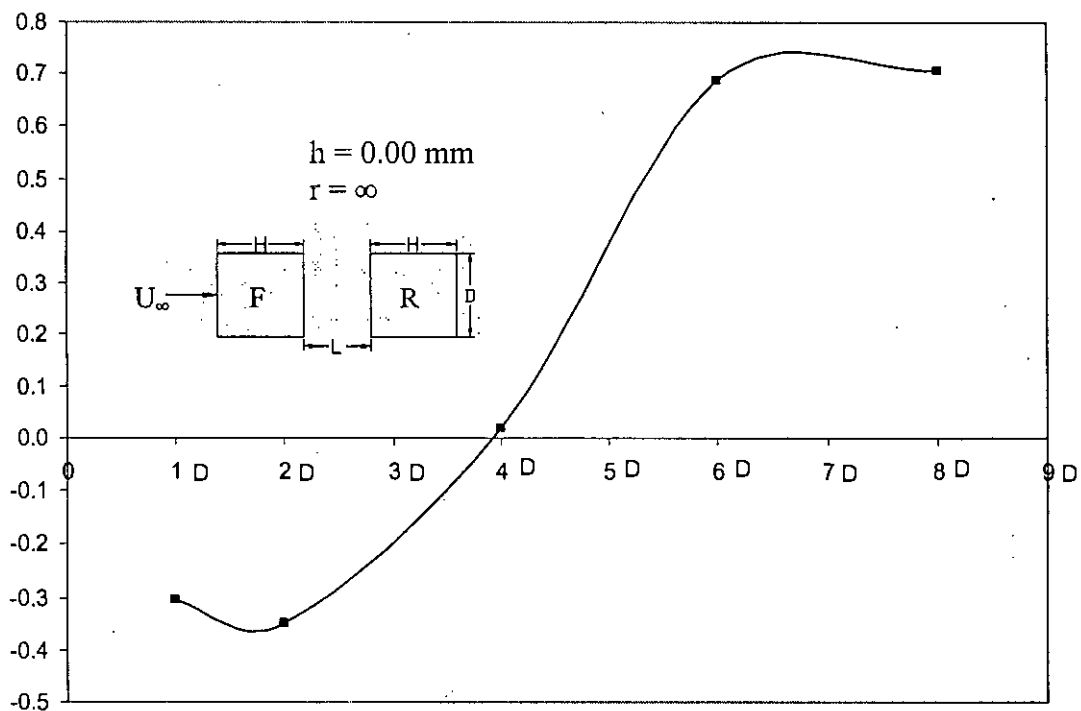
Figure 5.35: Variation of Drag Coefficient (C_d) with Interspace on Rear Square Cylinder in a Group.

Figure 5.36: Variation of Drag Coefficient (C_d) with Interspace on Rear Square Cylinder in a Group with Facet Width of 7.50mm.

Figure 5.37:   Variation of Drag Coefficient (C_d) with Interspace on Rear Square
Cylinder in a Group with Facet Width of 15.00mm.

Figure 5.38: Variation of Drag Coefficient (C_d) with Interspace on Rear Square
Cylinder in a Group with Facet Width of 22.50mm.

87

Figure 5.39: Variation of Drag Coefficient (C_d) with Interspace on Rear Square Cylinder in a Group with Facet Width of 30.00mm.

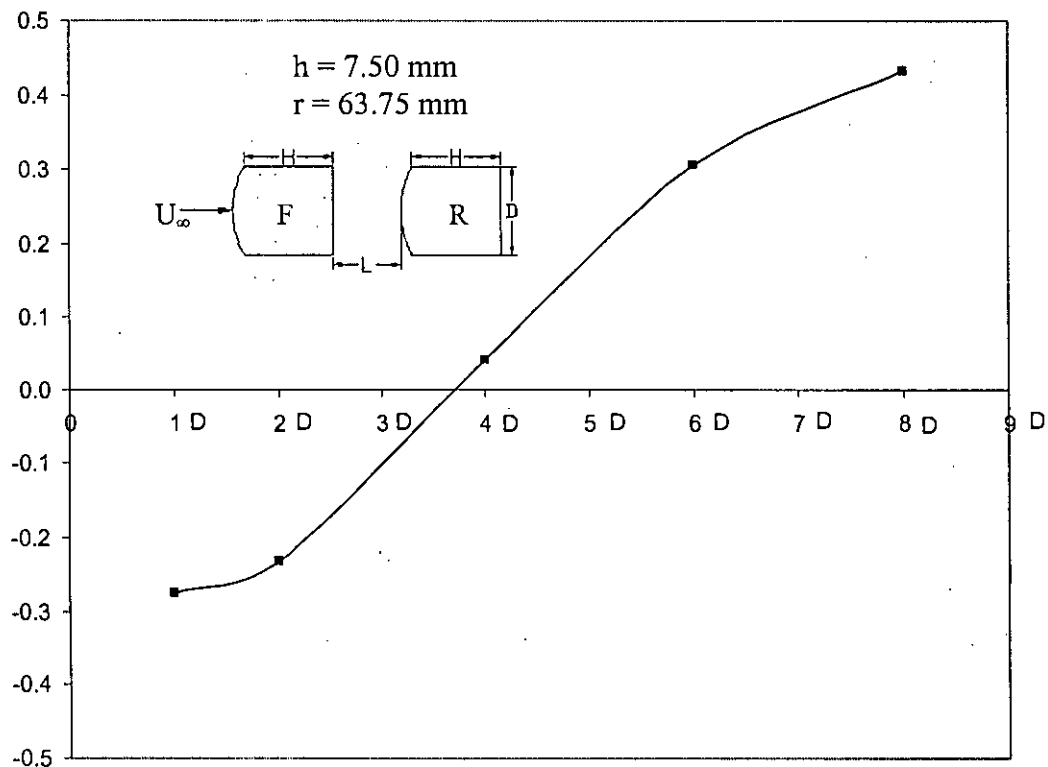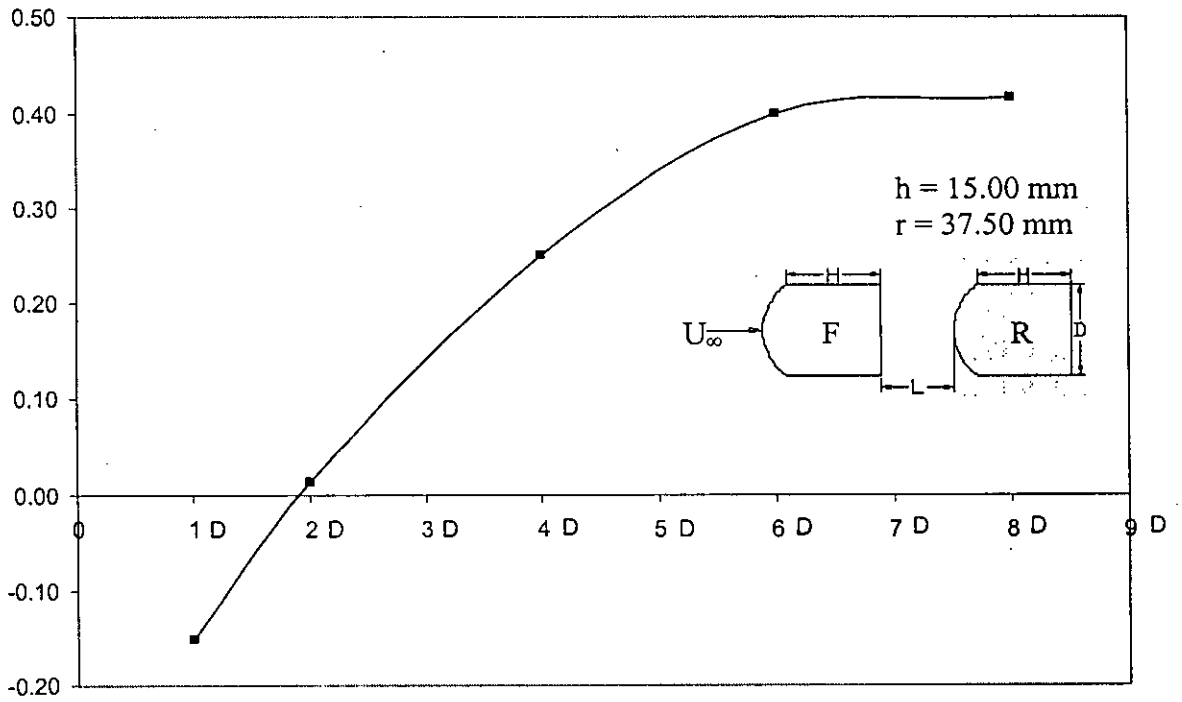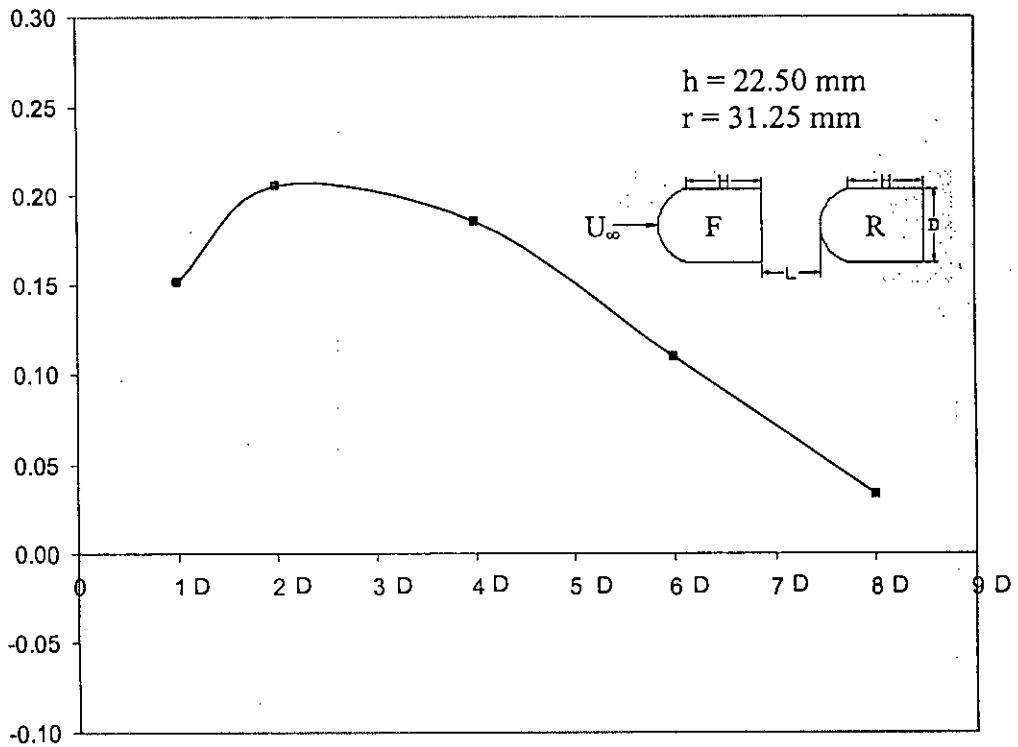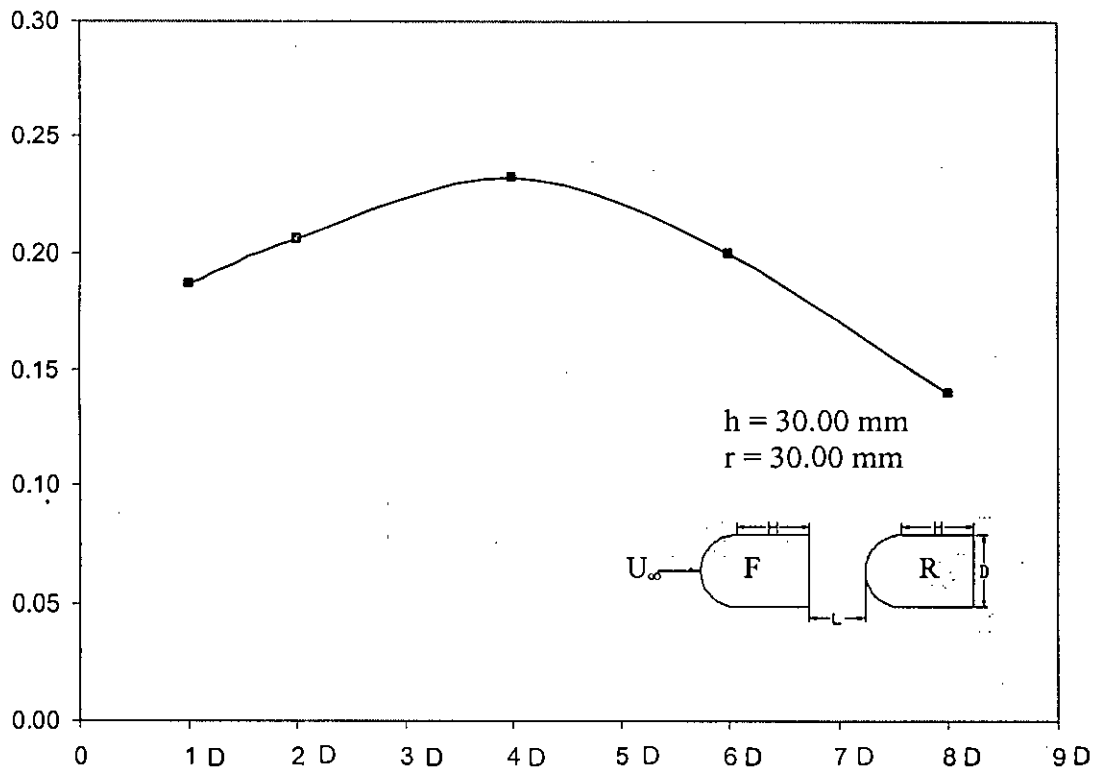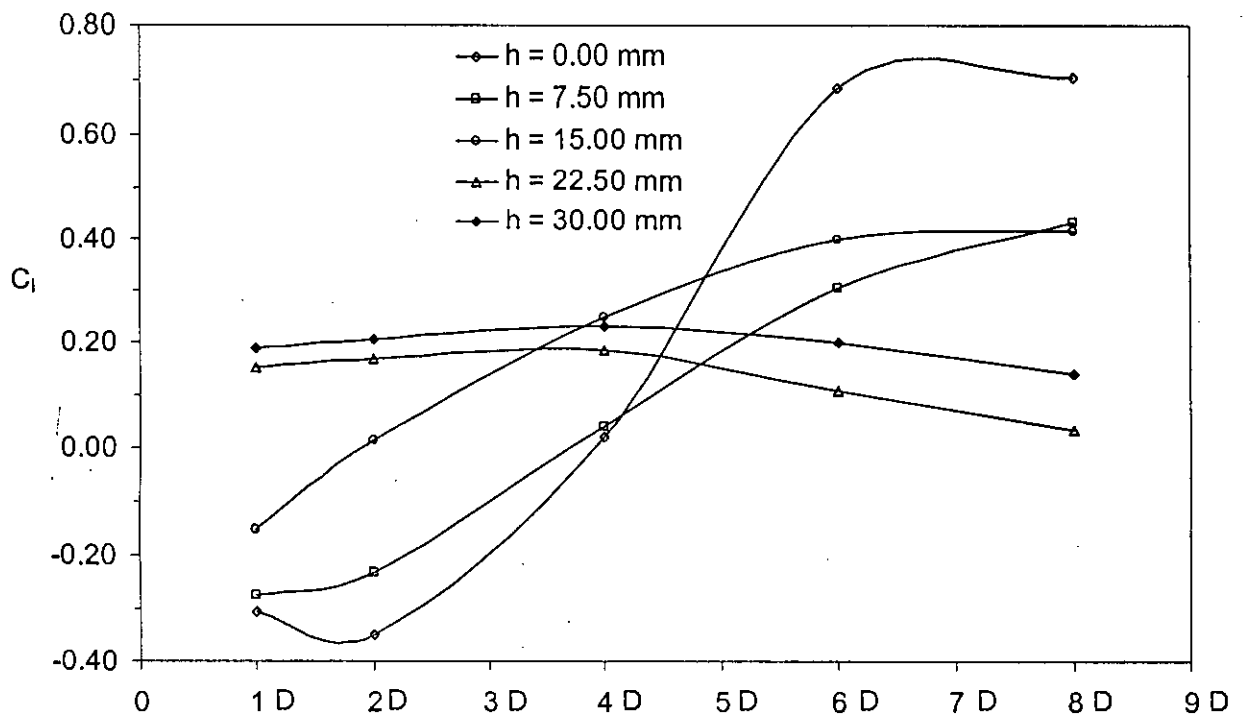Figure 5.40: Variation of Drag Coefficient (C_d) with Interspace on Rear Square Cylinder in a Group with Different Facet Widths.

CHAPTER - 6

CONCLUSIONS AND RECOMMENDATIONS

The following conclusions can be drawn from the experimental investigation of flow around square cylinder and cylinders with rounded facet. This chapter also includes the scope of extension and development of the present study.

6.1 Conclusions

1. At an angle of attack, $\alpha = 0^0$, no flow reattachment occurs on the surfaces of each isolated cylinder. However, the flow on the face B, face D and the face C is completely separated.

2. Flow reattachment occurs on face D of the single cylinder at small angle of attack and the location of reattachment shifts from the rear corner towards the front corner of the face D with increase in angle of attack.

3. At small angle of attack the C_P-value decreases considerably near the front corner of the face D of each cylinder in general.

4. The drags on the cylinders decrease with increase of the widths at the mid-point of the rounded facet i.e. with the decrease of the facet radius.

5. The C_P-values on the face B, face C and the face D of upstream cylinder reduce due to the presence of downstream cylinder.

6. The C_P-values on the face B, face C and the face D of upstream and downstream cylinders are always negative at any angle of attack. Whereas, these are negative in the case of single cylinder at angle of attack below 20^0.

7. The C_P-distributions on the face A of the downstream cylinders for longitudinal spacing, L= 1D and 2D are negative for both the two groups. Whereas, these are always positive in the case of single cylinder at any angle of attack below 40^0.

8. Due to the introduction of rounded facet, the drag coefficient decreases, however with facet width of 7.50 mm, the drag coefficient is more or less uniform with angle of attack up to 90^0 and gives the lower value.

9. Significant effect of inter space is observed on the drag coefficient of the upstream and downstream cylinder.

10. The stagnation point is found on the face A of either the single or the upstream cylinder in a group but on the face A of the downstream cylinder in a group no such stagnation point is found.

11. It appears from the investigation that there would be lower wind load on a building, which remains in the wake region produced by the building in the group.

12. From the investigation it is evident that after certain facet radius no further remarkable decrease in the drag coefficient is found, it may be taken into consideration by the relevant architect and engineer during performing their designs.

13. The outcome of the results may be applied for the design of the group of buildings while considering wind load.

6.2 Recommendations

1. The same experiment can be done with flow visualization technique to get a better understanding about the formation of wakes and vortex shedding pattern.

2. Further studies can be carried out by changing the formation of group i.e. one cylinder at upstream and two cylinders at downstream or two cylinders at upstream and one cylinder at downstream etc

3. Investigation of flow around staggered square and square cylinders with rounded facet at different angles of attack may be done.

4. The effect of surface roughness on the flow over isolated and group of square and rectangular cylinders can be investigated.

5. The effect of the Reynolds number may be investigated on the wind load of the

single as well as cylinders in a group.

6. Building models of various other shapes and sizes can be brought under this kind of investigation.

7. The test can also be conducted with different spacing and more cylinders.

8. The investigation of wind load can be performed by developing turbulent flow, with various turbulent intensity to see the effect of it.

REFERENCES

[1]   Ahmed N A and Back J (1996), "Destructive Wind Tunnel Tests", Unisearch Report no.23214-10, Australia.

[2]   Ahmed N A and Back J (1997), "Wind Tunnel Tests on Two Ventilators", Unisearch Report no.29295-01, Australia.

[3]   Allen H J and Vincent W G, "Wall Interference in a Two-dimensional Flow Wind Tunnel", NACA Report no. 782.

[4]   Anthony K C (1975), "Wind Engineering- The Personal View of a Practicing Engineer", Proceedings of the Fourth International Conference on Wind Effects on Buildings and Structures, London, U.K., pp.765-772.

[5]   Anwar A M M T (1996), "Wind Resistance on Non Engineered Housing in Implementing Hazard-Resistance Housing", Proceedings of the 1st International Housing and Hazards Workshop to Explore Practical Building for Safety Solutions held in Dhaka, Bangladesh, pp.11-17.

[6]   Baines W D (1963), "Effects of Velocity Distribution on Wind Loads and Flow Patterns on Buildings", Proceedings of a Symposium on Wind Effects on Buildings and Structures, Teddington, U.K., pp.197-225.

[7]   Barriga A R, Crowe C T and Roberson J A (1975), "Pressure Distributions on a Square Cylinder at a Small Angle of Attack in a Turbulent Cross Flow", Proceedings of the 4th International Conference on Wind Effects on Buildings, London, U.K., pp.89-93.

[8]   Bearman, P W and Truman D M (1971), "An Investigation of the Flow around Rectangular Cylinders", The Aeronautical Quarterly, Vol. 23, pp.229-237.

[9]   Bearman P W and Wadcock AJ (1973), "The Interaction between a Pair of Circular Cylinders Normal to a Stream", Journal of the Fluid Mechanics, Vol. 61, pp.499-511.

[10]   Bostock B R and Mair W A (1972), "Pressure Distributions and Forces on Rectangular and D-shaped Cylinders", The Aerodynamical Quarterly, Vol. 23, pp.499-511.

[11]   Bradbury L J S (1975), "Pulsed wire anemometer measurements on the flow past a normal flat plate in uniform and sheared flow", Proceedings of the 4th

International Conference on Wind Effects on Building and structures, Heathrow, Cambridge University Press.

[12] Castro J P and Fackrell J E (1978), "A Note on Two-Dimensional Fence Flows with Emphasis on Wall Constraint", J. Indust. Aerodynamics, 3(1).

[13] Castro I P and Robins A G (1977), "The Flow around a Surface Mounted Cube in Uniform and Turbulent Streams", Journal of Fluid Mechanics, Vol.79, pp.305-335.

[14] Chowdhurry J R (1996), "Design and construction of Houses to Resist Natural Hazards", In Implementing Hazard Resistance Housing, Proceedings of the 1st International Housing and Hazards Workshop to Explore Practical Building for Safety Solutions held in Dhaka, Bangladesh, pp.11-17.

[15] Cheung J C K, Holmes J D, Melbourne W H, Lakshmanan N and Bowdith P (1997), "Pressures on a 1:10 Scale Model of the Texas Tech. Building", J. Wind Eng. Ind. Aerodyn. no.69-71, pp.529-538.

[16] Chisholm M P and Lewis J (1996), "Cyclone-Resistance domestic Construction in Bangladesh", In Implementing Hazard Resistance Housing, Proceedings of the 1st International Housing and Hazards Workshop to Explore Practical Building for Safety Solutions held in Dhaka, Bangladesh, pp.29-38.

[17] Cochran L S and Cermak J E (1992), "Full and Model Scale Cladding Pressures on the Texas Tech University Experimental Building", J. Wind Eng. Ind. Aerodyn. no.43, pp.1589-1600.

[18] Coudrey C F (1957), "The application of Maskell's Theory of Wind Tunnel Blockage in Every Large Solid Models", NPL-Aero Report 1247, HMSO.

[19] Davenport A G (1963), "The Relationship to Wind Structure to Wind Loading", Proceedings of the Conference on Wind Effects on Buildings and Structures, Vol. 1.

[20] Davis R W and Moore E F, "A Numerical Study of Vortex Shedding from Rectangular Cylinder", Journal of Fluid Mechanics, Vol. 116, pp.475-506.

[21] Franck N (1963), "Model Law and Experimental Technique for Determination of Wind Loads on Buildings", 1st International Conference on Wind Effects on Building and Structures, Teddington, London, HMSO.

[22] Gatshore I S (1930), "Two-Dimensional Turbulent Wake", Journal of Fluid Mechanics, Vol.30, Part-3, pp.533.

[23] Hua C K (1971), "The Behavior of Lift Fluctuations on the Square Cylinders in the Wind Tunnel Test", Proceedings of the 3rd International Conference on Wind Effects on. Buildings and Structures, Tokyo, Japan, pp. 911-920.

[24] Hussain H S and Islam O (1973), "Study of Wind Load on Buildings and Structures", Journal of the Institution of Engineers, Bangladesh, Vol.1, no.2-3.

[25] Islam A M T and Mandal A C (1990), "Experimental Analysis of Aerodynamic Forces for Cross-Flow on Single Rectangular Cylinder", Mechanical Engineering Research Bulletin, BUET, Dhaka, Vol.13, No.1, pp.36-51.

[26] Islam O (1976), "Possibilities of Wind Effect in Bangladesh", Department of Aeronautical and Mechanical Engineering, University of Salford, UK.

[27] Islam T (1988), "An Experimental Investigation of Wind Effect on Rectangular Cylinders", M. Sc. Thesis, BUET, Dhaka.

[28] Isyumov N and Davenport A G (1975), "Comparison of full scale and Wind Tunnel Measurements on Commerce Court Plaza", 1st. Indust. Aerodynamics, 1(2).

[29] Jensen M (1967), "Some Lessons Learned in Building Aerodynamics Research", Proceedings of the 2nd Conference on Wind Effects on Building and Structures, Vol. 1.

[30] Kelnhofer J (1971), "Influence of a Neighboring Building on Flat Roof Loading", Proceedings of the 3rd International Conference on Wind Effects on Buildings and Structures", Tokyo, Japan, pp.221-230.

[31] Keffer J F (1965), "The Uniform Distribution of a Turbulent Wake", Journal of Fluid Mechanics, Vol. 22, Part-1, pp.135.

[32] Koening K and Roshiko A (1985), "An Experimental Study of Geometrical Effects on the Drag and Flow Field of two Bluff Bodies Separated by a Gap", Journal of Fluid Mechanics, Vol. 156, pp.167-204.

[33] Lamb H (1932), "Hydrodynamics", Cambridge University Press.

[34] Lanoville A, Gatshore I S and Parkinsoon G V (1975), "An Explanation of Some Effects of Turbulence on Bluff Bodies", Proceedings of the 4th International Conference on Wind Effects on Buildings and Structures,

London, U.K, pp.333-341.

[35] Lawson T V (1975), "Wind Loading of Buildings, Possibilities from a wind Tunnel Investigation", University of Bristol, U.K. Report No. TVLI731A.

[36] Lee BE (1975), "The Effect of Turbulence on the Surface Pressure Field of a Square Prism", Journal of Fluid Mechanics, Vol. 69, pp.263-282.

[37] Leutheusser J (1971), "Static Wind Loadings of Grouped Buildings", Proceedings of the 3rd International Conference on Wind Effects on Buildings, Tokyo, Japan, pp.211-220.

[38] Mandal A C (1979), "A Study of Wind Effects on Square Cylinders", MSc. Thesis, BUET.

[39] Mandal A C and Farok G M G (2005), "An Experimental Investigation of Static Pressure Distributions on Square and Rectangular Cylinders with Rounded Corners", 4th International Conference on Heat Transfer, Fluids Mechanics and Thermodynamics, Cairo, Egypt.

[40] Maskell E C (1965), "A Theory of Blockage Effects on Bluff Bodies and Stalled Wings in a Closed Wind Tunnel", ARC R&M No.3400, HMSO.

[41] Matsumoto M, "The Dynamical Forces Acting on the Vibrating Square Prism in a Steady Flow", Proceedings of the 3rd International Conference on Wind Effects on Buildings and Structures, Tokyo, Japan, pp.921-930.

[42] Mchuri F G, Sherratt A F C and A S (1969), "Effect of the Free Stream Turbulence on Drag Coefficient of Bluff Sharp-Edged Cylinders", Nature, Vol.224, No. 5222, pp.908-909.

[43] Melbourne W (1978), "Criteria for Environmental Wind Conditions", 1st Indust. Aerodynamics, 3(2/3).

[44] Modi V J and Sherbiny S (1975), "Wall Confinement Effect on Bluff Bodies in Turbulent Flows" Proceedings of the Fourth International Conference on Wind Effects on Buildings and Structures, London, U.K, pp.121-132.

[45] Nakamura Y and Matsukawa T (1987), "Vortex Excitation of Rectangular Cylinders with a Long Side Normal to the Flow", Journal of Fluid Mechanics, Vol.180, pp.171-191.

[46] Nakamura Y and Ohya Y (1983), "The Effects of Turbulence on the Main Flow Past Square Rods", Journal of Fluid Mechanics, Vol.137, pp.331-345.

[47] Nakamura Y and Yujioha (1986), "Vortex Shedding from Square Prisms in Smooth and Turbulent Flows", Journal of Fluid Mechanics, Vol.164, pp.77-89.

[48] Okajima A (1982), "Strouhal Numbers of Rectangular Cylinders", Journal of Fluid Mechanics, Vol. 123, pp.379-398.

[49] Parkinson G V and Modi VJ (1967), "Recent Research on Wind Effects on Bluff Two Dimensional Bodies", Proceedings of International Research Seminar, Wind Effects on Buildings and Structures, Ottawa, Canada, pp.485-514.

[50] Pearlstein A J, Mantle WJ and National Science Foundation CTS 94-22770 (2000), "Stability and the Transition to Three-Dimensional in Flows Past Axisymmetric Bluff Bodies", the Summary of Engineering Research, College of. Engineering, University of Illinois at Urbana-Champaign, USA.

[51] Pearlstein A J F, Petteni L and Wang (2000), "Stability of the Wake Behind a Rotating Circular Cylinder", the Summary of Engineering Research, University of Illinois, USA.

[52] Peris R (1967), "Action Du Vont Sur Les cheminees De Grando Hantour", Proceedings of International Research Seminar, Wind Effects on Buildings and Structures, Ottawa, Canada, Vol. II, pp.243-282.

[53] Pope A and Harper J J (1996), "Low Speed Wind Tunnel testing", John Willy and Sons, New York.

[54] Roberson J A, Chi Yu Lin, Rutherford G S and Stine M D, "Turbulence Effects on Drag of Sharp-edged Bodies", Journal of Hydraulic Division, Vol. 98, no. HY7, pp.1187-1201.

[55] Roberson J A, Crowe C T and Tseng R (1975), "Pressure Distribution on Two and Three Dimensional Models at Small Angles of Attack in Turbulent Flow", Proceedings of the 2nd U.S. National Conference on Wind Engineering Research, Colorado.

[56] Robertson, J M (1975), "Pressure Field at Reattachment of Separated Flows", Proceedings of the 2nd U.S National Conference on Wind Engineering Research, Colorado.

[57] Roy UK, Seraj S M BUET, Bangladesh and Hodgson R L P, University of Exeter, UK (2000), "Pressure Distribution Characteristics on a Typical

Bangladeshi Rural Home", Journal of Institution of Engineers, Bangladesh, Multidisciplinary Vol. Mul-dis. 25, No. 1, P-62-67.

[58] Sakamoto H and Arie M (1983), "Vortex Shedding from a Rectangular Prism and a Circular Cylinder Placed Vertically in Turbulent Boundary Layer", Journal of Fluid Mechanics, Vol. 126, pp.147-165.

[59] Scruton C and Rogers E M E (1971), "Steady and Unsteady Wind Loading of Buildings and Structures", Proceedings R.Soc. A, 269, pp.353-85.

[60] Surry D (1991), "Pressure Measurements on the Texas Tech Building: Wind Tunnel Measurements and Comparison with Full Scale", J. Wind Eng. Ind. Aerodynamics. no.38, pp.235-247.

[61] Vickery B J (1966), "Fluctuating Lift and Drag on a Long Cylinder of Square Cross Section in a Smooth and in a Turbulent Stream", Journal of Fluid Mechanics, Vol.25, pp.481-491.

[62] Whitbread R E (1963), "Model Simulation of Wind Effects on Structures", Proceedings of a Symposium on Wind Effects on Buildings and Structures, Teddington, UK, pp. 283-301.